

**CO₂-Responsive Surfactants for Enhancing Heavy Oil Recovery:
from Fundamentals to Bench-Scale Demonstrations in Canadian Oil
Sands Extraction**

by

Yi Lu

A thesis submitted in partial fulfillment of the requirements for the degree of

Doctor of Philosophy

in

Chemical Engineering

Department of Chemical and Materials Engineering
University of Alberta

© Yi Lu, 2020

Abstract

Interfacial properties at the oil-water interface are of key importance to various operations in the petroleum industry, especially in the aqueous-based heavy oil recovery process. However, different operation stages often require different interfacial properties, which could be conflicted with each other at specific circumstances. Reducing oil-water interfacial tension (IFT) by adding surfactants benefits the heavy oil liberation from host rocks/solids, but soon becomes detrimental to the subsequent stage where the separation of heavy oil product from the aqueous phase prefers high IFT values. In this study, the CO₂-responsive surfactant series was designed to solve such interfacial problems and enhance heavy oil recovery. Responsive surfactants feature interfacial activity that can be switched on/off by external stimuli. Hence, they permit the modulation of interfacial property in a controllable manner, such that multiple requirements could be accomplished by one single chemical addition. In this study, CO₂ gas was selected as the stimuli because it is inexpensive, abundant in nature, and usually available onsite in the flue gas.

One of the major challenges in applying CO₂-responsive surfactants to large-scale petroleum industry concerns their CO₂ switchability and robustness under operating conditions. Our strategy is to design a series of CO₂-responsive surfactants with facile preparation and tunable switching pH, which allows a suitable reagent to be readily selected based on requirements. These CO₂-responsive surfactants were formed by combining monoethanolamine (MEA) with long-chain fatty acids (LCFAs) of variable chain lengths through electrostatic attraction. The tunability of switching pH for this group of surfactants was demonstrated by *in situ* probing of the CO₂-responsive characteristics at the oil/water interface using dynamic IFT measurements. It is shown that the switching pH of the CO₂-responsive surfactants was controlled by the hydrocarbon chain

length of LCFAs. More importantly, their switching behavior was found to be different at the interface and in the bulk solution, which is attributed to the enhanced molecular interactions at the interface. Since most applications require surfactants to be switched at the interface, the switching pH of CO₂-responsive surfactants is thereby most appropriate to be determined through their interfacial responses.

With comprehensive understandings of the interfacial activity and interfacial response, CO₂-responsive surfactants were assessed by their performance in heavy oil recovery, where the process was considered in two stages, heavy oil liberation from solids and heavy oil harvest from emulsions. It is demonstrated that the addition of CO₂-responsive surfactants facilitated the release of heavy oil from solid substrates by decreasing oil/water IFT. Meantime, surfactants also helped the aqueous medium carrying out more heavy oil by forming stable heavy oil-in-water (HO/W) emulsions. In a subsequent stage, however, it was difficult to separate the heavy oil from these surfactant-stabilized emulsions, resulting in severe production loss. In contrast, fast demulsification was achieved by activating the CO₂-responsiveness of responsive surfactants, and thereby, harvesting more effectively after phase separation. The sustainability of CO₂-responsive surfactants was also investigated in the recycled process water.

Finally, CO₂-responsive surfactants were applied to water-based Canadian oil sands extraction process and successfully enhanced ultra-heavy oil (bitumen) recovery in bench-scale demonstrations. Compared with conventional heavy oil recovery where the heavy oil product was harvested after spontaneous phase separation, the Canadian oil sands extraction collects the bitumen by flotation where air bubbles are used to capture the liberated bitumen in the aqueous phase. Nevertheless, the ability to switch off interfacial activity at the interface is also beneficial to the bitumen-air bubble attachment. Bench-scale bitumen flotation experiments were conducted

at ambient temperature using real Canadian oil sands ores. Bitumen recovery was significantly improved from 15.0 % to 50.4 % with the addition of CO₂-responsive surfactants and the activation of CO₂ switching.

This study demonstrates that the interfacial properties at the oil-water interface are essential to the aqueous-based heavy oil recovery process, and the ability to manipulate these interfacial properties precisely is a promising direction to develop the next generation processing aid for the petroleum industry.

Preface

This thesis is composed of a series of papers. Chapters 4-6 are research papers that has been published, submitted or still in preparation. The following is a statement of contributions made to the jointly authored papers contained in this thesis:

- **Chapter 1.** *Introduction.* This section is an original work by Yi Lu.
- **Chapter 2.** *Literature review.* This section is an original work by Yi Lu.
- **Chapter 3.** *Experimental.* This section is an original work by Yi Lu.
- **Chapter 4.** *CO₂-responsive surfactants and their interfacial switching mechanism.* A version of this chapter has been published as: **Y. Lu**, D. Sun, J. Ralston, Q. Liu, and Z. Xu “CO₂-Responsive Surfactants with Tunable Switching pH” in Volume 56, Issue 5 of *Journal of Colloid and Interface Science* by Elsevier with DOI: 10.1016/j.jcis.2019.08.110. Yi Lu was responsible for experimental design, data collection, interpretation and manuscript preparation. Z. Xu, Q. Liu and D. Sun conceived the project. Z. Xu, J. Ralston, and Q. Liu provided proofreading and valuable discussion of the manuscript.
- **Chapter 5.** *CO₂-responsive surfactants for conventional heavy oil recovery.* A manuscript based on this chapter is in preparation: **Y. Lu**, R. Li, R. Manica, D. Sun, Q. Liu, and Z. Xu. In preparation. Yi Lu was responsible for experimental design, data collection, interpretation and manuscript preparation. R. Li assisted in the contact angle measurements. Z. Xu, Q. Liu and D. Sun conceived the project. Z. Xu, Q. Liu, and R. Manica provided proofreading and valuable discussion of the manuscript.

- **Chapter 6.** *CO₂-responsive surfactants for the enhancement of ex-situ oil sands extraction: a bench-scale demonstration.* A manuscript based on this chapter is in preparation: **Y. Lu**, D. Sun, Q. Liu, and Z. Xu. In preparation. Yi Lu was responsible for experimental design, data collection, interpretation and manuscript preparation. Z. Xu, Q. Liu and D. Sun conceived the project. Z. Xu, and Q. Liu provided proofreading and valuable discussion of the manuscript.
- **Chapter 7.** *Conclusions and Future Perspectives.* This section is an original work by Yi Lu.

Dedicated to

my parents and my wife.

Acknowledgement

I would like to express my greatest gratitude and appreciation to:

- My supervisors, Prof. Zhenghe Xu and Prof. Qingxia Liu, not only for their tremendous patience, encouragement, supervisory, and education in my research field but also as mentors to my career and life;
- Prof. John Ralston from the University of Southern Australia for his knowledgeable suggestions and valuable inputs on proofreading parts of my thesis;
- Prof. Dejun Sun from Shandong University for conceiving this interesting project;
- Mr. James Skwarok and Ms. Jie Ru for their generous help in lab supporting;
- Ms. Lisa Carreiro, Ms. Laurie Kachmaryk and Ms. Lily Laser for administrative assistance;
- All the fellow members and friends in the group, in particular, Dr. Yeling Zhu, Dr. Ci Yan, Dr. Rogerio Manica, Dr. Zuoli Li, Dr. Rui Li, Dr. Chen Wang, Dr. Xiangyu Chen, and Mr. Xiao He for their kind discussions, collaborations, proofreading, and encouragements;
- Natural Sciences and Engineering Research Council of Canada (NSERC); Alberta Innovates-Energy and Environmental Solutions (AI-EES); and Leading Talents Program of Guangdong Province (K17253301) for financial support.

Table of Contents

Abstract	ii
Preface	v
Acknowledgement	viii
Table of Contents	ix
List of Figures	xiii
List of Tables	xx
List of Abbreviations	xxi
Chapter 1. Introduction	1
Chapter 2. Literature Review	6
2.1 Oil Sands Extraction	6
2.1.1 References.....	10
2.2 Responsive materials in the petroleum industry	11
2.2.1 Switchable interfacial activity.....	12
2.2.1.1 <i>Switchable surfactants</i>	13
2.2.1.2 <i>Switchable polymeric surfactants</i>	15
2.2.1.3 <i>Switchable particles</i>	16
2.2.2 Switchable solvent	19
2.2.3 Switchable viscosity.....	22
2.2.3.1 <i>Responsive polymeric viscosifier</i>	25
2.2.3.2 <i>Responsive self-assembled viscosifier</i>	29

2.2.4 References.....	33
Chapter 3. Experimental	40
3.1 Materials	40
3.2 Interfacial tension (IFT) measurement.....	42
3.2.1 Interfacial switching.....	42
3.2.2 Solution switching	42
3.3 Contact angle measurements.....	43
3.4 Integrated thin film drainage apparatus (ITFDA).....	44
3.5 Demulsification tests.....	47
3.6 Heavy oil liberation visualization cell	48
3.7 Induction timer.....	49
3.7.1 Bitumen surface preparation	49
3.7.2 Induction time measurement.....	49
3.8 Bitumen recovery from oil sands.....	50
3.9 References.....	52
Chapter 4. CO₂-Responsive Surfactants and Their Switching Mechanism	53
4.1 Introduction.....	53
4.2 Materials and methods	56
4.3 Results and Discussion	58
4.3.1 Interfacial activity	58
4.3.2 Determination of switching pH.....	60
4.3.3 Interfacial switching vs. Solution switching.....	64
4.3.4 Impacts on practical applications.....	75

4.3.4.1 Switching of emulsion stability	75
4.3.4.2 Switching of physical properties at bitumen-water interfaces.....	78
4.4 Conclusions.....	80
4.5 References.....	81
Chapter 5. CO₂-Responsive Surfactants for Conventional Heavy Oil Recovery.....	86
5.1 Introduction.....	87
5.2 Material and Methods	90
5.3 Results and Discussion	92
5.3.1 Effect of CO ₂ -responsive surfactants on heavy oil liberation.....	92
5.3.2 Effect of CO ₂ -responsive surfactants on heavy oil harvest	98
5.3.3 Life cycle of CO ₂ -responsive surfactants	105
5.4 Conclusions.....	111
5.5 References.....	113
Chapter 6. CO₂-Responsive Surfactants for the Enhancement of <i>Ex-Situ</i> Oil Sands Extraction: A Bench-Scale Demonstration.....	116
6.1 Introduction.....	116
6.2 Materials and Methods.....	120
6.3 Results and Discussion	122
6.3.1 Bitumen-air bubble attachment.....	122
6.3.2 Bitumen recovery.....	126
6.3.3 Froth quality.....	131
6.3.4 Salt effects.....	133
6.4 Conclusion	137

6.5 References.....	137
Chapter 7. Conclusions and Future Perspectives	140
7.1 Conclusions.....	140
7.2 Future perspectives	141
Bibliography	143

List of Figures

Figure 1.1. Schematic drawing of a water-based bitumen extraction process.....	2
Figure 1.2. Bitumen liberation and aeration.	3
Figure 2.1. (a) Typical process of the water-based extraction process; Schematic views of (b) the liberation stage and (c) the aeration stage.	8
Figure 2.2. (a) Molecular structure of pseudo-Gemini surfactants; (b) Enhancement of bitumen liberation by introducing interfacial activity; and (c) Enhancement of oil-water separation by activating CO ₂ switchability.	14
Figure 2.3. (a) Proposed concept of polymeric surfactants enhancing bitumen recovery in oil sands extraction; (b) Polymerization the thermal-responsive polymeric surfactant; and (c) Bottle tests of oil sands extraction.	16
Figure 2.4. Application of pH-responsive magnetic nanoparticles (MNPs) as recyclable stabilizers for oil-water separation.	17
Figure 2.5. Topography picture of calcite surfaces before (top) and after (bottom) nanoparticle treatment.....	18
Figure 2.6. (a) Wedge-shaped nanoparticle structure and forces; and (b) Wedge contact pressure.	19
Figure 2.7. (a) Proposed process of switchable hydrophilicity solvent (SHS) introduced as the non-ionic liquid for the bitumen recovery from oil sands; (b) Mechanism of the CO ₂ switching solvent; and (c) The mixture of carbonated water and CyNMe ₂ after the bitumen has been decanted (left) and the same mixture after the CO ₂ has been removed (right).	21

Figure 2.8. (a) Switchable solvent introduced as ionic liquid for the enhancement of oil sands extraction; (b) Amine-water system before CO ₂ injection (left) and forming homogeneous solution after CO ₂ injection (right); and (c) Mechanism of switchable solvent enhancing aqueous-nonaqueous hybrid oil sands extraction.....	23
Figure 2.9. (a) Simulated viscous fingering in a porous media flow; and (b) Illustration of using the pH-responsive amphiphilic system as displacing fluid in EOR.....	24
Figure 2.10. (a) Mechanisms of thermoviscosifying behavior; Recovery factors and flooding pressures using PAM or TVPs in core flooding tests at (b) 45 °C and (c) 85 °C. (C _{polymer} = 0.2 wt.%; Total dissolved solids = 101,000 mg/L; Injected rate = 2 mL/min).....	27
Figure 2.11. (a) Typical pH-responsive polyelectrolytes with a comb-like structure; (b) Intra-/Inter-molecular interactions for the thickening effect of polyelectrolytes at the high pH condition; and (c) Dissolution and switching mechanism of polyelectrolytes in the absence and in the presence of salt.	28
Figure 2.12. (a) Two-step synthesis protocol for the preparation of pH-responsive amphiphiles; (b) Effect of solution pH on the viscosity of amphiphile solution; and (c) Fraction of oil recovered using the amphiphile at different pH values.....	30
Figure 2.13. (a) Illustration of CO ₂ -EOR process using WAG injection technique; (b) Comparison of the effect of CO ₂ -responsive compound (octadecyl dipropylene triamine, ODPTA) with conventional surfactants, such as sodium dodecyl sulfate (SDS) and octadecyl dimethyl ammonium chloride (OTAC); The performance of ODPTA was further investigated by the effect of temperature at 7.8 MPa (c), the effect of pressure at 160 °C (d), and the effect of salinity at 7.8 MPa and 160 °C (e).....	32

Figure 3.1. Preparation of MEA-LCFA surfactants and the basis of CO ₂ switching with structures of four MEA-LCFA surfactants.....	41
Figure 3.2. Photography of a pendent drop in the IFT measurement.	43
Figure 3.3. Snapshots of high viscosity oil droplet receding on a silica surface in Milli-Q water.	44
Figure 3.4. Schematic drawing of the integrated thin film drainage apparatus (ITFDA).....	46
Figure 3.5. Procedures of the induction time measurement. (a) Bitumen surface preparation; and (b) Induction time measurement.	50
Figure 4.1. (a) Interfacial activity MEA-LCFA surfactants at the heptane/water interface; (b) Interfacial excess concentration estimated from the Gibbs adsorption isotherm.....	58
Figure 4.2. (a) Schematic illustration of probing <i>in-situ</i> CO ₂ -responses of surfactants at the oil/water interface; (b) Evolution of a pendant heptane droplet in MEA-OA aqueous solution upon direct addition of 1000 µl CO ₂ -saturated water into the aqueous phase; (c) Changes in dynamic IFT of 1 mM MEA-OA aqueous solution/heptane interface with the addition of different volumes of CO ₂ -saturated water; and (d) Switching pH determined from dynamic IFT data obtained by in-situ probing of interfacial responses of surfactants.	62
Figure 4.3. Two protocols were designed to distinguish switching mechanisms of MEA-LCFA surfactants at the oil/water interface and in bulk solution by CO ₂ addition: <i>Protocol 1</i> represents interfacial switching while <i>Protocol 2</i> represents solution switching. Protocol 1 was further modified by removing the original drop and generating a new oil drop in the switched solution, representing the experiment of Protocol 1 followed by Protocol 2.	65

Figure 4.4. Solution responses of MEA-LCFA surfactants obtained using solution switching protocol described in Figure 4.3. pH of the surfactant solutions was modified either by gentle CO ₂ bubbling (solid lines) or by HCl/NaOH titration (dash lines) at the heptane/water interface.	66
Figure 4.5. Dynamic IFT experiments following modified Protocol 1 at the heptane/water interface: (a) MEA-C; (b) MEA-LA; (c) MEA-MA; and (d) MEA-OA.	67
Figure 4.6. Responses at oil/water interface and in bulk solution of the MEA-LCFA surfactants to CO ₂ addition: (a) 1mM MEA-CA; (b) 1mM MEA-LA; (c) 1mM MEA-MA; and (d) 1mM MEA-OA.	69
Figure 4.7. (a) Schematic drawings to show two experimental protocols of coalescence time measurement corresponding to Protocol 1 or Protocol 2 described in Figure 4.3; (b) Coalescence time of two heptane droplets measured in 1 mM MEA-OA solutions with the solution conditions and switching protocols being chosen from the previous IFT experiments and labelled in the inset; and (c) Images captured during coalescence experiments at the contact time of 10000 ms from Left (case #1), Mid (case #2) and Right (case #4) corresponding to no switching, switching at the interface, and further switching at the interface.	71
Figure 4.8. Apparent pKa values of LCFAs reported in literature.	72
Figure 4.9. Schematic drawing of MEA-LCFA surfactants at the interface and in the bulk aqueous solution.	74
Figure 4.10. Visual observation of demulsifying heptane-in-water (v:v = 1:10) emulsions stabilized by MEA-OA by bubbling CO ₂ up to pH 6.30 and then HCl addition to pH 3.04.	76

Figure 4.11. Demulsification efficiency was evaluated qualitatively by emulsion stability, where heptane-in-water (v:v = 1:10) emulsions were stabilized by different MEA-LCFA surfactants.	77
Figure 4.12. (a) Attachment time of an air bubble to a bitumen surface in MEA-LCFA surfactants with and without CO ₂ bubbling; (b) Bitumen-air bubble contact in 1 mM MEA-LA solution for 1000 ms without CO ₂ bubbling; and (c) Bitumen-air bubble contact in 1 mM MEA-LA solution for 100 ms with CO ₂ bubbling.	79
Figure 5.1. Schematic diagram of the two major stages in heavy oil recovery process: (a) Heavy oil liberation; and (b) Heavy oil harvest.	89
Figure 5.2. (a) Snapshots of the high viscosity oil droplet receding on a silica surface in Milli-Q water; (b) Dynamic contact angle in the first 300 s; and (c) Static contact angles in different aqueous solutions.	94
Figure 5.3. (a) Typical images from the house-made heavy oil liberation visualization cell system; Temporary evolution of heavy oil liberation for the petroleum ores treated by MEA-LA solution (b) and MEA-OA solution (c).	95
Figure 5.4. Relationships between the ultimate DOL and the interfacial activity of the corresponding surfactant at the toluene/water interface.	98
Figure 5.5. (a) Demulsification of the stable heavy oil-in-water (HO/W) emulsions stabilized by CO ₂ -responsive surfactants with and without CO ₂ bubbling (aging time = 1 hour); Evolution of the heavy oil recovery ratio in a storage time of 1 month (b), as well as in the first 600 s after CO ₂ bubbling in the cases of different surfactant types (c), different MEA-LA concentration (d), and different volume ratio of the heavy oil (e).	99
Figure 5.6. Long term storage of heavy oil-in water emulsions.	102

Figure 5.7. Images for the coalescence process of toluene-diluted heavy oil droplets in CO ₂ -responsive surfactant solutions without and with the activation of interfacial CO ₂ switching.	103
Figure 5.8. CO ₂ -responsive surfactants in the heavy oil recovery process.....	105
Figure 5.9. Distribution coefficient of MEA, LA and OA when the pH value of the aqueous phase is 5.16 ± 0.35	107
Figure 5.10. FTIR spectrum of the toluene-diluted heavy oil containing a certain concentration of LA (a) and OA (b). The full spectrums are given as insets, whereas the characteristic peak of carboxylic group in fatty acids at the wavenumber of 1714 cm^{-1} is emphasized by zooming in the region from wavenumber 2000 cm^{-1} to 1650 cm^{-1}	109
Figure 5.11. Calibration curves for the fatty acids in toluene-diluted heavy oil. Concentrations of LA and OA in the extracted heavy oil samples were obtained by interpolating the values of the integrated area of FTIR patterns on the calibration curves.	109
Figure 5.12. Evaluation of the tailings water collected from the demulsification experiments by their bulk pH and interfacial activity at the toluene/water interface throughout three cycles: (a) 5 mM MEA-LA; and (b) 5 mM MEA-OA.....	111
Figure 6.1. (a) Schematic graph of typical CHWE process; (b) Bitumen liberation from sand grains with inset illustrating the liberation contact angle (θ_{lib}); and (c) Bitumen-air bubble attachment with inset illustrating the aeration contact angle (θ_{aera}).	117
Figure 6.2. Induction time of air bubble attachment to bitumen surface treated by CO ₂ -responsive surfactants with and without the CO ₂ bubbling.	124
Figure 6.3. Induction time of air bubble attaching to bitumen surface treated by CO ₂ -responsive surfactants or MEA solution after the bubbling of CO ₂ gas.	125

Figure 6.4. (a) Comparison of the bituminous froth in Milli-Q water and in 3 mM MEA-LA; and (b) Total bitumen recovery in bench-scale oil sands extraction experiments using CO ₂ - responsive surfactants as the processing aid and using CO ₂ gas as the secondary flotation gas.....	128
Figure 6.5. Comparison of bitumen recovery from the primary froth and the secondary froth in the cases of MEA-LA solution at different concentrations.	130
Figure 6.6. Comparison of bitumen recovery using CO ₂ or air as the secondary flotation gas, in the cases of no MEA-LA addition and 3 mM MEA-LA addition.	131
Figure 6.7. Evaluation of the froth quality by (a) froth composition; and by (b) bitumen-to-solid (B/S) ratio and bitumen-to-water (B/W) ratio.....	132
Figure 6.8. Ion concentration in the supernatant fluids, which were filtered from the mixture of CO ₂ -responsive surfactants and process water.	134
Figure 6.9. IFT measured at the toluene/aqueous interface of MEA-LA in the Milli-Q water or in the process water.....	135
Figure 6.10. Comparison of the bitumen recovery using MEA-LA as the processing aid in Milli- Q water and process water.	136

List of Tables

Table 3.1. Operation procedure of oil sands extraction experiments in M-BEU.	51
Table 4.1. Composition of CO ₂ -saturated water at pH 3.85.	61
Table 5.1. Molecular structures and key properties of the CO ₂ -responsive surfactants	90
Table 5.2. Fitting parameters in Eq. 5.2 for the real-time heavy oil liberation experiments.	97
Table 5.3. Coalescence time of toluene-diluted heavy oil stabilized by different aqueous solutions with or without CO ₂ addition.	104
Table 6.1. Major ions and their concentrations in the process water.	133

List of Abbreviations

AER	:	Alberta Energy Regulator
AFM	:	Atomic force microscopy
API	:	American Petroleum Institute gravity
B/W	:	Bitumen-to-water ratio
B/S	:	Bitumen-to-solid ratio
CA	:	Capric acid
CAT	:	Critical associating temperature
CCD	:	Charged-coupled device
CHWE	:	Clark hot water extraction
CyNMe ₂	:	Cyclohexyldimethylamine
DETA	:	Diethylenetriamine
DBL	:	Degree of bitumen liberation
DLS	:	Dynamic light scattering
DMCHA	:	<i>N,N</i> -dimethyl-cyclohexylamine
DOL	:	Degree of heavy oil liberation
EA	:	Ethyl acrylate
EOR	:	Enhanced oil recovery
FPS	:	Frames per second
FTIR	:	Fourier-transform infrared
HO/W	:	Heavy oil-in-water
HPAM	:	Partially hydrolyzed polyacrylamide
IC	:	Ion chromatography
IFT	:	Interfacial tension
ITFDA	:	Integrated thin film drainage apparatus
LA	:	Lauric acid
LCFAs	:	Long-chain fatty acids
LCST	:	Lower critical solution temperature
M-BEU	:	Modified bitumen extraction unit
MA	:	Myristic acid
MAA	:	Methacrylic acid

MEA	:	Mono-ethanolamine
MNP	:	Magnetic nanoparticles
O/W	:	Oil-in-water
OA	:	Oleic acid
ODPTA	:	Octadecyl dipropylene triamine
OTAC	:	Octadecyl dimethyl ammonium chloride
PAM	:	Polyacrylamide
SAGD	:	Stream assisted gravity drainage
SDS	:	Sodium dodecyl sulfate
SHS	:	Switchable hydrophilic solvent
SHTA	:	Switchable-hydrophilicity tertiary amine
TEPDA	:	<i>N,N,N',N'</i> -tetraethyl-1,3-propanediamine
TMAOH	:	Tetramethyl ammonium
TVP	:	Thermoviscosifying polymers
WAG	:	Water-alternating-gas
WLM	:	Worm-like micelle

Chapter 1. Introduction

Oil sands in northern Alberta contain around 10 wt.% of bitumen, 5 wt.% of water and 85 wt.% of mineral solids [1], and are considered to be one of the most important non-conventional petroleum resources. The ultimate goal of the oil sands extraction is to collect all possible bitumen in the oil sands ores elegantly using an energy-efficient and eco-friendly process.

Water-based oil sands extraction process is the most mature and commercialized technology in northern Alberta since it was first developed by Dr. Clark in 1920s [2]. Figure 1.1 is an illustration of a typical water-based extraction process. Mineable oil sands are first collected and then conditioned by process water. Within the hydrotransport pipelines, bitumen is liberated into aqueous phase spontaneously and carried out by the washing fluids. This process is considerable efficient, attributed to the hydrophilic nature of sand grains in northern Alberta [3]. The separation of bitumen from its host solids is referred as the '*bitumen liberation*' stage. Meanwhile, dispersed bitumen droplets are aerated by the entrained air bubbles in the pipeline, a process known as '*bitumen aeration*'. Subsequently, the mixture of aerated bitumen, process water, and solid wastes, enters gravitational separation vessels, where bitumen is separated out by flotation.

At the end of an extraction process, the bitumen-concentrated froth is harvested from the top stream, which typically contains around 60 wt.% of bitumen, 30 wt.% of water and 10 wt.% of solid. Bituminous froth will be sent to froth treatment units to produce higher quality oil for upgrading. The bottom streams of slurries are deposited to tailing ponds for tailing management. Both processes are essential to the oil sands industry but are beyond the scope of this thesis.

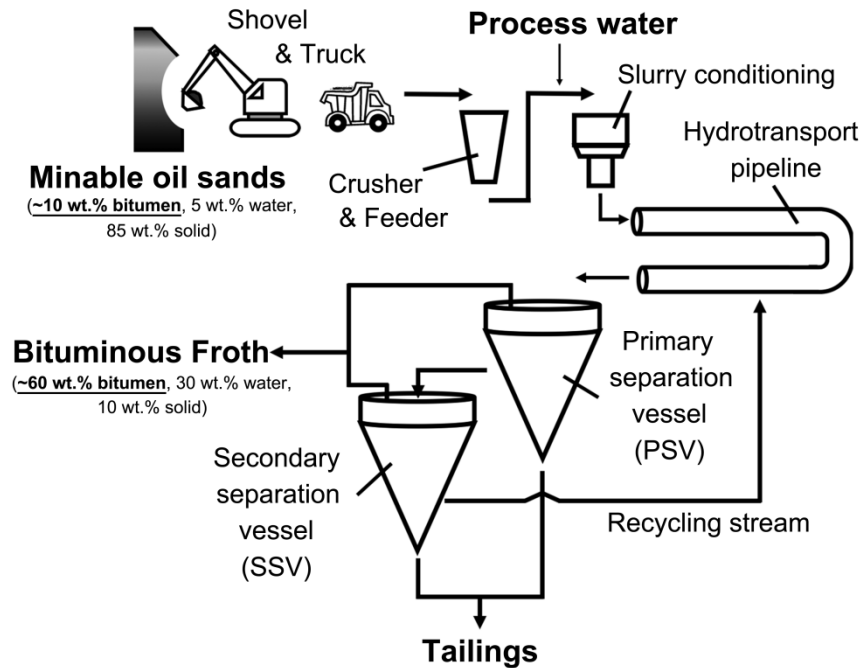


Figure 1.1. Schematic drawing of a water-based bitumen extraction process.

In order to achieve a higher bitumen recovery ratio, significant improvements are required from both the bitumen liberation and aeration stages. Unfortunately, these two stages appear to be in conflict in the sense of water-bitumen interfacial tension (IFT, γ_{WB}). In bitumen liberation, a low value of γ_{WB} is favorable [2], since the resulting small liberation contact angle (θ_{lib}) benefits the removal of bitumen from sand grains (Figure 1.2, left). On the other hand, decreasing γ_{WB} not only leads to the formation of stable bitumen-in-water emulsions, but also reflects as small aeration contact angle (θ_{aera}), which represents weak interaction between bitumen and air bubble [4] (Figure 1.2, right). In practice, “caustics” (e.g., sodium hydroxide, ammonium hydroxide) are used as the processing aids to enhance the bitumen recovery [2, 5, 6]. The addition of caustics releases natural surfactants [2] and thereby decreases the γ_{WB} . Optimum bitumen recovery is obtained by

controlling the pH of process water to the point where bitumen liberation is greatly facilitated while the compromise to bitumen aeration is acceptable.

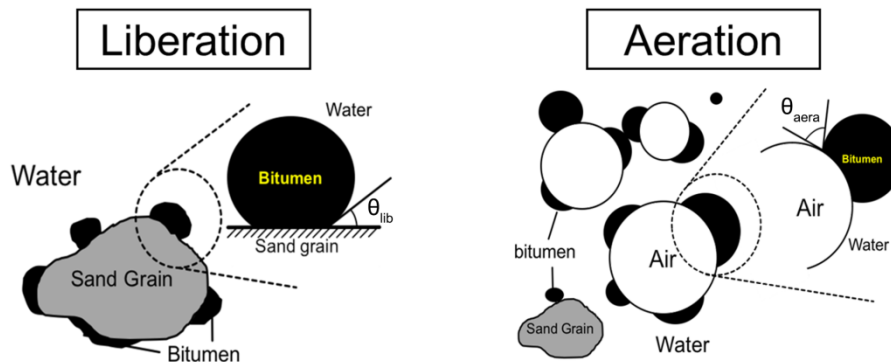


Figure 1.2. Bitumen liberation and aeration.

The next generation of water-based oil sands extraction industry needs to break through the limitation that originates from the conflicts between bitumen liberation and aeration. Namely, there are emerging requests to develop novel processing aids that can fulfill multiple interfacial requirements at different stages of operation in a simple, feasible and sustainable manner.

Responsive surfactants provide temporary interfacial activities at the oil/water interface, which are able to be switched off by external stimuli at the desired stage of operation. Theoretically, bitumen liberation is facilitated if responsive surfactants are added together with process water to lower the γ_{WB} . More importantly, these responsive surfactants can be switched off prior to the bitumen aeration. Thus, bitumen-air bubble attachment will be promoted once the hydrophobic nature of the bitumen surface is recovered.

CO₂-responsive surfactants, using CO₂ as the stimulus, are the most promising processing aids to oil sands extraction. CO₂ gas is available on site (e.g., abundant in flue gas), easily removable, and convenient to implement with no need of energy-intensive equipment.

The primary objective of this project is to develop CO₂-responsive surfactants that are feasible and efficient to enhance bitumen recovery in the water-based oil sands extractions process, utilizing their unique switchable interfacial activities to overcome the conflict between the bitumen liberation and aeration. In order to achieve this goal, this work also aims at understanding the switching behaviors of CO₂-responsive surfactants at the oil/water interface.

The following thesis is composed of seven chapters, including the literature reviews, colloidal and interfacial science studies, and applications in the petroleum industry. **Chapter 1** provides an overall introduction to this thesis. **Chapter 2** briefly reviews the current progress of oil sands extraction technology, as well as the development of responsive materials in the general petroleum industry. **Chapter 3** introduces the experimental methodologies and equipment used for this study. **Chapter 4** studies the switching mechanisms of CO₂-responsive surfactants, especially their behaviors at the oil/water interface. **Chapter 5** evaluates the performance of two CO₂-responsive surfactants for the conventional heavy oil recovery process, whereas **Chapter 6** presents the successful enhancement of bitumen recovery in bench-scale oil sands extraction demonstration. At the end of this thesis, **Chapter 7** concludes the major contributions of this project, as well as the recommendations for future research.

1.1 References

1. Masliyah, J., J. Czarnecki, and Z. Xu, *Handbook on theory and practice of bitumen recovery from Athabasca oil sands: Vol. I. Theoretical basis*. 2010: Kingsley Knowledge Publishing.
2. Masliyah, J., et al., *Understanding water- based bitumen extraction from Athabasca oil sands*. The Canadian Journal of Chemical Engineering, 2004. **82**(4): p. 628-654.
3. Mossop, G.D., *Geology of the Athabasca oil sands*. Science, 1980. **207**(4427): p. 145-152.
4. He, L., et al., *Effect of solvent addition on bitumen-air bubble attachment in process water*. Chemical Engineering Science, 2015. **137**: p. 31-39.
5. Flury, C., et al., *Effect of caustic type on bitumen extraction from canadian oil sands*. Energy & Fuels, 2014. **28**(1): p. 431-438.
6. Chen, T., et al., *Impact of salinity on warm water-based mineable oil sands processing*. The Canadian Journal of Chemical Engineering, 2017. **95**(2): p. 281-289.

Chapter 2. Literature Review

2.1 Oil sands extraction

Oil sands, also known as tar sands or bituminous sands, are considered to be one of the most important unconventional petroleum deposits [1]. Canada has one of the world's largest found oil sand reserves in northern Alberta, whereas others are located in Venezuela, Russia, and Kazakhstan. Compared to conventional oil, which can be produced from traditional wells, oil sands are relatively difficult and expensive to extract. Oil sands are usually described as a highly dense, highly viscous mixture of bitumen, water, sand, and clay, which contain high heavy metal content and a high carbon-to-hydrogen ratio. Therefore, numerous explorations and research projects have been performed over the decades in order to find a better and cheaper way to recover bitumen from oil sands.

Current methods of recovering bitumen from oil sands involve open-pit mining, mainly using Clark Hot Water Extraction (CHWE), and in-situ technique, mainly using Stream Assisted Gravity Drainage (SAGD). The difference between the two operations depends on the thickness of the overburden [2]. According to the Alberta Energy Regulator (AER), open-pit mining is limited to areas where the overburden thickness is less than 75m [3]. It is worth noting that open-pit mining is still the most mature and commercialized technique and produces about 50% of the total bitumen in Alberta oil sand industry, although the in-situ technique is considered to be the promising future.

The typical water-based extraction process can be summarized into four steps: slurry preparation, extraction, froth treatment, and tailing treatment (Figure 2.1a). Oil sand ores are collected by gigantic shovels and trucks in open-pit mines and then crushed into small pieces. After adding hot water and chemical aids, the resulting slurries have much lower viscosity, allowing hydro-transportation in pipelines. While transported in pipelines, bitumen would be liberated from sand grains and form tiny droplets. The release of bitumen is also referred to the liberation stage of oil sand extraction. After the liberation, air bubbles would be used to capture bitumen in water and create froth, which contains 60% bitumen, 30% water, and 10% solid. The remaining bottom would be treated as tailings. This process is called the aeration stage of oil sand extraction. The froth will be collected and treated with either naphthenic or paraffinic solvent in order to increase bitumen content by up to 99% [2].

Throughout the CHWE process, it is essential to liberate bitumen from the sand grains and allow them to be adsorbed onto the air bubbles. For the purpose of increasing the total bitumen recovery ratio, it is ideal to improve the efficiency in both liberation and aeration stages. Unfortunately, qualitative analysis reveals the problem that operation requirements for the efficiency enhancement for the two stages conflict with each other. In liberation, water-favorable bitumen surfaces are preferred in order to enhance the separation of bitumen and sand grains. Therefore, it is desirable to have either hydrophilic bitumen droplets, which is not realistic in most cases, or surface-active agents sitting on the water-bitumen interface. However, surface-active agents produce a fine water-bitumen emulsion, resulting in resistance to aeration. Tiny hydrophilized oil droplets are less able to be captured by air bubbles, which are hydrophobic [4]. In fact, this is also the reason why surface-active asphaltenes, which are naturally contained in the oil sand, are unfavorable in oil sand extraction [5].

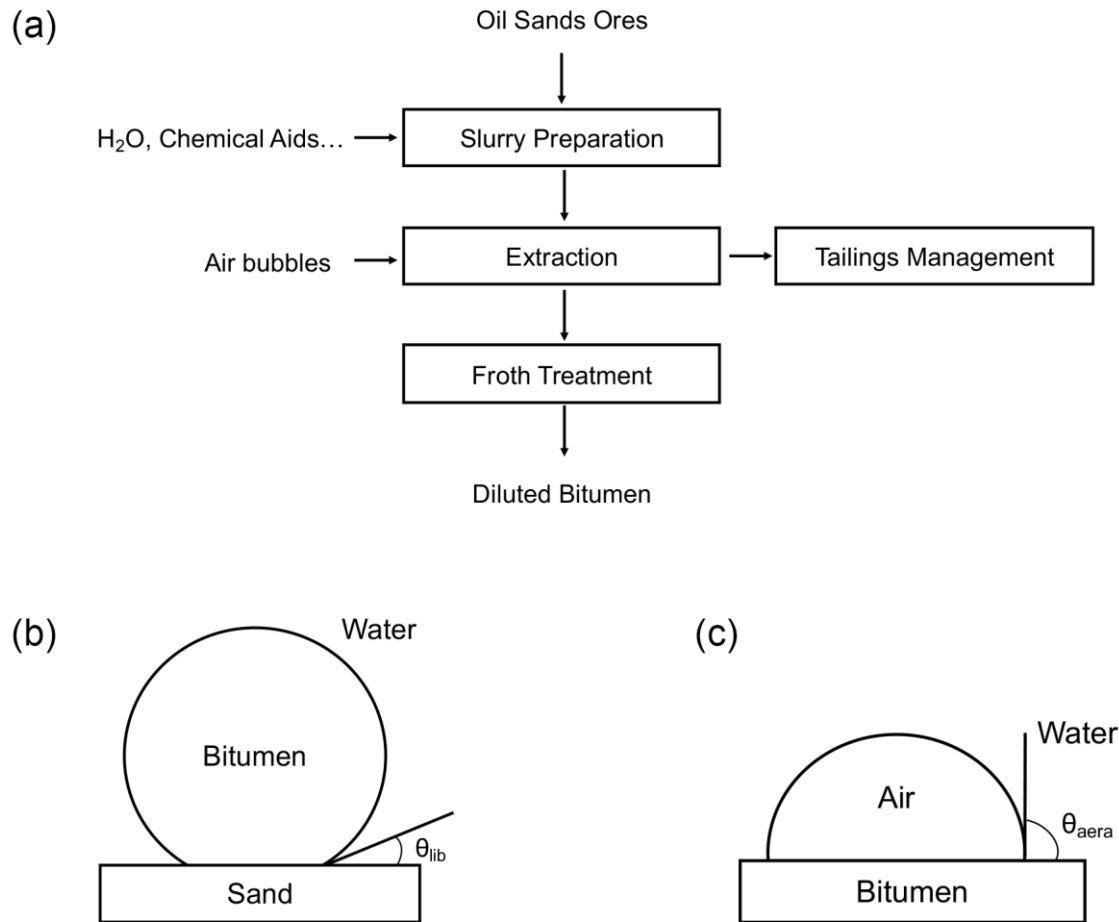


Figure 2.1. (a) Typical process of the water-based extraction process; Schematic views of (b) the liberation stage and (c) the aeration stage.

Quantitatively understanding of this conflict between liberation and aeration is explained by Young's equation. Figures 2.1b & 2.1c are the schemes for liberation and aeration, respectively, where θ s are the three-phase contact angles. Following the analysis above and described quantitatively, it is desirable to have a small θ in the liberation stage, which would enhance the separation of bitumen and sand grain. Meanwhile, the higher value of θ in the aeration stage would contribute to a better attachment among bitumen and air bubbles. In the liberation stage (Figure 2.1b), Young's equation gives:

$$\cos \theta_{lib} = \frac{\gamma_{SB} - \gamma_{SW}}{\gamma_{WB}} \quad \text{Eq. 2.1}$$

where θ_{lib} is the contact angle in the liberation stage, γ_{SB} , γ_{SW} , and γ_{WB} are the interfacial tensions between sand-bitumen, sand-water, and water-bitumen interfaces, respectively. Therefore, θ_{lib} could be minimized by either increasing γ_{SB} , decreasing γ_{SW} , or decreasing γ_{WB} . Similarly, in the aeration stage (Figure1c), Young's equation shows:

$$\cos \theta_{aera} = \frac{\gamma_{AB} - \gamma_{WB}}{\gamma_{WA}} \quad \text{Eq. 2.2}$$

where θ_{aera} is the contact angle in the aeration stage, γ_{AB} , γ_{WB} , and γ_{WA} are the interfacial tensions between air-bitumen, water-bitumen, and water-air interfaces, respectively. For the purpose of maximizing θ_{aera} , it is necessary to have lower γ_{AB} , higher γ_{WB} , or higher γ_{WA} . Considering that γ_{WB} is contradictory in those two stages, it is impossible to satisfy both requirements by traditional methods, i.e., adding normal surfactants. It should also be noted that pH would affect γ_{SW} and the release of natural surfactants in asphaltene as well [5, 6]. In general, liberation prefers base conditions, while aeration prefers neutral/acid conditions [7]. As a compromise to the conflict, the current industrial operation pH is ~ 8 [1].

Responsive materials, especially CO_2 -responsive surfactants, are potentially the answer to solve the problem. Responsive materials exhibit a dramatic and discontinuous change of their physical properties, i.e., change of solubility or amphiphilicity balance due to stimuli like temperature, pH variation. The main strategy of utilizing responsive surfactants is to introduce their surface activity in the liberation stage and switch to non-active in the aeration stage via the external changes.

2.1.1 References

1. Masliyah, J., et al., *Understanding water- based bitumen extraction from Athabasca oil sands*. Canadian Journal of Chemical Engineering, 2004. **82**(4): p. 628-654.
2. Masliyah, J., J. Czarnecki, and Z. Xu, *Handbook on theory and practice of bitumen recovery from Athabasca oil sands: Vol. I. Theoretical basis*. 2010: Kingsley Knowledge Publishing.
3. *Alberta mineable oil sands plant statistics monthly supplement*. 2016, Alberta Energy Regulator.
4. Jia, W., S. Ren, and B. Hu, *Effect of water chemistry on zeta potential of air bubbles*. International Journal of Electrochemical Science, 2013. **8**(4): p. 5828-5837.
5. Czarnecki, J. and K. Moran, *On the stabilization mechanism of water-in-oil emulsions in petroleum systems*. Energy & Fuels, 2005. **19**(5): p. 2074-2079.
6. Qiao, P., et al., *Interactions of asphaltene subfractions in organic media of varying aromaticity*. Energy & Fuels, 2018. **32**(10): p. 10478-10485.
7. Flury, C., et al., *Effect of caustic type on bitumen extraction from canadian oil sands*. Energy & Fuels, 2014. **28**(1): p. 431-438.

2.2 Responsive materials in the petroleum industry

In the petroleum industry, it is very common to see that different properties are required at the different stages in one continuous process, some of which could even conflict with each other. Sometimes, the oil needs to be emulsified with water, but soon required to be separated from the emulsion in the following step. Increasing the viscosity of the displacing fluids improves the mobility of heavy oil in the reservoir, but also causes injection and processing difficulties. Conventionally, each individual step requires one specific chemical addition, e.g., surfactants for emulsification and demulsifiers for demulsification. Such a strategy would lead to the waste of materials, the low efficiency of operation, as well as the accumulations of the pollutants in the near environment.

Responsive materials feature switchable properties upon external stimuli, such as temperature, pH, UV radiation, CO₂/N₂ gas, magnetic field, etc. They are capable of serving as multifunctional materials that could accomplish more than one requirement. Hence, successful implements of the responsive materials could significantly reduce the chemical additions, improve the process sustainability, and alleviate the environmental concerns. More importantly, their switching behavior that is subjected to a specific external stimulus could be activated when desired, similar to the “switch on/off” of a light bulb in daily life. Responsive materials have been considered as the frontier technology for designing “smart” processes and have attracted numerous interests from various fields, including the petroleum industry, pharmaceuticals, controlled drug delivery, sensors, cosmetics, and soil/water remediations. In this section, we focus on the recent progress of responsive materials in the petroleum industry due to our specific interests.

Major challenges of applying responsive materials to the petroleum industry include the difficulty in materials preparation, the complicity of operating conditions, and economic efficiency. Responsive materials are typically difficult to synthesis or expensive, either of which restricts their potentials in large-scale applications. Besides, it is also essential to choose an appropriate trigger for the activation of responsive behavior, which should be economically and environmentally favorable.

2.2.1 Switchable interfacial activity

Controlling interfacial activity is of critical importance to various operations in the petroleum industry [1]. The introduction of interfacial activity could efficiently decrease the oil-water interfacial tension (IFT), reducing the capillary pressure in porous media, and alter the wettability of reservoir solids. Petroleum oil often contains various natural surfactants, e.g., naphthenic acids, asphaltenes, and resins. Besides, amphiphilic molecules such as surfactants, polymers, or particles could also be added to provide the desired interfacial activity. However, strong interfacial activity is problematic to the oil-water separation, which would lead to detrimental impacts on heavy oil harvesting and upgrading, as well as dramatically increase the quantity of tailings water. Typical strategies to alleviate the interfacial problem involve the optimization of surfactant dosage but with compromised performance, the addition of a secondary processing aid (e.g., demulsifiers), or the application of physical forces (e.g., centrifugation or electrical field). The concept of switchable interfacial activity is to permit precise modulation of the interface through responsive materials, and thereby overcome the technical difficulties as mentioned above.

2.2.1.1 Switchable surfactants

Surfactants are widely used to decrease the oil-water IFT. Recent developments of conventional surfactants in the petroleum industry have been reviewed in detail [2, 3]. With the comprehensive understanding of interfacial science, surfactants with switchable interfacial activity have been considered as the next generation processing aid. Lu et al. reported pseudo-Gemini surfactants with CO₂ switchability that were easily synthesized by diamines and fatty acids [4]. These surfactants were capable of facilitating the bitumen liberation from sand grains, as well as promoting oil-water separation after CO₂ bubbling (Figure 2.2). The same group also developed a series of CO₂-responsive surfactants with easy-tunable switching pH, such that the concept could be expanded to various operating conditions [5, 6].

Responsive surfactants were also developed to transport heavy oil in pipelines. Heavy oil transportation in pipelines is usually accompanied by significant difficulties, including paraffin precipitations, instability of asphaltenes, multiphase flow, clogging, and corruptions [7]. These phenomena could be even worse for the heavy oil with low API (American Petroleum Institute gravity) and high viscosity ($> 10^3$ mPa·s). In efforts to alleviate such situations, Lu and his coworkers investigated CO₂ switchable emulsions to improve the heavy oil flows in hydro-transportation [8, 9]. At the end of the pipelines, CO₂ gas was bubbled to release the heavy oil in emulsions, whereas the aqueous phase could be recycled.

Microemulsions stabilized by responsive surfactants have recently gained numerous interests as a novel technique to assist surfactant flooding enhanced oil recovery (EOR) process [10, 11]. Microemulsions are transparent, thermodynamically stable emulsions have droplet sized smaller than 100 nm [12-14]. Microemulsions feature high oil capacity, thereby are capable of carrying a

decent amount of crude oil from the reservoir through washing. The responsive characters then allow oil products to be separated from the emulsions. Brown et al. developed CO₂-responsive microemulsions based on reactive ionic liquids, which was proposed as the replacement to conventional cleaning agents and emulsifiers [15, 16]. A few CO₂-responsive microemulsion systems were also reported for broad aspects of applications, such as oil recovery, contaminated soil remediation, and drilling fluids recovery [17-19]. However, researchers are still challenging the robustness of microemulsions in porous media [14], which is critical to the petroleum industry.

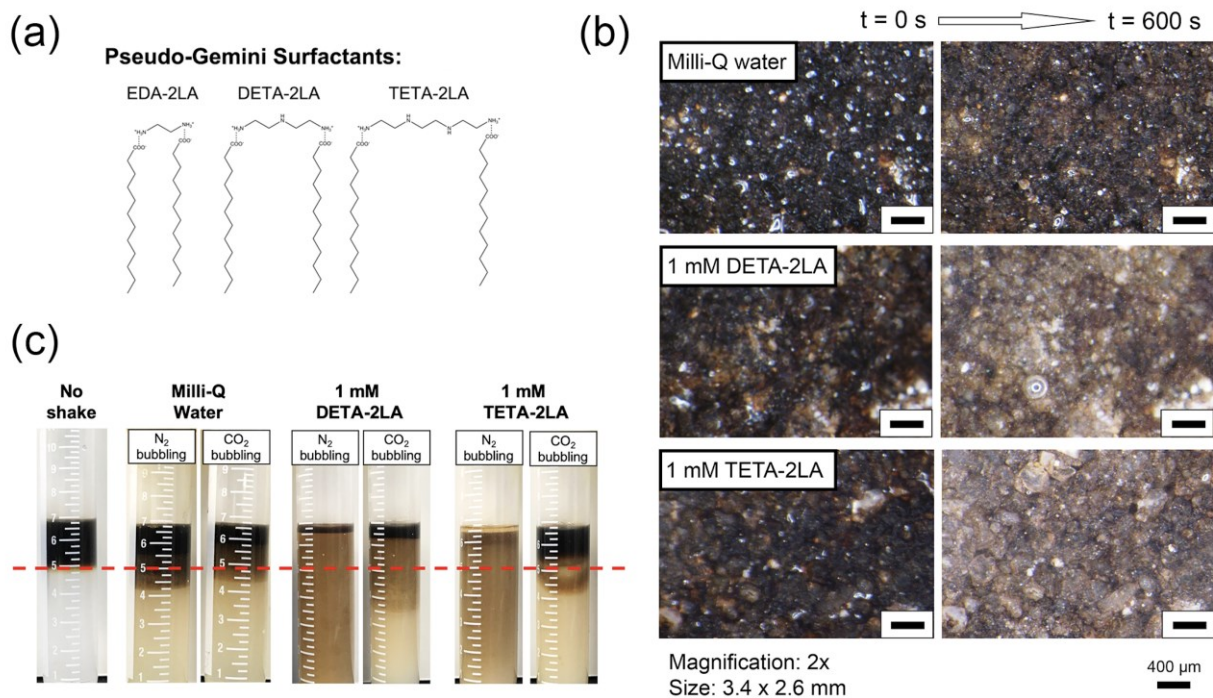


Figure 2.2. (a) Molecular structure of pseudo-Gemini surfactants; (b) Enhancement of bitumen liberation by introducing interfacial activity; and (c) Enhancement of oil-water separation by activating CO₂ switchability. (Modified from ref. [4])

2.2.1.2 Switchable polymeric surfactants

Polymers have been extensively studied as processing aids to the EOR application for decades [20, 21]. They could serve as the interfacial modifiers and the fluid viscosifiers. In this section, we focus on the responsive polymeric surfactants that majorly influence the interfacial properties. Polymeric viscosifiers will be reviewed in the following section.

There are several attempts being made to develop thermo-responsive polymeric surfactants for the oil sands extraction process [22-24]. It is known that thermo-responsive polymers exhibit coil-globule transition as the environment temperature increases above its lower critical solution temperature (LCST) [25], where they transform from water-soluble to water-insoluble. Hence, polymeric surfactants could be designed as the block copolymer that is composed of a thermal-responsive block and another balancing block. The interfacial activity of polymeric surfactants becomes switchable when the thermo-responsive block performs its LCST transition behavior, which breaks the natural amphiphilicity balance. The proposed concept of thermo-responsive polymeric surfactants is shown in Figure 2.3 [24]. Although these approaches are of great scientific importance, as well as open avenues for responsive materials, the use of thermal response is economically unfavorable because of the enormous energy consumption to change bulk temperature, especially when considering the large scale of oil sands industry. Besides, the costs for precise copolymerization are often expensive as well.

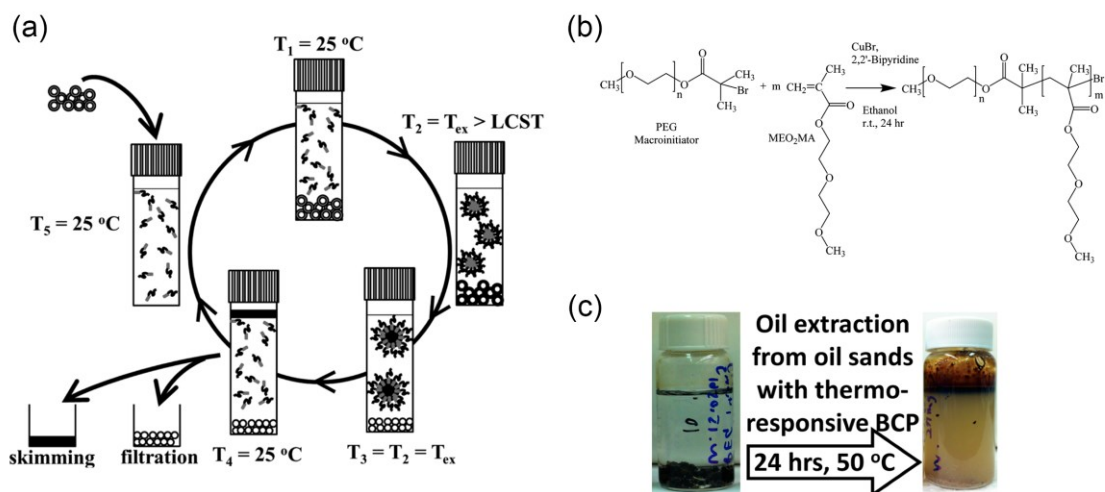


Figure 2.3. (a) Proposed concept of polymeric surfactants enhancing bitumen recovery in oil sands extraction; (b) Polymerization the thermal-responsive polymeric surfactant; and (c) Bottle tests of oil sands extraction. (Modified from ref. [24])

2.2.1.3 Switchable particles

Over the past years, there are numerous researches showing the potential of particles in the petroleum industry, including exploration, drilling, production, and refinery. Particles could be designed as the *in-situ* sensing materials to estimate the reservoir temperature/pressure [26], map the real-time oil reservoir evolution [27], and detect the waterfront of displacing fluid [28, 29]. Particles with interfacial activity were also reported to stabilize oil-in-water emulsions [30] or soften rigid films caused by asphaltenes [31, 32]. In the upstream operations, particles were explored to serve as catalysts [33] or reduce the fouling effect [34]. Indeed, particle characterization and modification have been considered as the frontier technology to the future industry.

Stimuli-responsive particles have also been studied extensively in the past decade. Particles could respond to the external change either according to the surface characters of solid cores (e.g., graphene oxide response to bulk pH [35]), or by grafting functional groups. Tang et al. summarized the current development of stimuli-responsive particles, as well as their potential applications [36]. However, there are still a few reports about the stimuli-responsive particles in the petroleum industry. Wang and coworkers reported pH-responsive magnetic nanoparticles (MNPs) for efficient emulsification of crude oil-in-water and facile oil-water separation (Figure 2.4) [37]. He et al. further improved the concept by synthesizing Janus particles with magnetic responsiveness [31]. Besides, Tang proposed pH-responsive particles based on cellulose nanoparticles for heavy oil harvesting, of which the system is surfactant-free and biocompatible [38].

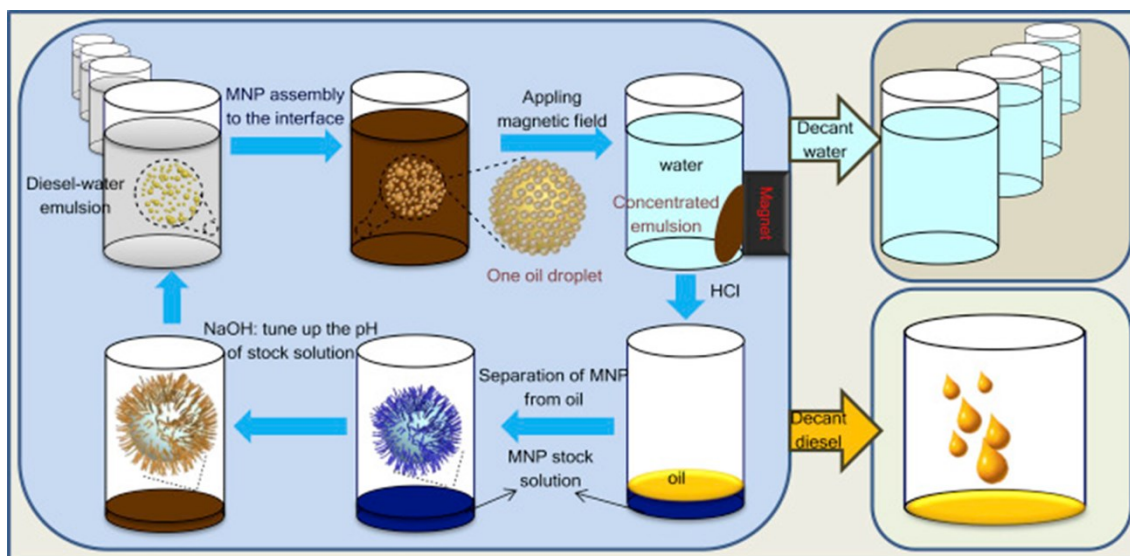


Figure 2.4. Application of pH-responsive magnetic nanoparticles (MNPs) as recyclable stabilizers for oil-water separation [37].

One of the biggest obstacles of applying responsive particles in the petroleum industry is their behaviors in the complex reservoir conditions. In the EOR process, for example, several

mechanisms have been proposed for the particles enhancing heavy oil liberation, including wettability alternation, IFT reduction, and disjoining pressure. The presence of particles also decreases the oil-water IFT, which is essential to the liberation of heavy oil from solids [39]. On the other hand, particles are capable of altering the surface wettability by adsorbing onto the solid surface (coating mechanism) and removing the original adsorbed molecules (cleaning mechanism), as proposed by Hammond and Unsal [40]. Al-Ansari et al. investigated the calcite surfaces by atomic force microscopy (AFM) before and after the nanoparticle flooding treatment [41]. Experimental images clearly indicated that particles had a dramatic influence on the surface morphology (Figure 2.5). In addition, the spreading of nanoparticles on the solid surface is a complicated phenomenon. It is commonly accepted that a wedge-film would be formed at the oil-water-solid three-phase contact line (Figure 2.6) [42, 43]. Such phenomena could build up disjoining pressure up to 5×10^4 Pa in the vertex region, facilitating the oil-solid separation and allowing the fluid to spread further [43, 44].

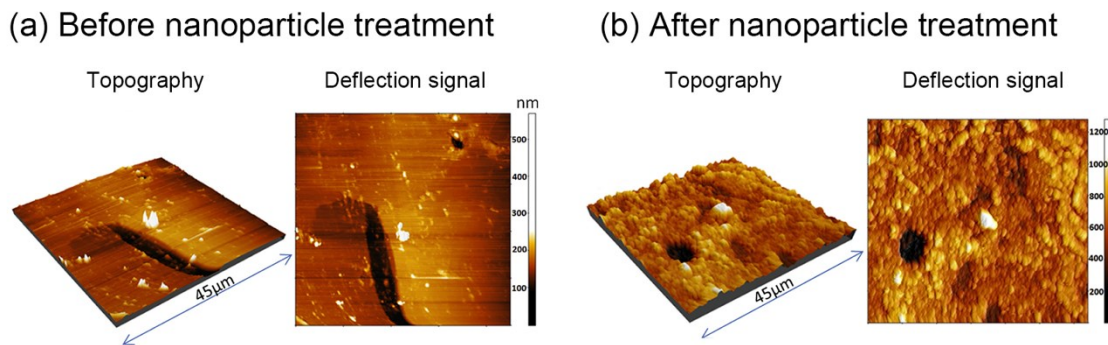


Figure 2.5. Topography picture of calcite surfaces before (top) and after (bottom) nanoparticle treatment. (Modified from ref. [41])

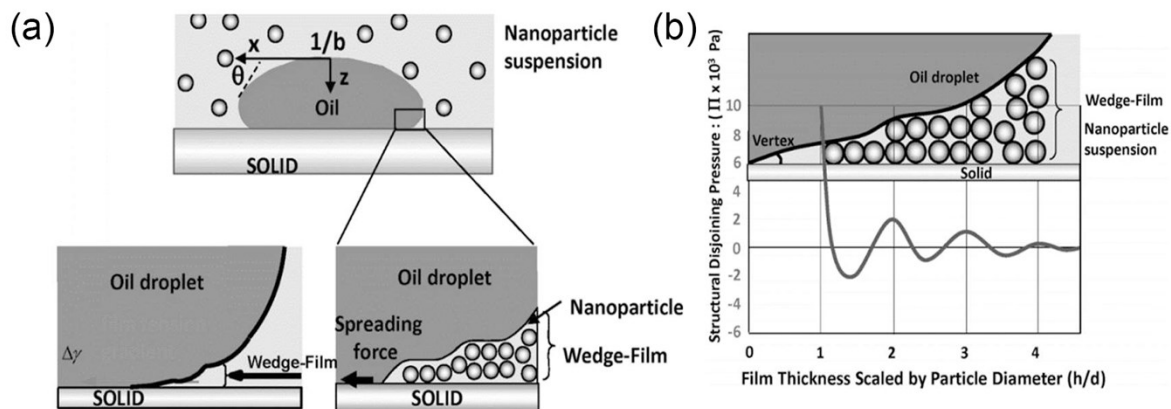


Figure 2.6. (a) Wedge-shaped nanoparticle structure and forces; and (b) Wedge contact pressure [44].

2.2.2 Switchable solvent

Solvent extraction is a promising technique to extract heavy oil from unconventional petroleum reservoir due to its low operating temperature, high extraction rate, and universal applicability. However, traditional solvents are usually challenged by the costs of solvent recovery and the inevitable solvent loss [45]. More recently, solvents with switchable polarity had been exploited as a green substitution to the traditional solvents. Switchable solvents are non-ionic liquids (low polarity, hydrophobic) that can convert to ionic liquid (high polarity, hydrophilic) when exposing to the external stimuli [46, 47]. To the best of our knowledge, switchable solvents mostly respond to CO_2/N_2 gas. Their nature as ionic liquids features low volatility, whereas their switchable character permits efficient recycling of the solvents.

Switchable solvents could be introduced in their non-ionic form to dissolve hydrocarbon resources, and then switch to ionic form to separate the high-quality petroleum product and recycle the solvent. Holland et al. first investigated the use of a switchable hydrophilic solvent (SHS) for

enhancing bitumen recovery from oil sands [48]. Their proposed process is illustrated in Figure 2.7, where cyclohexyldimethylamine (CyNMe₂) exhibits reversible CO₂ switchability. It is worth mentioning that water was not involved in the bitumen extraction, until being used for the recycle of switchable solvents. Similar strategies have been applied to various non-conventional petroleum resources, and the recovery ratio is typically higher than 90 % [48-50]. In addition, SHS had also been demonstrated to weaken the asphaltene self-association interactions and reduce the size of asphaltene aggregations [51], which exhibit further implications for the upgraders.

Solvent loss is still the biggest obstacle for commercializing the switchable solvent from the perspectives of both the petroleum industry and environmental regulators. Although the switchable solvents are proposed with a straightforward recovery method, the recovery ratio of SHS still could not meet the requirements to the best of our knowledge. Holland et al. indicated that the best method applied resulted in a solvent loss of 0.06 g CyNMe₂ per gram of solvent-free bitumen [48]. Merchan-Arenas reported that only 54 - 60 % of the SHS (*N,N*-dimethyl-cyclohexylamine, DMCHA) could be recycled and reinjected into the extraction process [49]. These issues were caused by the insufficient protonation/deprotonation during the CO₂ switching process, which led to incomplete phase separation. Besides, bitumen with high viscosity is also considered as a potential hindrance to the recovery of the switchable solvent due to its low mobility [45].

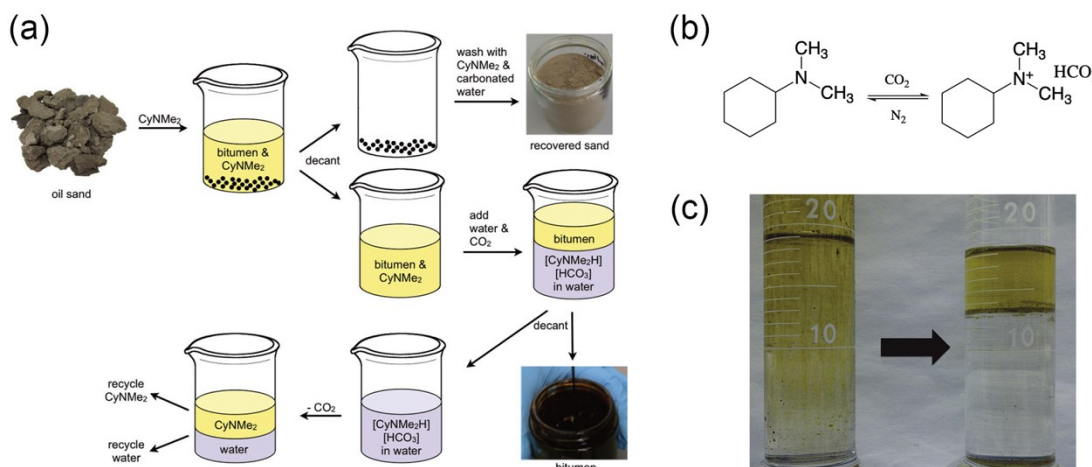


Figure 2.7. (a) Proposed process of switchable hydrophilicity solvent (SHS) introduced as the non-ionic liquid for the bitumen recovery from oil sands; (b) Mechanism of the CO₂ switching solvent; and (c) The mixture of carbonated water and CyNMe₂ after the bitumen has been decanted (left) and the same mixture after the CO₂ has been removed (right). (Modified from ref. [48])

Switchable solvents could also be introduced in their ionic form, typically in combination with the aqueous phase, where they serve as both the solvent and the interfacial modifier. Sui et al. used switchable-hydrophilicity tertiary amine (SHTA) in recovering heavy hydrocarbon from oil sands [52]. A general illustration of the extraction process is shown in Figure 2.8. A cosolvent (toluene) was added to further reduced the bitumen viscosity. It was addressed that the improvement of processability should be attributed to the formation of ion pairs at the bitumen surfaces, which inhibited the bitumen-solid interactions. The same group later claimed a similar approach using a CO₂ switchable solvent with diamine structure (*N,N,N',N'*-tetraethyl-1,3-propanediamine, TEPDA), but in the absence of the cosolvent [53].

Applying switchable solvents in their ionic forms has been demonstrated with the promising recyclability as well as the significant reduction in solid entrainment. Switchable solvents combined with the aqueous phase could be recycled for at least four times and only exhibited a slight decrease in the extraction efficiency [52, 53]. Besides, Li et al. emphasized that both the solid entrainment in the oil product and the solvent loss to solid wastes were sharply reduced (more than 50 %) in comparison with those without water addition [53]. Once again, such a phenomenon should be attributed to the decreased interaction between bitumen and solid. However, the physical and chemical properties of the solid surface are often location-dependent according to the origin and geological characters of the petroleum reservoir. Since the approach of combining switchable solvent with water is highly dependent on the replacement of bitumen-solid interactions by bitumen-solvent ion pairs, this strategy might be affected by the solid properties, as well as the affinity between bitumen and switchable solvent. Hence, it may not be as universally applicable as the non-ionic switchable solvent extraction. Nevertheless, further exploration is definitely needed to investigate the feasibility of switchable solvents in various petroleum resources.

2.2.3 Switchable viscosity

The viscosity of the displacing fluid is of critical importance to the EOR process. When displacing the original crude oil by *in-situ* waterflooding, it is commonly seen that water fluids flow much faster than the oil phase due to the viscosity differences, leaving most of the oil products behind without efficient recovery. This phenomenon is known as the viscous fingering (Figure 2.9a), which dramatically influences the *in-situ* flow behavior and typically causes negative impacts on the recovery ratio [54, 55]. In efforts to prohibit the viscous fingering, the conventional approach is to increase the viscosity of the displacing fluid and to match that of the interacting fluid to form a uniform interface [56, 57]. Polymer-assisted flooding has been reported with good performances

in the reservoirs with oil viscosity between 10 to 150 mPa·s [57-59]. However, the upper limit of oil viscosity is subjected to injection difficulties. Since the aqueous displacing fluid is needed to contain a comparable viscosity as the target crude oil, tremendous efforts are demanded to pump in these highly viscous solutions.

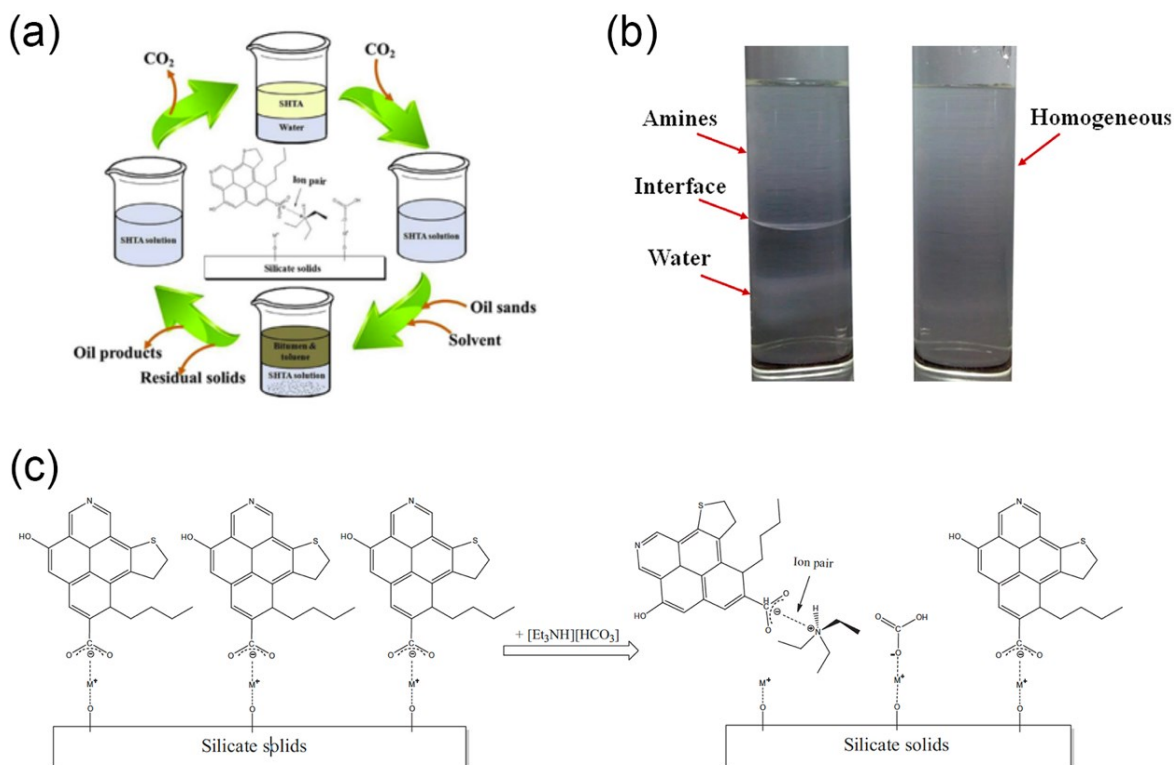


Figure 2.8. (a) Switchable solvent introduced as ionic liquid for the enhancement of oil sands extraction; (b) Amine-water system before CO₂ injection (left) and forming homogeneous solution after CO₂ injection (right); and (c) Mechanism of switchable solvent enhancing aqueous-nonaqueous hybrid oil sands extraction. (Modified from ref. [52])

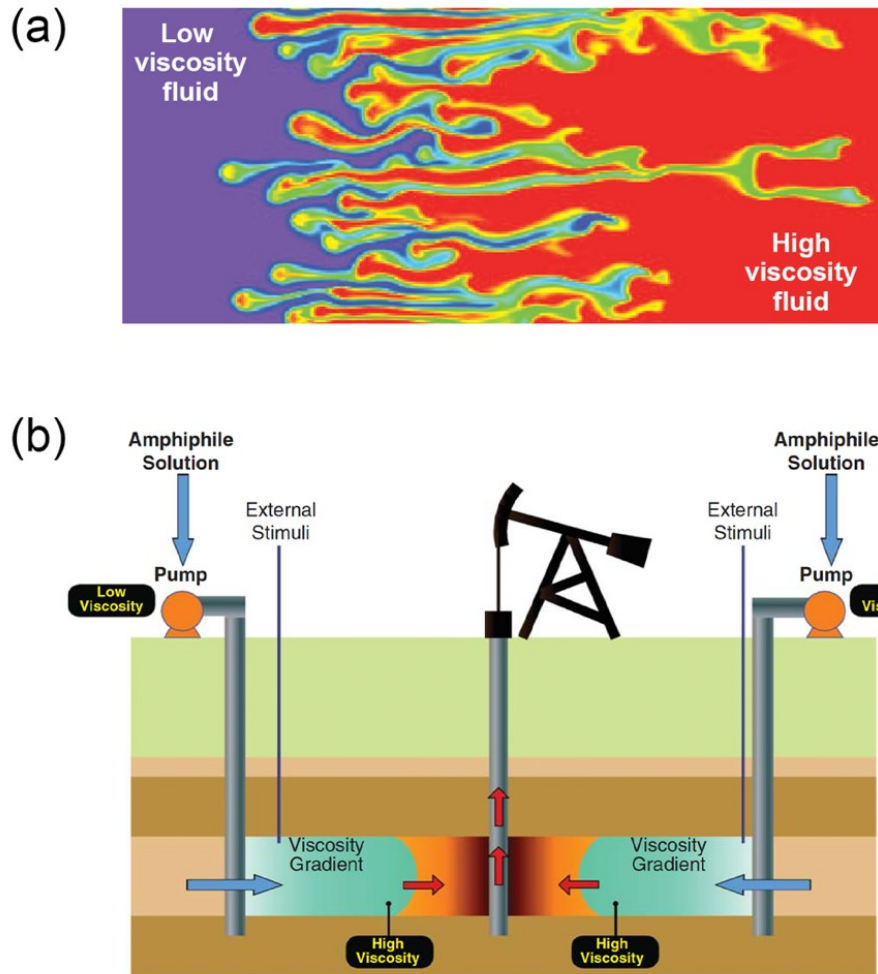


Figure 2.9. (a) Simulated viscous fingering in a porous media flow (Modified from ref. [55]); and (b) Illustration of using the pH-responsive amphiphilic system as displacing fluid in EOR [57].

Displacing fluids containing responsive viscosifiers could be designed with the easy-to-flow property during the pump-in stage, while also capable of depositing high viscosity explicitly in the oil-rich regions. The concept is schematically illustrated in Figure 2.9b. External stimuli are introduced *in situ* to trigger the increase of fluid viscosity, such that the fingering effect could be diminished, and the oil recovery is enhanced. There are several attempts to prove this novel

concept using responsive polymers or responsive self-assemblies. However, the current development of switchable viscous fluids in EOR is still facing numerous challenges, including the choice of proper stimuli, complicated *in situ* environment, high salinity and high temperature operating conditions, and the loss of viscosifier due to the adsorption.

2.2.3.1 Responsive polymeric viscosifier

Polymers are the most widely used viscosifier to thicken the displacing fluid in EOR. For example, the aqueous solution of polyacrylamide (PAM) or its derivatives has been studied for decades as effective additives to enhance the oil recovery [60]. Despite the pumping difficulties for highly viscous polymer solutions as mentioned, conventional polymers also suffer from thermal-thinning properties and salt-screening effect, i.e., reduced viscosity at high temperature and high salinity conditions. Both factors further impede their applications in harsh EOR operating conditions.

Thermoviscosifying polymers (TVPs) are a special type of polymer, of which the solution viscosity exhibits an increase when the temperature rises above their corresponding critical associating temperature (CAT). Hourdet and his coworkers recognized the thermoviscosifying behaviors when grafting side chains with LCST behavior onto a water-soluble polymer backbone [61-63]. Micro-domains were thereby generated at high temperatures, which interact with each other through hydrophobic interaction and increase solution viscosity by entanglement (Figure 2.10a). In the past decade, TVPs have been extensively investigated as promising additives to enhance the oil recovery from hot petroleum reservoirs since their thermal-responsive behaviors correspond well with the demands in EOR. Feng's group developed a series of TVPs for EOR applications from laboratory demonstrations to pilot-scale implementations [64-66]. Similar concepts were also conducted by other groups using various types of TVPs and under different

reservoir conditions [67-70]. It was demonstrated that TVPs exhibited better sweep efficiencies and mobility controls in the core flooding tests if compared with the conventional PAM addition (Figure 2.10b & 2.10c). Correspondingly, TVP solutions resulted in higher increment in the oil recovery factor after water flooding (16.4 % at 45 °C and 15.5 % at 85 °C), whereas the increment of recovery factor by PAM solutions decreased at elevated temperature (12.0 % at 45 °C and 9.20 % at 85 °C) [66]. In general, TVPs have great potentials to be utilized in EOR, especially for reservoirs with high temperatures and high salinity. More interestingly, the thermoviscosifying behavior could even be largely enhanced with increasing salt concentration, suggesting the good salinity tolerance of TVPs in EOR operation [71]. Li et al. utilized such salt-responsive phenomena and successfully developed the viscosifying polymer for fracturing shale oil reservoirs [72].

The thickening of polymer solution could also be achieved by introducing pH-responsive moieties. It is known that polyelectrolytes with more than one charged group changes their conformation at different pH conditions, thereby affecting the solution viscosity. Typically, polyanions experience high viscosity at high pH and low viscosity at low pH, whereas polycations exhibit the opposite [20, 73]. Tam and coworkers designed pH-responsive polyelectrolytes with a comb-like structure, comprising of a random copolymer of methacrylic acid (MAA), ethyl acrylate (EA), and hydrophobically modified macromonomers (Figure 2.11a) [74, 75]. These polymer latexes exhibit swelling behavior at high pH conditions and significantly increase the solution viscosity. Araujo et al. demonstrated that the exceptional thickening capability of comb-like polyelectrolytes is the combination of electrostatic repulsion, intra-/inter-molecular association, and EA block association (Figure 2.11b) [76]. However, to the best of our knowledge, pH-responsive polymers as “smart” viscosifier were not explored as extensively as the TVPs in EOR applications due to several technical difficulties. The presence of dissolved ions would greatly reduce the viscosity of

polyelectrolyte solutions due to the screening of charges (Figure 2.11c) [75]. The local mechanical stress also affects the formation of the polymer network, concerning the polymer performance when bypassing the porous medium in the petroleum reservoir [77]. Besides, the interaction between charged polyelectrolytes and natural surfactants have a pronounced influence on the thickening effect [20, 78].

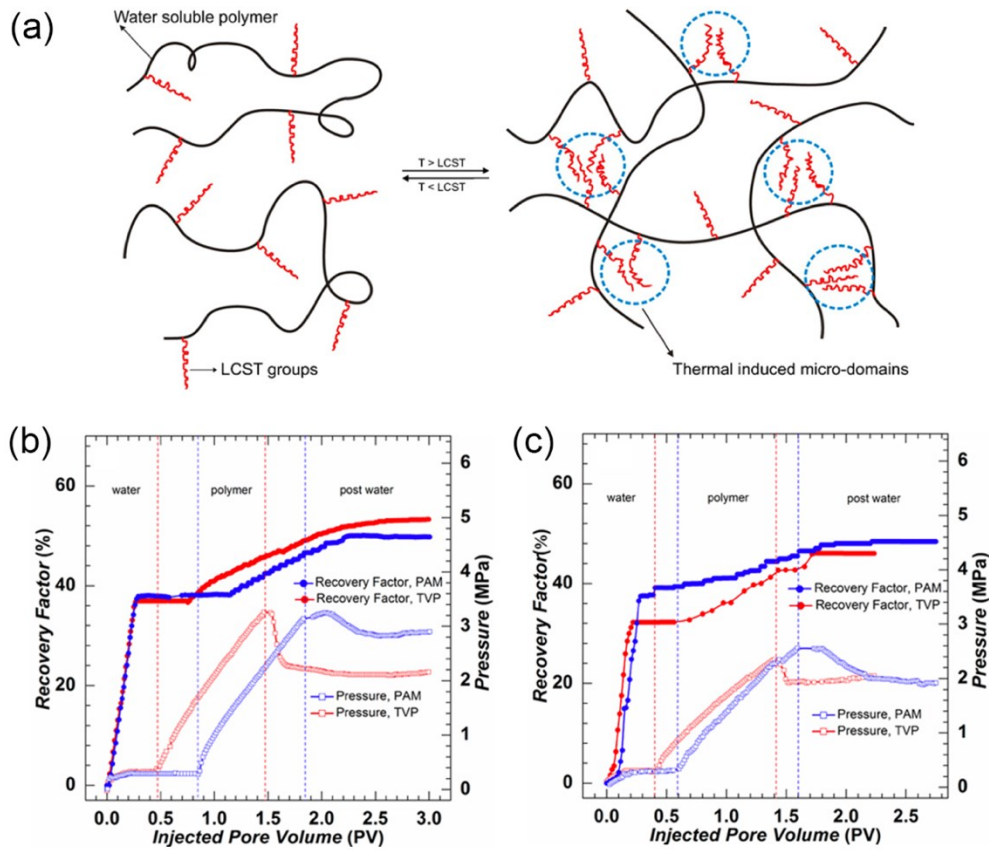


Figure 2.10. (a) Mechanisms of thermoviscosifying behavior (Modified from ref. [63]); Recovery factors and flooding pressures using PAM or TVPs in core flooding tests at (b) 45 °C and (c) 85 °C. ($C_{\text{polymer}} = 0.2 \text{ wt.}\%$; Total dissolved solids = 101,000 mg/L; Injected rate = 2 mL/min). (Modified from ref. [66])

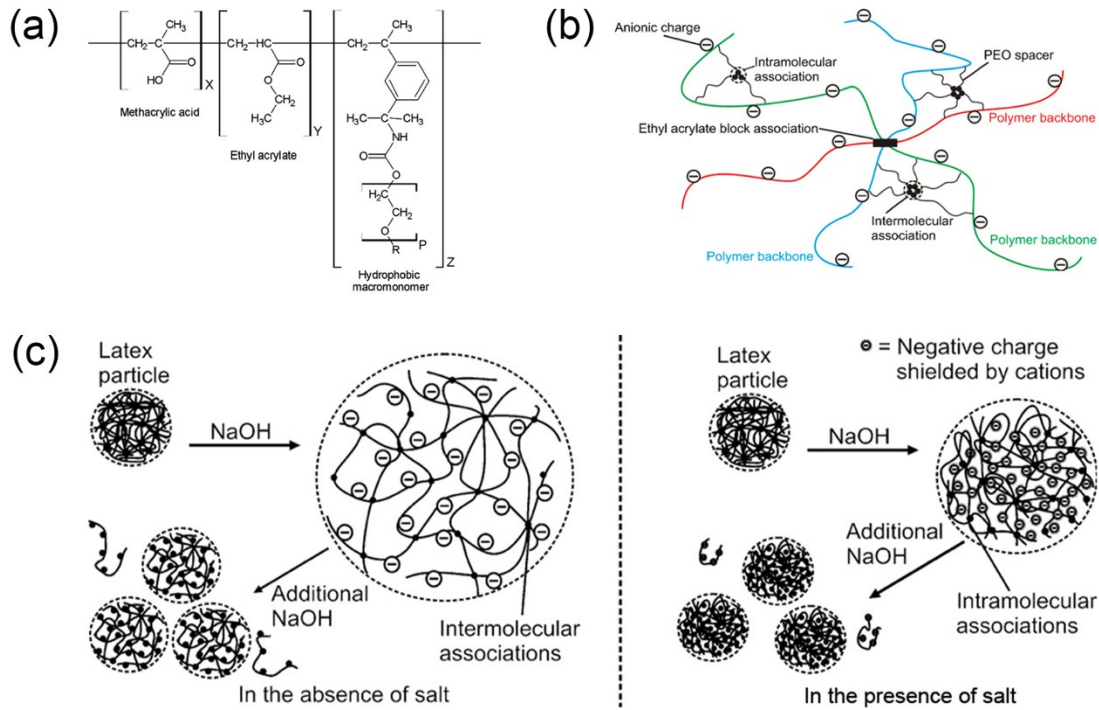


Figure 2.11. (a) Typical pH-responsive polyelectrolytes with a comb-like structure [74]; (b) Intra-/Inter-molecular interactions for the thickening effect of polyelectrolytes at the high pH condition [76]; and (c) Dissolution and switching mechanism of polyelectrolytes in the absence and in the presence of salt [75].

There are also several attempts to develop responsive polymeric viscosifiers for EOR applications despite thermal- and pH- responses. Philippova and Khokhlov reported “water-responsive” polymers that could find the water influx by itself and block the unwanted flows of displacing fluids [79]. Zhong et al. proposed a novel associative polymer with a good salt-thickening effect, that also exhibits heat-thickening and shear thickening properties at low shear stress [80]. Zhang and coworkers developed self-adaptive polymers that automatic response to the applied stress [81]. When flowing through the converging sections of the porous medium, polymer aggregations disassembled due to the local shear and elongated force, helping the displacing fluid enter the pore

throat regions. In the diverging area, polymers regain intermolecular interactions and reinforce the solution viscosity. Further investigations are needed to assess the viability and feasibility of these novel responsive polymers.

2.2.3.2 Responsive self-assembled viscosifier

Self-assembly structures are also promising candidates to construct responsive viscosifiers in the aqueous solution. Worm-like micelles (WLMs) are the elongated flexible self-assemblies formed by the aggregation of amphiphiles [82], which exhibit remarkable viscoelastic properties above threshold concentrations. Moreover, the dynamic structures of WLMs could be influenced by external conditions (stimuli), whereas such morphology changes are usually reversible. Akbulut and his coworkers reported the use of the pH-responsive amphiphilic system in EOR [57]. WLMs were assembled by the combination of an amino amide (*N*-oleicamidopropyl-*N,N*-dimethylamine) and maleic acid (Figure 2.12a), which could increase its viscosity 12 times by changing the pH from 4 to 8 in a reversible manner (Figure 2.12b). WLMs were proved to be effective as the displacing fluid in column experiments (Figure 2.12c). The same group also proposed a similar approach using a thermal-responsive amphiphile with WLMs formation as well as good salinity tolerance [83]. Since the *in-situ* EOR is usually operated at the elevated temperature, responsive amphiphiles could be injected on the ground at ambient temperature and self-adapted to high viscosity according to the environment temperature.

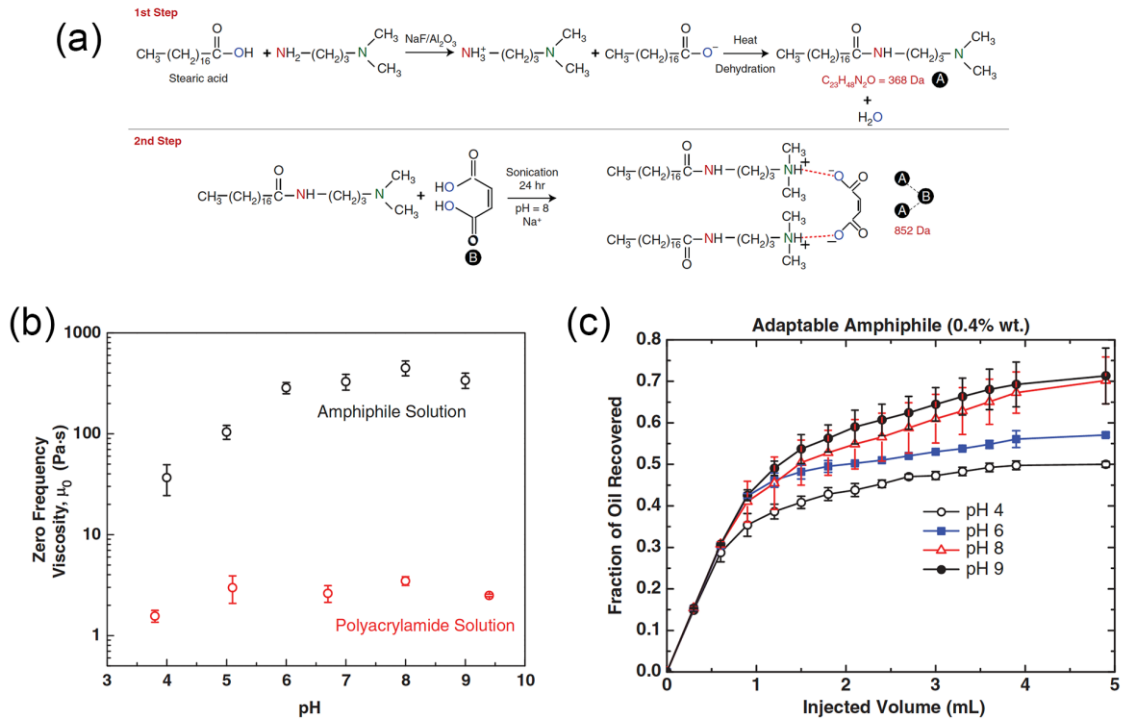


Figure 2.12. (a) Two-step synthesis protocol for the preparation of pH-responsive amphiphiles; (b) Effect of solution pH on the viscosity of amphiphile solution; and (c) Fraction of oil recovered using the amphiphile at different pH values. (Modified from ref. [57])

In the petroleum reservoirs with ultra-low permeability, the EOR process using CO₂ flooding (CO₂-EOR) is one of the most promising techniques to improve sweep efficiency. However, the high mobility of CO₂ and the reservoir heterogeneity are considered to be the two major issues needed to be tackled [84]. CO₂ has low density and high mobility. Thereby, they tend to migrate either upward to the top of the reservoir or sideways to the regions with relatively higher permeability, both of which could be prevented by controlling system viscosity. Since CO₂ gas is already involved in the process, it is quite intuitive to design a CO₂-responsive viscosifier to alleviate the above-mentioned concerns. Li et al. investigated the use of CO₂-responsive chemical (*N*-erucamidopropyl-*N,N*-dimethylamine) for mobility control in the CO₂-EOR process using

water-alternating-gas (WAG) injection [85]. During the WAG process (Figure 2.13a), water and gas (CO₂) are injected into the wellbore alternatively, which provides a natural platform for the responsive viscosifier to be switched reversibly. In the ideal scenario, the fluid viscosity maintains a low value before the contact with CO₂ and exhibits a sharp increase by forming WLMs structures after the contact with CO₂. Later on, the same group further improved the concept by screening more CO₂-responsive compounds at high temperature, high pressure, and high salinity conditions, which simulates the *in situ* operation [86]. It was demonstrated that the long-chain polyamine, ODPTA (octadecyl dipropylene triamine), displayed promising mobility control capability in the sand-pack flooding experiments in comparison with conventional surfactants (Figure 2.13b). More importantly, ODPTA exhibited extraordinary CO₂ foaming capability at high temperature (160 °C), high pressure (7.8 MPa), and high salinity (200,000 ppm with 1000 ppm Ca²⁺). Similarly, Zhang et al. screened five kinds of chemicals with various CO₂-responsive groups for the CO₂-EOR process combined with hydraulic fracturing [87]. Yang and his coworkers also claimed that CO₂-responsive WLMs formed by the combination of sodium dodecyl sulfate (SDS) and diethylenetriamine (DETA) could enhance CO₂ flooding [88]. In general, switching the fluid viscosity *in situ* has a significant impact on improving the oil recovery and broadening the reservoir processability. WLMs that contain CO₂-responsive moieties are believed to have a good affinity with the CO₂-EOR process.

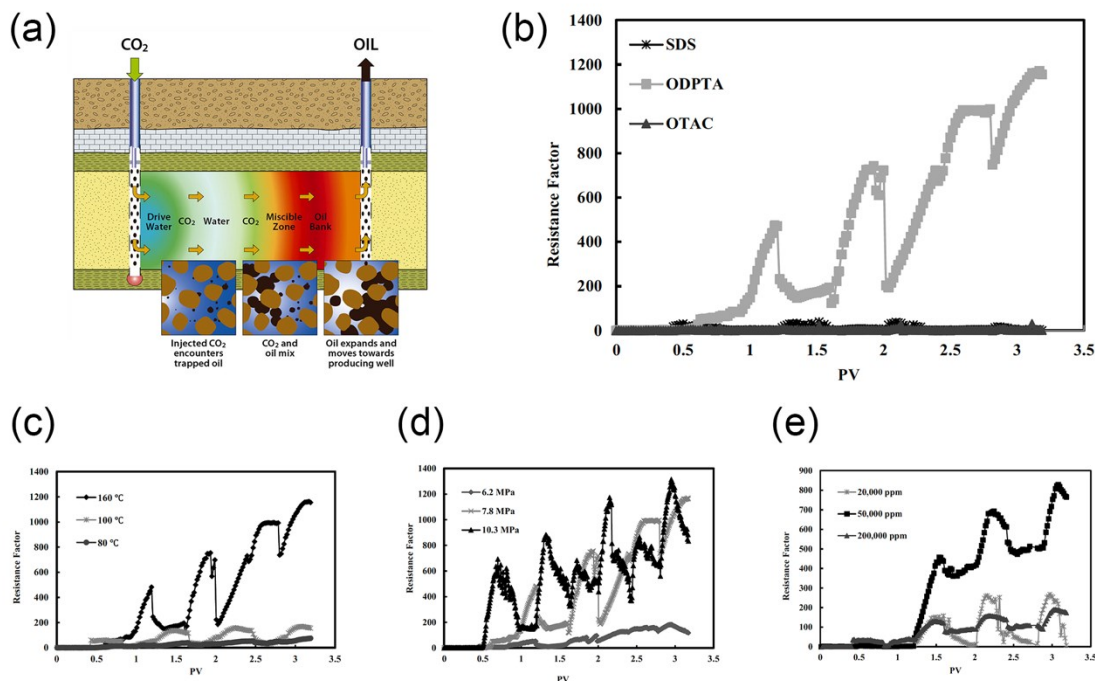


Figure 2.13. (a) Illustration of CO₂-EOR process using WAG injection technique; (b) Comparison of the effect of CO₂-responsive compound (octadecyl dipropylene triamine, ODPTA) with conventional surfactants, such as sodium dodecyl sulfate (SDS) and octadecyl dimethyl ammonium chloride (OTAC); The performance of ODPTA was further investigated by the effect of temperature at 7.8 MPa (c), the effect of pressure at 160 °C (d), and the effect of salinity at 7.8 MPa and 160 °C (e). (Figure a was modified from ref. [89], while Figures b-e was modified from ref. [86])

Although numerous responsive WLMs had been reported in various petroleum applications, as discussed above, there are still concerns about the feasibility of WLMs assemblies in harsh EOR operating conditions. Compared to polymers, WLMs feature dynamic assembly properties through non-covalent interactions. Such characters enable easy design of the responsive behavior but also result in difficulties in maintaining stable properties upon the disruption from environmental

changes. The viscoelastic property of WLMs solutions could be significantly reduced in the presence of light crude oil due to the transformation from WLMs to spherical micelles [90, 91]. Hence, it would be more suitable to apply responsive WLMs to the petroleum reservoir with heavy or ultra-heavy oil. Besides, there is still a lack of evidence whether WLMs would remain their entangled structures when passing through the porous medium. The mechanical strength of WLMs might be challenged by the pore throats, where the local radius becomes extremely small. To alleviate such concern, Zhu et al. reported that the addition of a pre-flush slug or post-flush of polymer (partially hydrolyzed polyacrylamide, HPAM) would remarkably increase the oil recovery factor from WLMs-assisted process [92]. To the best of our knowledge, however, there is no further investigation of this system in the responsive WLMs systems. Furthermore, economic efficiency is perhaps the most significant limitation to commercialize WLMs in EOR applications. The formation of WLMs requires the high concentration of the amphiphiles, typically above 4 wt.% [3], which is not viability in large-scale circumstances. In addition to high chemical dosage, the adsorption onto the solid surfaces could further consume the amphiphiles, leading to less efficiency of WLMs formation, lower fluid viscosity, even the transformation from WLMs to spherical micelles [90]. There are emerging demands to develop the building blocks for WLMs with weak adsorption characters. Despite the challenges in current technology, we still believe that responsive WLMs still provide great opportunities to the EOR applications.

2.2.4 References

1. He, L., et al., *Interfacial sciences in unconventional petroleum production: from fundamentals to applications*. Chemical Society Reviews, 2015. **44**(15): p. 5446-94.
2. Negin, C., S. Ali, and Q. Xie, *Most common surfactants employed in chemical enhanced oil recovery*. Petroleum, 2017. **3**(2): p. 197-211.
3. Sun, L., et al., *Recent advances of surfactant-stabilized N₂/CO₂ foams in enhanced oil recovery*. Fuel, 2019. **241**: p. 83-93.

4. Lu, Y., et al., *Pseudo-gemini biosurfactants with CO₂ switchability for enhanced oil recovery (EOR)*. Tenside Surfactants Detergents, 2019. **56**(5): p. 407-416.
5. Lu, Y., et al., *CO₂-responsive surfactants with tunable switching pH*. Journal of Colloid and Interface Science, 2019. **557**: p. 185-195.
6. Lu, Y., et al. *Controlling interfacial property through cost-efficient, CO₂-responsive assemblies for the enhancement of bitumen recovery*. in *Abstracts of papers of the American Chemical Society*. 2019. Orlando: American Chemical Society, 1155 16th st, NW, Washington, DC 20036 USA.
7. Ashrafzadeh, S. and M. Kamran, *Emulsification of heavy crude oil in water for pipeline transportation*. Journal of Petroleum Science and Engineering, 2010. **71**(3-4): p. 205-211.
8. Lu, H.S., et al., *Application of CO₂-triggered switchable surfactants to form emulsion with XinJiang heavy oil*. Journal of Dispersion Science and Technology, 2014. **35**(5): p. 655-662.
9. Lu, H.S., et al., *CO₂-switchable oil/water emulsion for pipeline transport of heavy oil*. Journal of Surfactants and Detergents, 2015. **18**(5): p. 773-782.
10. Nazar, M.F., S.S. Shah, and M.A. Khosa, *Microemulsions in enhanced oil recovery: a review*. Petroleum Science and Technology, 2011. **29**(13): p. 1353-1365.
11. Tagavifar, M., *Microemulsion viscosity and its implications for chemical EOR: Experimental results and a model*. 2015, The University of Texas at Austin: Research Showcase in Petroleum and Geosystems.
12. De Gennes, P.G. and C. Taupin, *Microemulsions and the flexibility of oil/water interfaces*. The Journal of Physical Chemistry, 1982. **86**(13): p. 2294-2304.
13. Cates, M.E., et al., *Theory of microemulsions: comparison with experimental behavior*. Langmuir, 1988. **4**(4): p. 802-806.
14. Perazzo, A., et al., *Emulsions in porous media: From single droplet behavior to applications for oil recovery*. Advances in Colloid and Interface Science, 2018. **256**: p. 305-325.
15. Brown, P., et al., *CO₂-responsive microemulsions based on reactive ionic liquids*. Langmuir, 2014. **30**(15): p. 4267-4272.
16. Brown, P., et al., *CO₂-reactive ionic liquid surfactants for the control of colloidal morphology*. Langmuir, 2017. **33**(31): p. 7633-7641.
17. Zhang, Y., et al., *CO₂-Responsive microemulsion: Reversible switching from an apparent single phase to near-complete phase separation*. Green Chemistry, 2016. **18**(2): p. 392-396.
18. Chen, X., et al., *CO₂-responsive o/w microemulsions prepared using a switchable superamphiphile assembled by electrostatic interactions*. Journal of Colloid and Interface Science, 2019. **534**: p. 595-604.
19. Liu, D., et al., *Conversion of a surfactant-based microemulsion to a surfactant-free microemulsion by CO₂*. Soft Matter, 2019. **15**(3): p. 462-469.

20. Wever, D.A.Z., F. Picchioni, and A.A. Broekhuis, *Polymers for enhanced oil recovery: A paradigm for structure–property relationship in aqueous solution*. Progress in Polymer Science, 2011. **36**(11): p. 1558-1628.
21. Raffa, P., A.A. Broekhuis, and F. Picchioni, *Polymeric surfactants for enhanced oil recovery: A review*. Journal of Petroleum Science and Engineering, 2016. **145**: p. 723-733.
22. Long, J., et al., *Improving oil sands processability using a temperature-sensitive polymer*. Energy & Fuels, 2011. **25**(2): p. 701-707.
23. Han, C., *Design and synthesis of temperature switchable non-ionic block copolymers for application to oil sands extraction*. 2016, University of Alberta.
24. Yang, B. and J. Duhamel, *Extraction of oil from oil sands using thermoresponsive polymeric surfactants*. ACS Applied Materials & Interfaces, 2015. **7**(10): p. 5879-89.
25. Tiktopulo, E.I., et al., *Domain coil-globule transition in homopolymers*. Macromolecules, 1995. **28**(22): p. 7519-7524.
26. Jahagirdar, S.R., *Oil-microbe detection tool using nano optical fibers*, in *SPE Western Regional and Pacific Section AAPG Joint Meeting*. 2008, Society of Petroleum Engineers: Bakersfield, California, USA. p. 7.
27. Li, J. and M. Meyyappan, *Real time oil reservoir evaluation using nanotechnology*. Jan. 2011. U.S. Patent No. 7,875,455. 25
28. Al-shehri, A.A., et al., *Illuminating the reservoir: magnetic nanomappers*, in *SPE Middle East Oil and Gas Show and Conference*. 2013, Society of Petroleum Engineers: Manama, Bahrain. p. 10.
29. Rahmani, A.R., et al., *Crosswell magnetic sensing of superparamagnetic nanoparticles for subsurface applications*. SPE Journal, 2015. **20**(05): p. 1067-1082.
30. Suleimanov, B.A., F.S. Ismailov, and E.F. Veliyev, *Nanofluid for enhanced oil recovery*. Journal of Petroleum Science and Engineering, 2011. **78**(2): p. 431-437.
31. He, X., et al., *Magnetically responsive Janus nanoparticles synthesized using cellulosic materials for enhanced phase separation in oily wastewaters and water-in-crude oil emulsions*. Chemical Engineering Journal, 2019. **378**: p. 122045.
32. Ko, S., et al., *Accelerated oil droplet separation from produced water using magnetic nanoparticles*, in *SPE Annual Technical Conference and Exhibition*. 2014, Society of Petroleum Engineers: Amsterdam, The Netherlands. p. 14.
33. Mohajeri, A., et al., *Hydrodesulphurization nanocatalyst, its use and a process for its production*. 2010. U.S. Patent Application No. 12/629,835.
34. Sotto, A., et al., *Doping of polyethersulfone nanofiltration membranes: antifouling effect observed at ultralow concentrations of TiO₂ nanoparticles*. Journal of Materials Chemistry, 2011. **21**(28): p. 10311-10320.
35. Kim, J., et al., *Graphene oxide sheets at interfaces*. Journal of the American Chemical Society, 2010. **132**(23): p. 8180-8186.
36. Tang, J., P.J. Quinlan, and K.C. Tam, *Stimuli-responsive Pickering emulsions: recent advances and potential applications*. Soft Matter, 2015. **11**(18): p. 3512-3529.

37. Wang, X., et al., *Developing recyclable pH-responsive magnetic nanoparticles for oil–water separation*. *Polymer*, 2015. **72**: p. 361-367.
38. Tang, J., R.M. Berry, and K.C. Tam, *Stimuli-responsive cellulose nanocrystals for surfactant-free oil harvesting*. *Biomacromolecules*, 2016. **17**(5): p. 1748-1756.
39. Hendraningrat, L., S. Li, and O. Torsæter, *A coreflood investigation of nanofluid enhanced oil recovery*. *Journal of Petroleum Science and Engineering*, 2013. **111**: p. 128-138.
40. Hammond, P.S. and E. Unsal, *Spontaneous imbibition of surfactant solution into an oil-wet capillary: wettability restoration by surfactant–contaminant complexation*. *Langmuir*, 2011. **27**(8): p. 4412-4429.
41. Al-Anssari, S., et al., *Wettability alteration of oil-wet carbonate by silica nanofluid*. *Journal of Colloid and Interface Science*, 2016. **461**: p. 435-442.
42. Wasan, D.T. and A.D. Nikolov, *Spreading of nanofluids on solids*. *Nature*, 2003. **423**(6936): p. 156-159.
43. McElfresh, P.M., D.L. Holcomb, and D. Ector, *application of nanofluid technology to improve recovery in oil and gas wells*, in *SPE International Oilfield Nanotechnology Conference and Exhibition*. 2012, Society of Petroleum Engineers: Noordwijk, The Netherlands. p. 6.
44. Agista, M.N., K. Guo, and Z. Yu, *A state-of-the-art review of nanoparticles application in petroleum with a focus on enhanced oil recovery*. *Applied Sciences*, 2018. **8**(6): p. 871.
45. Yang, Z., et al., *Recent advances of CO₂-responsive materials in separations*. *Journal of CO₂ Utilization*, 2019. **30**: p. 79-99.
46. Jessop, P.G., et al., *Reversible nonpolar-to-polar solvent*. *Nature*, 2005. **436**(7054): p. 1102-1102.
47. Jessop, P.G., et al., *A solvent having switchable hydrophilicity*. *Green Chemistry*, 2010. **12**(5): p. 809-814.
48. Holland, A., et al., *Separation of bitumen from oil sands using a switchable hydrophilicity solvent*. *Canadian Journal of Chemistry*, 2012. **90**(10): p. 805-810.
49. Merchan-Arenas, D.R. and C.C. Villabona-Delgado, *Chemical-enhanced oil recovery using N,N-dimethylcyclohexylamine on a Colombian crude oil*. *International Journal of Chemical Engineering*, 2019. **2019**.
50. Li, X.J., et al., *Cleaner and sustainable approach of washing oil sands using CO₂-responsive composite switchable water (CSW) with lower volatility*. *Journal of Cleaner Production*, 2019. **236**.
51. Mozhdehei, A., N. Hosseinpour, and A. Bahramian, *Dimethylcyclohexylamine switchable solvent interactions with asphaltenes toward viscosity reduction and in situ upgrading of heavy oils*. *Energy & Fuels*, 2019. **33**(9): p. 8403-8412.
52. Sui, H., et al., *Understanding the roles of switchable-hydrophilicity tertiary amines in recovering heavy hydrocarbons from oil sands*. *Chemical Engineering Journal*, 2016. **290**: p. 312-318.

53. Li, X., et al., *A hybrid process for oil-solid separation by a novel multifunctional switchable solvent*. Fuel, 2018. **221**: p. 303-310.
54. Fanchi, J.R., *Chapter 6 - Fluid properties and model initialization*, in *Principles of applied reservoir simulation (Fourth Edition)*, J.R. Fanchi, Editor. 2018, Gulf Professional Publishing. p. 101-120.
55. Christie, M.A., et al., *Error analysis and simulations of complex phenomena*. Los Alamos Science, 2005. **29**(6).
56. Yegin, C., et al., *Next-generation displacement fluids for enhanced oil recovery*, in *SPE Oil and Gas India Conference and Exhibition*. 2017, Society of Petroleum Engineers: Mumbai, India. p. 29.
57. Chen, I., et al., *Use of pH-responsive amphiphilic systems as displacement fluids in enhanced oil recovery*. SPE Journal, 2014. **19**(06): p. 1,035-1,046.
58. Taber, J.J., F.D. Martin, and R.S. Seright, *EOR screening criteria revisited - Part 1: Introduction to screening criteria and enhanced recovery field projects*. SPE Reservoir Engineering, 1997. **12**(03): p. 189-198.
59. Taber, J.J., F.D. Martin, and R.S. Seright, *EOR screening criteria revisited - Part 2: Applications and impact of oil prices*. SPE Reservoir Engineering, 1997. **12**(03): p. 199-206.
60. Sorbie, K., *Polymer-improved oil recovery, 115 glasgow*. Scotland: Blackie & Son, 1991: p. 126-163.
61. Hourdet, D., F. L'allouret, and R. Audebert, *Reversible thermo-thickening of aqueous polymer solutions*. Polymer, 1994. **35**(12): p. 2624-2630.
62. L'allouret, F., et al., *Reversible thermoassociation of water-soluble polymers*. Revue de l'Institut Français du Pétrole, 1997. **52**(2): p. 117-128.
63. Bokias, G., et al., *Hydrophobic interactions of poly(N-isopropylacrylamide) with hydrophobically modified poly(sodium acrylate) in aqueous solution*. Macromolecules, 1997. **30**(26): p. 8293-8297.
64. Wang, Y., et al., *A novel thermoviscosifying water-soluble polymer for enhancing oil recovery from high-temperature and high-salinity oil reservoirs*. Advanced Materials Research, 2011. **306-307**: p. 654-657.
65. Chen, Q., et al., *Thermoviscosifying polymer used for enhanced oil recovery: rheological behaviors and core flooding test*. Polymer Bulletin, 2013. **70**(2): p. 391-401.
66. Li, X.E., et al., *Comparative studies on enhanced oil recovery: thermoviscosifying polymer versus polyacrylamide*. Energy & Fuels, 2017. **31**(3): p. 2479-2487.
67. Kamal, M.S., et al., *Rheological properties of thermoviscosifying polymers in high-temperature and high-salinity environments*. The Canadian Journal of Chemical Engineering, 2015. **93**(7): p. 1194-1200.
68. Guo, Y., et al., *Flow behavior through porous media and microdisplacement performances of hydrophobically modified partially hydrolyzed polyacrylamide*. SPE Journal, 2016. **21**(3): p. 688-705.

69. Viken, A.L., et al., *Thermothickening and salinity tolerant hydrophobically modified polyacrylamides for polymer flooding*. Energy & Fuels, 2018. **32**(10): p. 10421-10427.
70. Sarsenbekuly, B., et al., *Evaluation of rheological properties of a novel thermo-viscosifying functional polymer for enhanced oil recovery*. Colloids and Surfaces A: Physicochemical and Engineering Aspects, 2017. **532**: p. 405-410.
71. Liu, X., et al., *Effect of inorganic salts on viscosifying behavior of a thermoassociative water-soluble terpolymer based on 2-acrylamido-methylpropane sulfonic acid*. Journal of Applied Polymer Science, 2012. **125**(5): p. 4041-4048.
72. Li, X.e., et al., *A salt-induced viscosifying smart polymer for fracturing inter-salt shale oil reservoirs*. Petroleum Science, 2019. **16**(4): p. 816-829.
73. Afolabi, R.O., et al., *Hydrophobically associating polymers for enhanced oil recovery – Part A: A review on the effects of some key reservoir conditions*. Journal of Petroleum Science and Engineering, 2019. **180**: p. 681-698.
74. Dai, S., et al., *Light scattering of dilute hydrophobically modified alkali-soluble emulsion solutions: Effects of hydrophobicity and spacer length of macromonomer*. Macromolecules, 2000. **33**(19): p. 7021-7028.
75. Wang, C., K.C. Tam, and R.D. Jenkins, *Dissolution behavior of hase polymers in the presence of salt: Potentiometric titration, isothermal titration calorimetry, and light scattering studies*. The Journal of Physical Chemistry B, 2002. **106**(6): p. 1195-1204.
76. Araujo, E., et al., *Pyrene excimer kinetics in micellelike aggregates in a C₂₀-HASE associating polymer*. Langmuir, 2000. **16**(23): p. 8664-8671.
77. Tan, H., K.C. Tam, and R.D. Jenkins, *Network structure of a model HASE polymer in semidilute salt solutions*. Journal of Applied Polymer Science, 2001. **79**(8): p. 1486-1496.
78. English, R.J., et al., *Hydrophobically modified associative polymer solutions: rheology and microstructure in the presence of nonionic surfactants*. Industrial & Engineering Chemistry Research, 2002. **41**(25): p. 6425-6435.
79. Philippova, O.E. and A.R. Khokhlov, *Smart polymers for oil production*. Petroleum Chemistry, 2010. **50**(4): p. 266-270.
80. Zhong, C., W. Wang, and M. Yang, *Synthesis and solution properties of an associative polymer with excellent salt-thickening*. Journal of Applied Polymer Science, 2012. **125**(5): p. 4049-4059.
81. Zhang, Y., et al., *Enhancing oil recovery from low-permeability reservoirs with a self-adaptive polymer: A proof-of-concept study*. Fuel, 2019. **251**: p. 136-146.
82. Dreiss, C.A., *Chapter 1. Wormlike micelles: An introduction*, in *wormlike micelles: advances in systems, characterisation and applications*. 2017, The Royal Society of Chemistry. p. 1-8.
83. Talari, J.V., *Temperature sensitive supramolecular assemblies for enhanced oil recovery*. 2016. Texas A&M University
84. Ahmed, S., et al. *A review on CO₂ foam for mobility control: enhanced oil recovery*. 2017. Singapore: Springer Singapore.

85. Li, D., et al., *CO₂-sensitive foams for mobility control and channeling blocking in enhanced WAG process*. Chemical Engineering Research and Design, 2015. **102**: p. 234-243.
86. Li, D., et al., *CO₂-sensitive and self-enhanced foams for mobility control during CO₂ injection for improved oil recovery and geo-storage*. Chemical Engineering Research and Design, 2017. **120**: p. 113-120.
87. Zhang, Y., et al., *Smart mobility control agent for enhanced oil recovery during CO₂ flooding in ultra-low permeability reservoirs*. Fuel, 2019. **241**: p. 442-450.
88. Yang, Z., et al., *New method based on CO₂-switchable wormlike micelles for controlling CO₂ breakthrough in a tight fractured oil reservoir*. Energy & Fuels, 2019. **33**(6): p. 4806-4815.
89. Halland, E.K., et al., *CO₂ storage atlas: Norwegian continental shelf*. Norwegian Petroleum Directorate, 2014.
90. Feng, Y., Z. Chu, and C.A. Dreiss, *Applications of smart wormlike micelles, in smart wormlike micelles: design, characteristics and applications*. 2015, Springer Berlin Heidelberg: Berlin, Heidelberg. p. 79-91.
91. Shibaev, A.V., et al., *How a viscoelastic solution of wormlike micelles transforms into a microemulsion upon absorption of hydrocarbon: new insight*. Langmuir, 2014. **30**(13): p. 3705-3714.
92. Zhu, D., et al., *Laboratory study on the potential EOR use of HPAM/VES hybrid in high-temperature and high-salinity oil reservoirs*. Journal of Chemistry, 2013. **2013**.

Chapter 3. Experimental

All experiments were conducted at room temperature (23 ± 1 °C) unless otherwise specified.

3.1 Materials

Capric acid (CA) (99%, Fisher Scientific), lauric acid (LA) (99%, Fisher Scientific), myristic acid (MA) (99%, Fisher Scientific), oleic acid (OA) (>95%, Fisher Scientific), monoethanolamine (MEA) (>99%, Sigma-Aldrich), heptane (>99.5%, Fisher Scientific) and toluene (>99.5%, Fisher) were used as received without further purification. CO₂ gas (medical grade, Praxair) was also used as received. Milli-Q water was supplied by ThermoFischer Barnstead Nanopure ultrapure water purification system (resistivity > 18 MΩ·cm, $\gamma_{\text{heptane/water}} = 50.9$ mN/m, $\gamma_{\text{toluene/water}} = 36.3$ mN/m). Hydrochloride (HCl) (1 N solution, Sigma-Aldrich) and sodium hydroxide (NaOH) (1 N solution, Fisher Scientific) were diluted by Milli-Q water prior to their use.

Surfactant solutions were prepared by simple mixing of MEA with LCFA at 1:1 M ratio in Milli-Q water. Surfactant solutions were sonicated at 50 °C for 5 h in a sonication water bath and then shaken on a custom-designed shaker for 48 h. Figure 3.1 shows the reactions that take place during sample preparation. Prior to its use, each surfactant solution was sonicated at 50 °C for 1 h. This is to eliminate any precipitations that may have occurred during storage. Compounds prepared as such are denoted as MEA-LCFA [e.g., MEA-CA for monoethanolamine – capric acid] and their structures are shown in Figure 3.1.

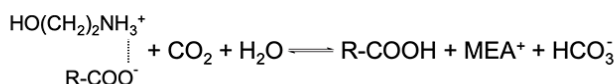
The petroleum ores in this study were Canadian oil sands ores (Athabasca, site AC, 2016) provided by Syncrude Canada Ltd. The ores contained 11.4 wt.% of heavy oil, 3.7 wt.% of water and 84.9 wt.% of solids. The solid particles less than 44 μm in size, which is also known as the fines, had a

content of 22.0 wt.% of total solids in this oil sands ores. The ore composition was determined by the Dean Stark apparatus and was consistent with previous reports [1, 2]. The heavy oil (bitumen) sample, which was also provided by Syncrude Canada Ltd, was collected from the predominantly fed to the vacuum distillation unit. The process water used was from the Aurora process water on September 2016.

Sample Preparation:



Switching Mechanism:



MEA-LCFA Surfactants:

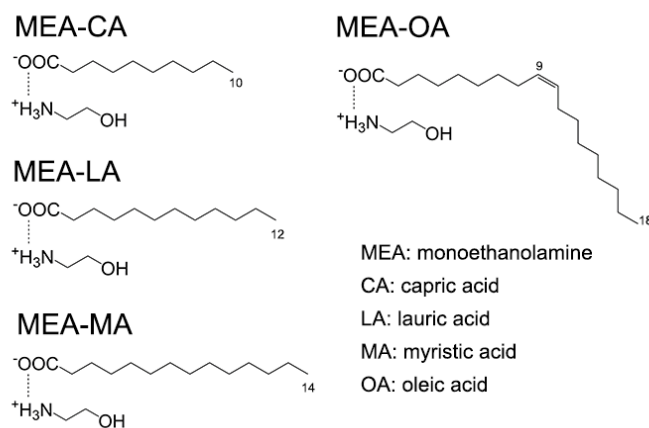


Figure 3.1. Preparation of MEA-LCFA surfactants and the basis of CO₂ switching with structures of four MEA-LCFA surfactants.

3.2 Interfacial tension (IFT) measurement

Interfacial tension (IFT) was measured using the pendant drop method on a T200 Theta Optical Tensiometer (Biolin Scientific) (Figure 3.2). A pendant oil drop was first generated at the tip of a “J-shape” needle while submerged in the surfactant solution. Images of the pendant drop were captured by a high-speed CCD camera at one frame/second (FPS) rate. IFT is analyzed by fitting the drop shape in accordance with the Young-Laplace equation [3, 4] using OneAttension software provided by Biolin Scientific. The IFT of the heptane/water interface was found to be 50.9 ± 0.1 mN/m, while that of toluene/water interface was 36.3 ± 0.2 mN/m, both of which were in good agreement with the values reported in the open literature [5].

3.2.1 Interfacial switching

The interfacial responses of MEA-LCFA surfactants at the oil/water interface were determined by measuring the change of dynamic IFT during the switching process. A pendant drop (heptane or toluene, 15 μ l) was first generated in the surfactant solution (1 mM, 3 ml). Surfactants were allowed to adsorb onto the oil/water interface until an equilibrium was reached, i.e., the rate of IFT change was undetectable (<0.02 mN/min). CO₂-responses were then activated by adding a certain volume of CO₂-saturated water into the aqueous phase (denoted as $t = 0$ s). CO₂-saturated water was prepared by bubbling CO₂ in Milli-Q water for 600 s. Dynamic IFTs were recorded until a new equilibrium was reached.

3.2.2 Solution switching

The responses of MEA-LCFA surfactants in the bulk solution were characterized by their equilibrium IFT values. The solution pH was first manipulated by gentle CO₂ bubbling, or by

HCl/NaOH titration. IFTs were then measured when the surfactant adsorption was equilibrated at the interface. The major difference between interfacial switching and solution switching is that the surfactants were already switched in the bulk solution before the IFT measurements in solution switching.

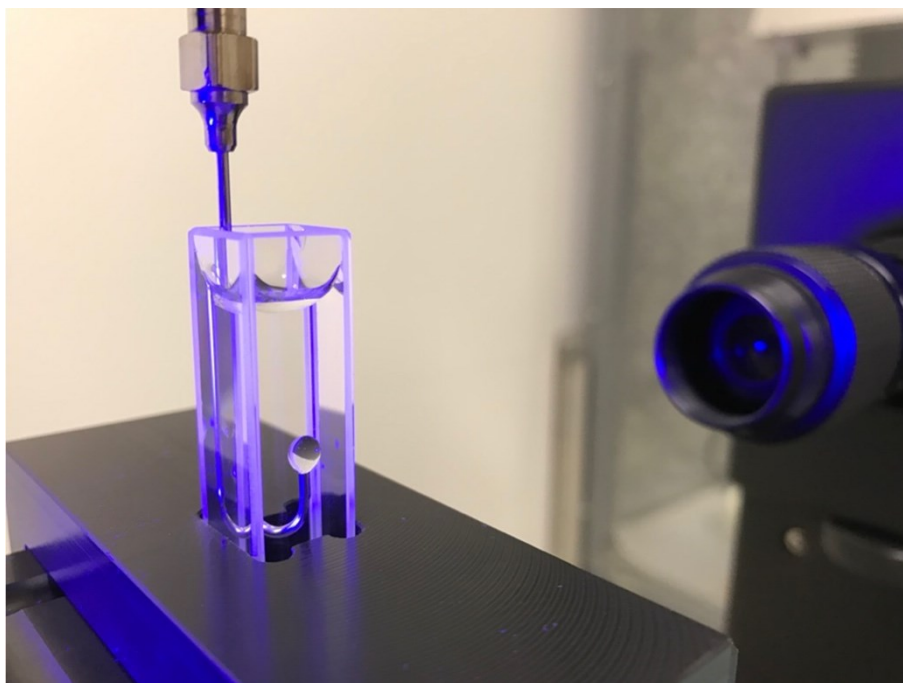


Figure 3.2. Photography of a pendent drop in the IFT measurement.

3.3 Contact angle measurements

The contact angle in the aqueous phase was obtained by a custom-designed micropipette system, where an inverted optical microscope (Zeiss Axiovert 200) was combined with micromanipulators. Experiments of an oil drop receding on a solid surface in water were performed as described in previously [6, 7]. Briefly speaking, a submillimeter size oil droplet ($\sim 5 \times 10^{-4} \text{ mm}^3$) (polybutene oil N190000, viscosity = $810 \pm 10 \text{ Pa}\cdot\text{s}$, Cannon Instrument Co.) was delivered onto a spherical silica cap, which had been pretreated by an air plasma cleaner (Harrick Plasma) for 300 s. The

measurement was initiated by placing the oil-covered silica surface into the aqueous solution, while the whole process was recorded by a charge-coupled device (CCD) camera at one frame/second (FPS) rate. Typical images are shown in Figure 3.3. Dynamic contact angles in the aqueous phase were obtained by analyzing the sequence of recorded images with a custom-programmed Matlab code [6]. Contours of the oil drop and the solid on the image was recognized due to the high greyscale contrasts at the interface, such that the values of the aqueous-phase contact angle could be evaluated at the intersections of two boundaries. Each condition was conducted at least twice.

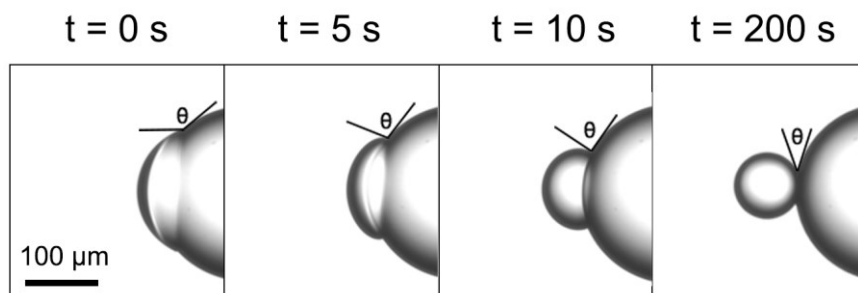


Figure 3.3. Snapshots of high viscosity oil droplet receding on a silica surface in Milli-Q water.

3.4 Integrated thin film drainage apparatus (ITFDA)

The coalescence time of two heptane droplets in surfactant solutions was measured by a custom-designed integrated thin film drainage apparatus (ITFDA). The setup of this instrument is shown in Figure 3.4 and more details on this instrument can be found elsewhere [8, 9]. A general operating procedure for determining the coalescence time of two heptane droplets is as followed. A steel cell was first filled with 15 ml surfactant solutions (1 mM). The cell was placed on a three-dimensional micro-translation stage, which enabled precise positioning and alignment. A heptane droplet ($d = 2 \text{ mm}$) was generated at the tip of the glass tube, which was suspended in the aqueous phase. The

droplet was brought into contact with a Teflon plate located on the inner bottom of the chamber. The heptane droplet remained on the Teflon surface when the glass tube was lifted, forming a semicircular heptane drop of ~ 0.5 mm height. Then, another heptane droplet ($d = 2$ mm) was generated at the tip of the glass tube and suspended in the aqueous surfactant solutions. The bottom heptane droplet, moving together with the steel cell, was aligned to the top droplet with the help of a CCD camera by manually adjusting the translation stage. The top droplet was then brought to a distance of $175 \mu\text{m}$ above the bottom drop. Both droplets were aged in the solution for a sufficient period of time to allow the surfactants to adsorb until an equilibrium was reached. During the coalescence time measurement, the top droplet was moved down towards the bottom droplet by the speaker at an approaching speed of 0.3 mm/s and a total displacement of $187.5 \mu\text{m}$ representing an overlapping distance of $12.5 \mu\text{m}$. The two droplets remained in contact for 120 seconds. The CCD camera recorded the whole process and the coalescence time of two heptane droplets was determined by analyzing the video recorded.

The influence of MEA-LCFA surfactants on the attachment time of ultra-heavy crude oil (bitumen) to air bubbles in water was also investigated by the ITFDA. Details on the experimental setup were described in previous studies [10]. In general, the top droplets in Figure 3.4 was replaced by a pendant air bubble, whereas the bottom Teflon surface in Figure 3.4 was coated by bitumen obtained from Syncrude Canada Ltd. (Fort McMurray, Canada). To ensure a smooth bitumen surface, the Teflon plate with a thin layer of bitumen was heated gently for 300 seconds. After cooling down to room temperature, the bitumen surface was immersed into the surfactant solution (1 mM) for 30 minutes, mimicking the bitumen extraction process in the industry [10, 11]. CO_2 was then bubbled through the solution for 600 seconds to activate the responsiveness of surfactants. The bitumen-coated Teflon plate was taken out and transferred into the steel cell in

Figure 3.4. The clear solution was taken from the previous beaker to ensure the same chemical environment but with better visibility. An air bubble ($d = 2$ mm) was then generated from the glass tube and kept in the solution for 300 seconds prior to the bitumen-air bubble attachment measurement in order to ensure the equilibrium of surfactant adsorption. The air bubble was then moved downwards towards the bitumen surface. Air bubble was in contact with the bitumen surface for a controlled period of time, and the state of attaching or no attaching was recorded. Each contact time was repeated for 50 times for a certain bitumen surface. Bitumen-air bubble attachment time is defined as the contact time where there is an overall 50% possibility for the air bubbles successfully attaching onto the bitumen surface. Each contact time was repeated for 50 times for a certain bitumen surface and each condition was conducted in at least triplicate.

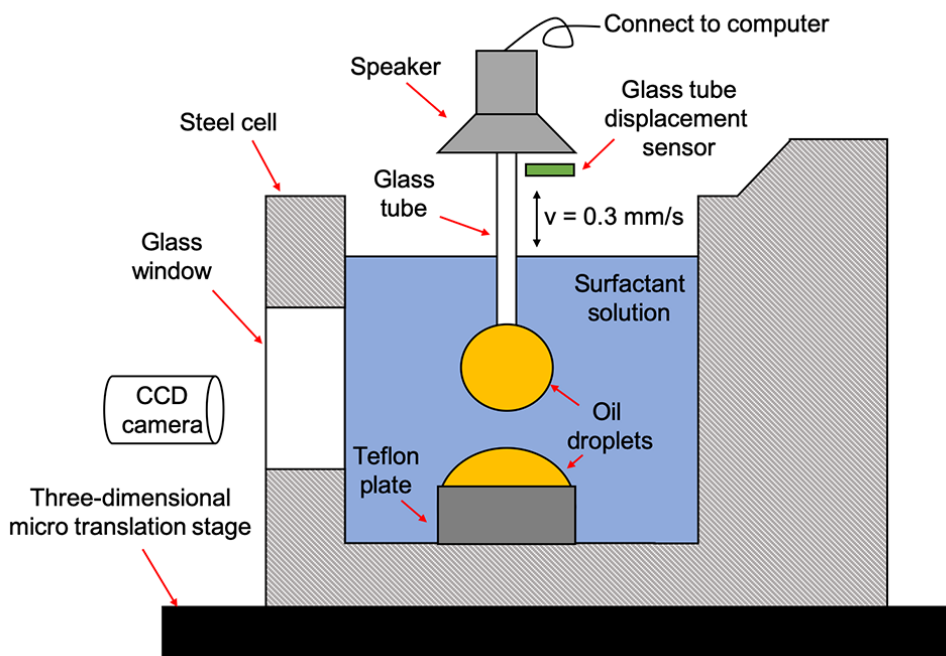


Figure 3.4. Schematic drawing of the integrated thin film drainage apparatus (ITFDA).

3.5 Demulsification tests

Demulsification of heptane-in-MEA-LCFA aqueous solution emulsions was evaluated by comparing the visual appearance of emulsions with CO₂ bubbling. Emulsions were prepared by vortex mixing of 1 ml heptane with 10 ml MEA-LCFA surfactant solution (20 mM) in a glass bottle for 60 s. Demulsification was conducted by continuous bubbling of CO₂ into the prepared emulsions. Emulsions were photographed periodically to evaluate their stability with or without CO₂ bubbling. Micrographs of emulsions were obtained using an optical microscope (Zeiss Axioskop 40). Droplet size distribution in the emulsions were analyzed by dynamic light scattering (DLS) method with a 173° back scattering angle (Zetasizer Nano S, Malvern Instruments®).

Demulsification of heavy oil-in-surfactant aqueous solution emulsions was assessed by comparing their stability with and without CO₂ bubbling. Due to the high viscosity of the heavy oil samples (2.22×10^3 Pa·s), the heavy oil used in this part of the study was diluted by toluene (1 wt.% heavy oil in toluene). Diluted heavy oil (15 ml) was mixed with surfactant aqueous solution (5 mM, 15 ml) in a glass vial. The mixture was then homogenized by a homogenizer (VWR® 250) at 30,000 rpm for 60 s. The demulsification process was conducted by continuous bubbling of CO₂ into the emulsions for sufficient time until no visual change was observed (typically required ~ 120 s). Demulsification efficiency was evaluated by the volume of the black heavy oil in the upper layer.

Post-demulsification experiments were conducted by analyzing the heavy oil product in the upper layer and the aqueous solution in the bottom layer. The heavy oil extracted from emulsions was collected and analyzed by FTIR spectrum (Agilent Technologies, Cary 600 Series FTIR Spectrometer). Oil samples were injected into a sample holder of two parallel KBr windows at a fixed spacing of 0.1 mm. The aqueous solutions in the bottom layer was considered as the tailings

water. They were also collected and investigated by their IFT values at the toluene/water interface and bulk pH values.

3.6 Heavy oil liberation visualization cell

Heavy oil liberation from the petroleum ores was studied by a custom-designed liberation visualization cell system. Details on the experimental setup could be found elsewhere [12, 13]. In general, petroleum ores were first placed at the bottom of a sample holder and flattened by a small hammer to ensure a flat surface was exposed. Aqueous solution of CO₂-responsive surfactants was then added carefully into the sample holder until the ores were fully covered. The liberation process was monitored by a stereo-optical microscope (Olympus SZX 10) coupled with a high-resolution digital camera. Images of the heavy oil liberating from their host solids were captured consecutively for a duration of 600 s starting from the addition of surfactant solution. The “*degree of heavy oil liberation (DOL)*” as a function of the run time was analyzed off-line by an image processing method also given in a previous report [13]. Briefly speaking, the regions covered by heavy oil were naturally distinguished as the “dark areas” whereas the “bright regions” can be considered as the solids. The value of DOL was defined as the percentage of the continuous disappearance of “dark areas” in comparison to the “dark areas” in the initial image ($t = 0$ s). The initial image was defined to have a DOL value of zero, indicating no occurrence of liberation. Since the heavy oil liberation is typically really fast in the first few seconds [12, 14] and any dislocation of the initial image may lead to unreliable results, a video was recorded simultaneously with the solution addition, such that the initial image could be obtained accurately. The initial image was determined as the first image where the surface of the petroleum ores was just covered by the surfactant solution. Each experimental condition was conducted at least three times.

3.7 Induction timer

Bitumen-air bubble attachment was studied by determining the induction time of bitumen-air bubble attachment in aqueous solutions [10]. Details of the experimental setup can be found in previous studies [10, 15]. In general, this two-step experiment involves the bitumen surface preparation and the induction time measurement.

3.7.1 Bitumen surface preparation

Bitumen surface was treated by CO₂-responsive surfactants following the procedure shown in Figure 3.5. Generally, a Teflon plate was coated with a thin layer of bitumen and heated gently for 5 minutes to produce a smooth bitumen surface. After cooling down to room temperature, the bitumen-coated Teflon plate was held by a tweezer and immersed into the surfactant solution with the bitumen surface facing downwards, while gentle stirring was applied simultaneously (Figure 3.5a). The sample was immersed in the solution for 30 minutes to ensure equilibrated adsorption of the surfactants at the bitumen-water interface. CO₂ was then bubbled through the solution for 10 minutes to activate the CO₂ responsiveness. A glass wall was used to prevent incidental bubble attachment. The bitumen surface was then taken out and transferred into a clean rectangular cell (Figure 3.5b). Clear solution was taken from the previous beaker to ensure the same chemical environment but with better visibility.

3.7.2 Induction time measurement

An air bubble ($d = 2$ mm) was generated from the glass tube and kept in the solution for 300 seconds prior to the bitumen-air bubble attachment measurement in order to ensure the equilibrium of surfactant adsorption. The air bubble was then moved downwards towards the bitumen surface.

Air bubble was in contact with the bitumen surface for a controlled period of time, and the state of attaching or no attaching was recorded. Each contact time was repeated for 50 times for a certain bitumen surface. Bitumen-air bubble attachment time is defined as the contact time where there is an overall 50% possibility for the air bubbles successfully attaching onto the bitumen surface. Experiments were conducted in triplicate. The induction time is defined as the contact time at which 50% of air bubbles attach to the bitumen surface and thereby suffer significant deformation when retreated.

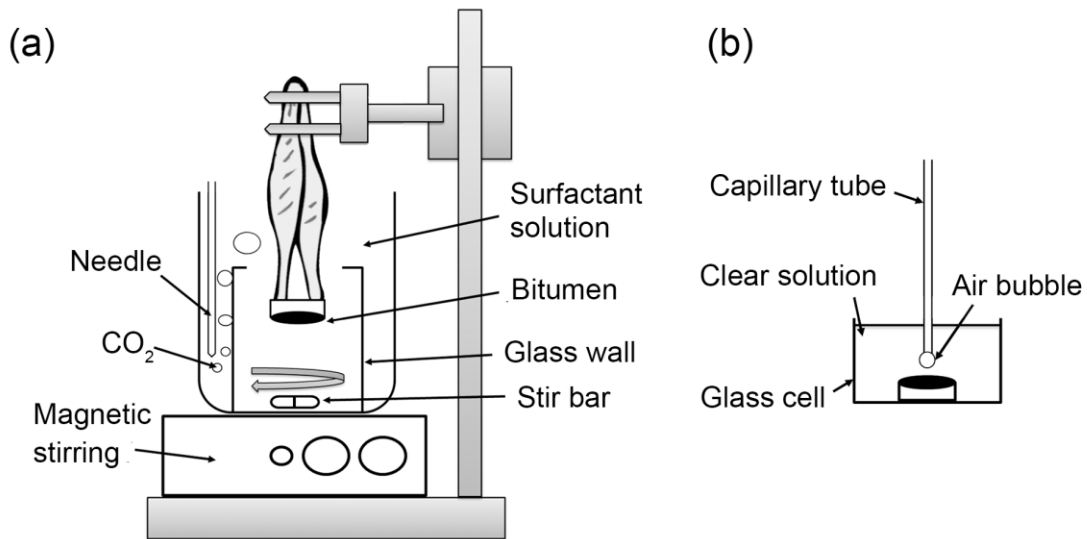


Figure 3.5. Procedures of the induction time measurement. (a) Bitumen surface preparation; and (b) Induction time measurement.

3.8 Bitumen recovery from oil sands

Bitumen recovery experiments were carried out in a modified bitumen extraction unit (M-BEU). M-BEU consisted of a 1-L stainless steel cell modified with water jacket, an impeller, an adjustable AC motor (KBAC series, NEMA 4X/IP65, equipped with a tachometer from JoneTM) and a mass

flow controller (AALBORG[®] GFC17). Circulating water at constant temperature of 23 ± 1 °C from a thermal water bath was pumped through the water jacket to ensure ambient temperature condition.

The operation procedure is summarized in Table 3.1. Briefly speaking, the oil sands extraction contained three continuous stages: slurry condition, primary flotation and secondary flotation, which mimicked the oil sands ores in hydrotransport pipeline, PSV and SSV, respectively. Each stage was operated for 10 minutes. In the slurry condition stage, 500 ± 1 g of thawed oil sands ores were added into the M-BEU cell, which contained 150 g of surfactant solution. The mixing speed was set as 600 rpm while the external air flow was set as 150 ml/min. In the primary flotation stage, another 900 g surfactant solution was added. The agitator was kept running at 600 rpm, but the air flow was turned off. The primary bituminous froth was collected and weighted in a cellulose Soxhlet extraction thimble (Whatman[™] 2800432, single wall). At last, in the secondary flotation stage, the mixing speed was raised up to 800 rpm, while CO₂ flow was input at the flow rate of 50 ml/min. The secondary froth was also collected and weighted in another thimble. The bitumen recovery ratio and froth quality were analyzed by the Dean-Stark apparatus using toluene as the refluxing solvent [16].

Table 3.1. Operation procedure of oil sands extraction experiments in M-BEU.

	Slurry condition	Primary flotation	Secondary flotation
Addition	150 g solution	900 g solution	--
Mixing speed	600 rpm	600 rpm	800 rpm
Air flow	150 ml/min Air	--	50 ml/min CO ₂
Duration	10 min	10 min	10 min

3.9 References

1. Zhu, Y., et al., *Biodiesel-assisted ambient aqueous bitumen extraction (BA³BE) from athabasca oil sands*. Energy & Fuels, 2018.
2. Lu, Y., et al., *Pseudo-gemini biosurfactants with CO₂ switchability for enhanced oil recovery (EOR)*. Tenside Surfactants Detergents, 2019. **56**(5): p. 407-416.
3. Young, T., III. *An essay on the cohesion of fluids*. Philosophical transactions of the royal society of London, 1805(95): p. 65-87.
4. Berg, J.C., *An introduction to interfaces & colloids: the bridge to nanoscience*. 2010: World Scientific.
5. Dean, J.A., *Lange's handbook of chemistry*. 1999: New york; London: McGraw-Hill, Inc.
6. Li, R., et al., *Spontaneous displacement of high viscosity micrometer size oil droplets from a curved solid in aqueous solutions*. Langmuir, 2019. **35**(3): p. 615-627.
7. Yeung, A., et al., *On the interfacial properties of micrometre-sized water droplets in crude oil*. Proceedings of the Royal Society of London. Series A: Mathematical, Physical and Engineering Sciences, 1999. **455**(1990): p. 3709-3723.
8. Wang, L., et al., *Measurement of interactions between solid particles, liquid droplets, and/or gas bubbles in a liquid using an integrated thin film drainage apparatus*. Langmuir, 2013. **29**(11): p. 3594-603.
9. Wang, L., Z. Xu, and J.H. Masliyah, *Dissipation of film drainage resistance by hydrophobic surfaces in aqueous solutions*. The Journal of Physical Chemistry C, 2013. **117**(17): p. 8799-8805.
10. Gu, G., et al., *Effects of physical environment on induction time of air-bitumen attachment*. International Journal of Mineral Processing, 2003. **69**(1): p. 235-250.
11. Masliyah, J., J. Czarnecki, and Z. Xu, *Handbook on theory and practice of bitumen recovery from Athabasca oil sands: Vol. I. Theoretical basis*. 2010: Kingsley Knowledge Publishing.
12. Srinivasa, S., et al., *Study of bitumen liberation from oil sands ores by online visualization*. Energy & Fuels, 2012. **26**(5): p. 2883-2890.
13. He, L., et al., *Image analysis of heavy oil liberation from host rocks/sands*. The Canadian Journal of Chemical Engineering, 2015. **93**(6): p. 1126-1137.
14. He, L., et al., *Enhancing bitumen liberation by controlling the interfacial tension and viscosity ratio through solvent addition*. Energy & Fuels, 2014. **28**(12): p. 7403-7410.
15. Chen, T., et al., *Impact of salinity on warm water-based mineable oil sands processing*. Canadian Journal of Chemical Engineering, 2017. **95**(2): p. 281-289.
16. Bulmer, J. and J. Starr, *Syncrude analytical methods for oil sand and bitumen processing*. AOSTRA, Edmonton, 1979.

Chapter 4. CO₂-Responsive Surfactants and Their Switching Mechanism

One of the major challenges in applying CO₂-responsive surfactants concerns their tunable switchability and robustness under operating conditions. We hypothesize that combining monoethanolamine (MEA) with long-chain fatty acids (LCFAs) of variable chain lengths through electrostatic attraction could develop a series of CO₂-responsive surfactants with tunable switching pH. The tunability of switching pH for this group of surfactants was detected by *in situ* probing of the CO₂-responsive characteristics at the oil/water interface using dynamic interfacial tension (IFT) measurements. Two protocols were applied to distinguish interfacial response and solution response. The key importance of interfacial response was demonstrated by two essential applications of CO₂-responsive surfactants: demulsification of stable emulsions, and alternation of the interfacial properties of ultra-heavy crude oil-water interfaces. The switching pH of the CO₂-responsive surfactants was controlled by the hydrocarbon chain length of LCFAs. More importantly, their switching behavior was found to be different at the interface and in the bulk solution, which is attributed to the enhanced molecular interactions at the interface. Since most applications require surfactants to be switched at the interface, it is thereby most appropriate to determine the switching pH through their interfacial responses.

4.1 Introduction

Chemical processes that require the control of interfacial activities at the oil/water interface often benefit from the removal of interfacial-active materials in a subsequent stage. Interfacial activities can be introduced by surfactants, polymers, and particles. They are used to enhance emulsion stability, encapsulation of drugs or reactants, removal of oil stains, treatment of oily waste waters,

etc. For some applications, however, interfacial activities are only needed temporarily, and the ability to switch off these interfacial activities at some point is highly favorable if not necessary for downstream operations, such as separating a specific component, releasing drugs at the target, or eliminating pollutants. Unfortunately, it is relatively difficult to remove conventional interfacial-active materials once they adsorb at the interface. Traditional strategies to resolve this problem include optimizing the dosage of surface-active materials for compromised performance, adding a secondary processing aid, or applying physical forces such as centrifugation or electrical field.

Stimuli-responsive surfactants feature switchable interfacial activities, allowing them to modulate the oil-water interfacial properties in a controllable manner. Responsive surfactants can be switched from interfacial-active to interfacial-inactive using external stimuli, such as temperature, pH, CO₂/N₂ and/or UV radiation. Therefore, responsive surfactants can be applied to enhance a particular process by introducing a desirable interfacial activity in one stage, and then be switched to a surface inactive state for a subsequent stage. Stimuli-responsive surfactants have been investigated in fields such as enhanced oil recovery [1, 2], heavy oil transportation through pipelines [3], oil-water separation [4-7], soil remediation [8, 9], microreactors [10, 11], and controlled drug delivery [12-15].

Stimuli-responsive surfactants, whose interfacial activities are triggered by CO₂, have attracted recently great scientific and practical interests. Surfactants can respond to CO₂ by forming carbamic acid/carbamate [16] or urea [17], or by the protonation of functional groups due to the pH decrease taking place during CO₂ solvation. In general, the first process is rather slow and irreversible at ambient temperature, restricting their fields of utilization [18], while the latter process is more common. For CO₂-responsive surfactants using protonation, the functional groups

can be either anionic (e.g., carboxylates [5, 19, 20] and phenolates [8]), or cationic (e.g., tertiary amines [21], amidines [3, 4], and melamines [22]). CO₂-responsiveness originates from the change in interfacial activity between the protonated and deprotonated forms of the surfactant. Although numerous CO₂-responsive surfactants have been developed, significant challenges remain before they can be used in practical applications.

For CO₂-responsive surfactants to be used in commercial applications, it is essential to identify their switching conditions, where the sharp response can be activated. Both states of interfacial activity should be realized promptly under the switching conditions. However, the desired switching is often different from process to process, while onsite operating conditions can be complicated and location-dependent. It is both time-consuming and economically nonviable to design specific CO₂-responsive surfactants for every potential application, which may only be feasible to limited situations. A more logical approach is to develop a series of CO₂-responsive surfactants which are easy to synthesize and possess both a tunable switching pH and a well-understood switching mechanism. This would permit a suitable reagent to be readily selected for the desired application.

Long-chain fatty acids (LCFAs) are commonly used to construct CO₂-responsive surfactants [5, 8, 20]. LCFAs are interfacially active in their deprotonated form at high pH and switch to less active once protonated at low pH [8, 19]. The midpoint of this transformation is known as the apparent pK_a of LCFAs, where half of the species is protonated and the other half remains deprotonated. Therefore, the switching condition of LCFA-based surfactants should be correlated with their apparent pK_a values. More importantly, the apparent pK_a of LCFAs is adjustable by changing the length of hydrocarbon chain [23-27] or by decorating with side groups [19]. The switching pH is thus tunable by applying different types of LCFAs.

The nature of the counter-ion in LCFAs also plays an important role [28]. Common salt form of LCFAs, e.g., sodium or potassium ion as the counter-ion, has low solubility in water at room temperature due to a high Krafft point [28, 29]. Enhancement of solubility of LCFAs in water may be achieved by using bulky cations, such as tetraalkylammoniums [29-31], alkanolamines [19, 30, 32], ethylenediamines [5, 20], and choline [29]. The large head group of these cations prevents the chain crystallization of LCFA at room temperature [28]. Counter-ions with simple structures such as monoethanolamine (MEA) or tetramethyl ammonium (TMAOH) were considered to facilitate scientific interpretation of the results. Foams and emulsions produced from MEA salts were reported to be more stable than that from TMAOH salts [30]. Hence, MEA was selected as the counter-ion in the current study.

In this study, we developed a series of CO₂-responsive surfactants by the association of MEA with LCFAs. The switching pH of the MEA-LCFA surfactants in response to CO₂ addition was determined by probing dynamic IFT at the oil/water interface. We identified significant differences in interfacial switching and solution switching when MEA-LCFA surfactants respond to CO₂ addition, which is also a primary focus of this study.

4.2 Materials and methods

Surfactant solutions were prepared by simple mixing of MEA with LCFA at 1:1 M ratio in Milli-Q water. Surfactant solutions were sonicated at 50 °C for 5 h in a sonication water bath and then shaken on a custom-designed shaker for 48 h. Compounds prepared as such are denoted as MEA-LCFA [e.g., MEA-CA for monoethanolamine – capric acid].

Interfacial tension (IFT) was measured by T200 Theta Optical Tensiometer (Biolin Scientific) using the pendant drop method. The interfacial responses of MEA-LCFA surfactants at the

oil/water interface were determined by measuring the change of dynamic IFT during the switching process as described in Section 3.2.1. The responses of MEA-LCFA surfactants in the bulk solution were characterized by their equilibrium IFT values as described in Section 3.2.2.

The coalescence time of two heptane droplets in surfactant solutions was measured by a custom-designed integrated thin film drainage apparatus (ITFDA). The details of this instrument can be found elsewhere [33, 34] and in Section 3.4. Briefly speaking, two heptane droplets were first submerged in the surfactant solution for a sufficient period of time to achieve the equilibrium of surfactants adsorption. After that, the droplets were brought in contact for 120 seconds, while the whole process was recorded by a high-speed camera. The coalescence time of two heptane droplets was determined by analyzing the video recorded. In an effort to correlate the coalescence time and the IFT, we kept similar treatments of the heptane-water interface as in the IFT measurements. For the interfacial responses, both heptane droplets were first generated and aged in the surfactant solution, then treated by a known amount of CO₂-saturated water to activate CO₂-responses at the interface, and allowed an equilibration time of 300 seconds to ensure the surfactants reaching the new equilibrium of adsorption after the switch. After that, the coalescence time was measured. For the solution responses, the pH of the surfactant solution was firstly modified by CO₂-saturated water prior to the generation of heptane droplets. The same operating procedure was applied to obtain the coalescence time. Experiments were conducted in triplicate. The influence of MEA-LCFA surfactants on the attachment time of ultra-heavy crude oil (bitumen) to air bubbles in water was also investigated by the ITFDA using a modified method as previous described in Section 3.4.

Demulsification of heptane-in-MEA-LCFA aqueous solution emulsions was evaluated by comparing the visual appearance of emulsions with CO₂ bubbling. Emulsions were prepared by vortex mixing of 1 ml heptane with 10 ml MEA-LCFA surfactant solution (20 mM) in a glass

bottle for 60 s. Demulsification was conducted by continuous bubbling of CO₂ into the prepared emulsions.

4.3 Results and Discussion

4.3.1 Interfacial activity

The interfacial activities of MEA-LCFA surfactants were first determined by measuring interfacial tensions (IFT). As shown in Figure 4.1a, all surfactants were interfacially active and could reduce significantly the heptane/water IFT. Surfactants constructed by LCFAs with longer hydrocarbon chains length were more interfacially active, as expected, except for the MEA-OA at high concentrations. At 1 mM concentration of surfactants in the aqueous phase, the order of interfacial activity is MEA-OA \approx MEA-MA > MEA-LA > MEA-CA. This concentration is used mainly in the following analysis.

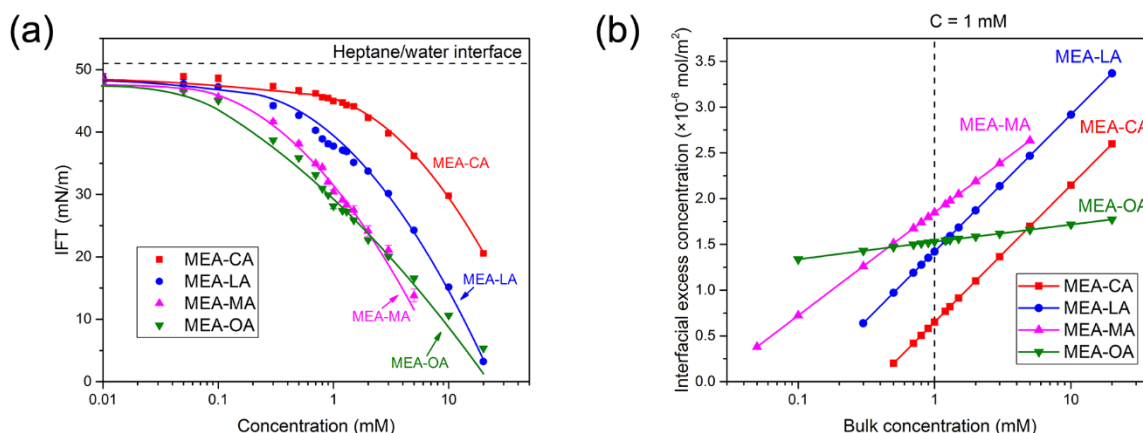


Figure 4.1. (a) Interfacial activity MEA-LCFA surfactants at the heptane/water interface; (b) Interfacial excess concentration estimated from the Gibbs adsorption isotherm.

The interfacial excess concentration of MEA-LCFA surfactants was estimated using the Gibbs adsorption isotherm equation. The Gibbs adsorption isotherm equation is a two-dimensional analogous of the Gibbs-Duhem equation and describes the excess amount of surfactants adsorbed at the interface in comparison with that dissolved in bulk [35, 36]. For the i -th component in a surfactant system, it has the following form [37]:

$$\Gamma_i = - \frac{d\gamma}{d\mu_i} \quad (4.1)$$

where γ is the IFT, Γ_i and μ_i are the interfacial excess concentration and the chemical potential of the i -th component, respectively. Higher values of Γ represent stronger adsorption at the interface. Chemical potentials obey the relation $\mu_i \approx RT \ln C_i$ for ideal systems, where R is the gas constant, T is the temperature, C_i is the concentration of the i -th compound. Considering all existing species in the surfactant solution, and the charge neutrality in the bulk solution and at the interface, the following equation can be derived [35]:

$$\Gamma = - \frac{1}{RT} \frac{d\gamma}{d \ln [C_{LCFA^-} \cdot C_{MEA^+}]} \quad (4.2)$$

where C_{LCFA^-} and C_{MEA^+} are the bulk concentration of $LCFA^-$ and MEA^+ . Details of the derivation and calculation are given in the journal publication [38]. The relationship between the interfacial excess concentration and bulk concentration is plotted in Figure 4.1b. The results confirm that a longer hydrocarbon chain leads to a stronger adsorption onto the interface, except for MEA-OA at high concentrations. The excess concentration of MEA-OA at the interface is the highest at low concentration but gradually surpassed by the others as the bulk concentration increases. The peculiar trend of MEA-OA should be attributed to the unsaturated bond in OA, which restricts the

compaction of surfactants at the interface [24]. Such a limitation becomes more significant when the interfacial concentration of surfactant is high. The order of interfacial excess is MEA-MA > MEA-OA > MEA-LA > MEA-CA at 1 mM surfactant concentration.

4.3.2 Determination of switching pH

The interfacial responses of the surfactants at the heptane/water interface was demonstrated by the changes in dynamic IFT using the probing strategy illustrated in Figure 4.2a. Surfactants were first adsorbed to the oil/water interface until the equilibrium was achieved at their natural pH. A known volume of freshly prepared CO₂-saturated water was added gently into the cuvette at t = 0 s, and the dynamic IFTs were recorded for 300 s. The motivation of such an experimental procedure is to probe the responses of the surfactant at the oil/water interface directly.

Prior to the experiments, it is also essential to estimate the CO₂ concentration in CO₂-saturated water for quantitative analysis. Fresh CO₂-saturated water was prepared daily by bubbling CO₂ into Milli-Q water for 10 minutes. pH of the CO₂-saturated water was measured to be 3.85 ± 0.03. CO₂ concentration could be calculated throughout the dissociation constants (K_{a1}, K_{a2}, K_{app}) and the aqueous pH value. When CO₂ dissolves in water, it forms carbonic acid (H₂CO₃), which further dissociates into bicarbonate (HCO₃⁻) and carbonate ion (CO₃²⁻). The equilibriums of every composition in the CO₂-saturated water can be written as following:

$$K_{a1} = \frac{[H^+][HCO_3^-]}{[H_2CO_3]} \quad (4.3)$$

$$K_{a2} = \frac{[H^+][CO_3^{2-}]}{[HCO_3^-]} \quad (4.4)$$

$$K_{\text{app}} = \frac{[\text{H}^+][\text{HCO}_3^-]}{[\text{H}_2\text{CO}_3] + [\text{CO}_2(\text{aq})]} \quad (4.5)$$

$$[\text{H}^+] = [\text{OH}^-] + [\text{HCO}_3^-] + 2[\text{CO}_3^{2-}] \quad (4.6)$$

where the values of dissociation constants (K_{a1} , K_{a2} , K_{app}) at room temperature can be found in literatures [39]. Since $[\text{H}^+]$ and $[\text{OH}^-]$ can be obtained from aqueous pH, the concentration of each compositions in CO_2 -saturated water can thereby be calculated.

Table 4.1. Composition of CO_2 -saturated water at pH 3.85.

Species	CO_2 (aq)	H_2CO_3	HCO_3^-	CO_3^{2-}	CO_2 concentration
Concentration (mM)	44.6	0.0798	0.141	4.69×10^{-8}	44.8

Note: $K_{a1} = 2.50 \times 10^{-4}$; $K_{a2} = 4.69 \times 10^{-11}$; $K_{\text{app}} = 4.47 \times 10^{-7}$ from ref.[39].

As mentioned, CO_2 -saturated water used in this study was measured to be 3.85. Thus, the concentration of each composition in CO_2 -saturated water is shown in Table 4.1. CO_2 concentration was calculated as the summation of CO_2 in all forms. It has to be noted that only a small volume of CO_2 -saturated water was added into a large volume of surfactant solution. CO_2 concentration was largely diluted in the dynamic IFT measurements. In general, CO_2 concentrations in the surfactant solutions were 1.44 mM, 3.44 mM, 6.40 mM, and 11.2 mM after the addition of 100 μl , 250 μl , 500 μl , and 1000 μl of CO_2 -saturated water, respectively.

A noticeable change in drop shape was observed immediately after the CO_2 addition, a clear evidence of an IFT change. Figure 4.2b shows the evolution of a pendant heptane droplet in 1 mM MEA-OA solution after the addition of 1000 μl CO_2 -saturated water. The heptane drop evolved

gradually to a more spherical shape, indicating an increase in IFT. Solution turbidity also increased as a result of insoluble nature of the protonated OA.

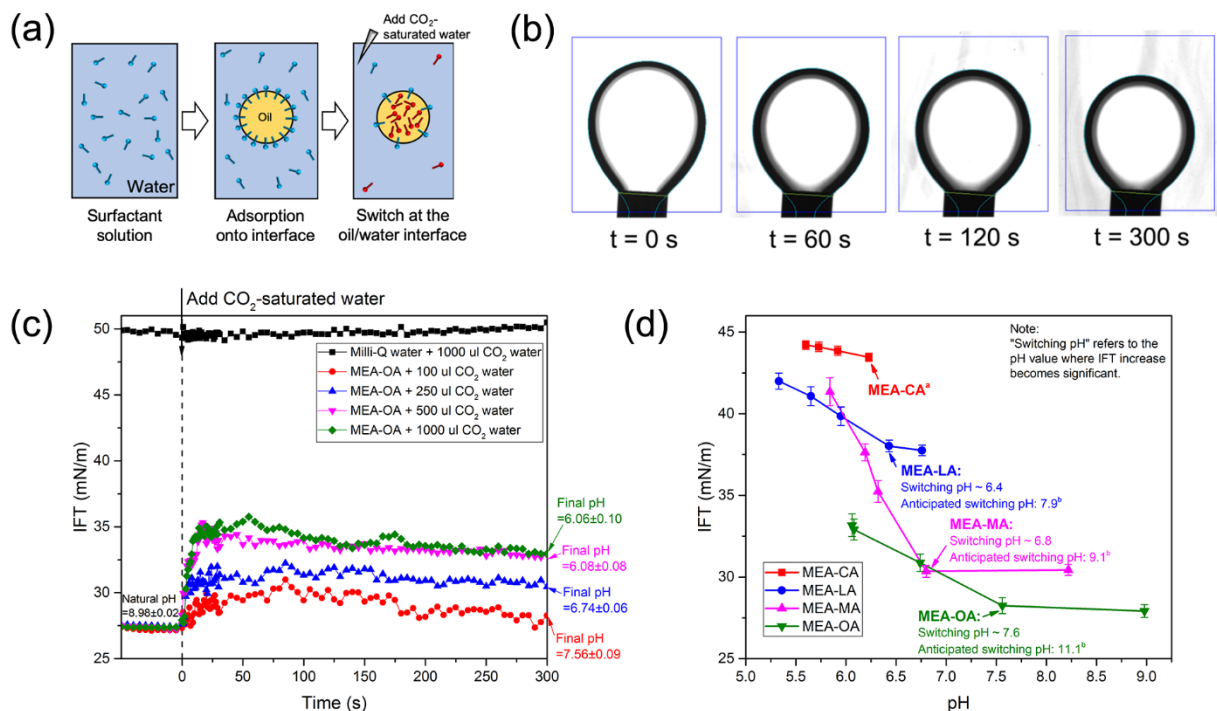


Figure 4.2. (a) Schematic illustration of probing *in-situ* CO₂-responses of surfactants at the oil/water interface; (b) Evolution of a pendant heptane droplet in MEA-OA aqueous solution upon direct addition of 1000 μ l CO₂-saturated water into the aqueous phase; (c) Changes in dynamic IFT of 1 mM MEA-OA aqueous solution/heptane interface with the addition of different volumes of CO₂-saturated water; and (d) Switching pH determined from dynamic IFT data obtained by *in-situ* probing of interfacial responses of surfactants. ^a The interfacial response of MEA-CA was not significant. ^b The anticipated switching pH was calculated from the apparent pK_a values of the LCFAs from refs [8, 24, 26, 27].

The interfacial responses of MEA-OA are illustrated by their changes in dynamic IFT upon CO₂ addition as shown in Figure 4.2c. The heptane-Milli-Q water interface was non-responsive to the addition of CO₂ in solution, which suggests that the observed changes in IFT were attributed to responses of the MEA-LCFA surfactants at the interface. The response occurred immediately after CO₂ additions as shown by a significant increase in the IFT within the first 60 seconds of CO₂ addition. Increasing the volume of CO₂-saturated water addition led to a more significant change in dynamic IFT, which was the consequence of more completed OA⁻ protonation. MEA-CA was the only compound which displayed nearly a negligible change in IFT (Figure 4.2d). This reflects the relatively strong acidity of CA (pK_a = 6.4 [27]) as well as the best water solubility (0.87 mmol/L in H₂O [40]) among the four fatty acids examined.

The relationship between pH and IFTs provides key information to determine the switching pH, where the interfacial responses of surfactants can be activated. For easy discussion, we define the switching pH in this study as the pH where the increase in the IFT becomes significant, indicating a significant or complete loss in interfacial activity of the surfactants. Equilibrium IFTs were obtained from the dynamic IFT experiments and plotted against their corresponding solution pH in Figure 4.2d. The interfacial responses of MEA-LCFA surfactants was confirmed to be a direct consequence of decreasing pH during CO₂ addition, which caused the protonation of fatty acids. LCFA is interfacially active in its deprotonated form and switches to less active after being protonated. Therefore, the fraction of protonated LCFA, usually known as the degree of protonation, is expected to be directly related to the responsive behavior. The degree of LCFA protonation can be derived from their corresponding apparent pK_a values reported in the literature. Based on the definition of switching pH in this study, the anticipated switching pH was estimated as the pH value where the degree of LCFA protonation is 0.05. Figure 4.2d shows that the

switching pH of MEA-LCFA surfactants was tunable, increasing gradually with increasing hydrocarbon chain length. Surprisingly, the switching pH for interfacial response was much lower than expected, especially for LCFAs with longer hydrocarbon chains, e.g., MEA-MA and MEA-OA.

4.3.3 Interfacial switching vs. Solution switching

Switching pH of CO₂-responsive surfactants is essential for both fundamental studies and practical applications. The objective of this research is to construct a series of CO₂-responsive surfactants with the switching pH being tunable by using different LCFAs. The most ideal scenario would be the case where the apparent pK_a of LCFAs could predict the switching pH for the activation of interfacial responses. Experimental data revealed that the switching pH was tunable, but the switching pH could not be simply predicted from pK_a values of LCFAs. It is thereby critical to understand the origin of such a lower switching pH than the anticipation from pK_a values of LCFAs, and also to determine whether or not the switching pH obtained from *in situ* probing methods (e.g., dynamic IFT experiments) could be used to interpret macroscopic colloidal phenomena. The switching pH determined from the dynamic IFT experiments was explicitly related to the responses of these responsive surfactants at the oil/water interface. Apparent pK_a values of LCFAs reported in literature were mostly measured in the bulk aqueous phase, which may not be appropriate for interpreting interfacial behavior. We showed that the CO₂-responses at the oil/water interface deviate significantly from that in the solution phase for MEA-LCFA surfactants and designed diagnostic experiments to identify the mechanisms involved.

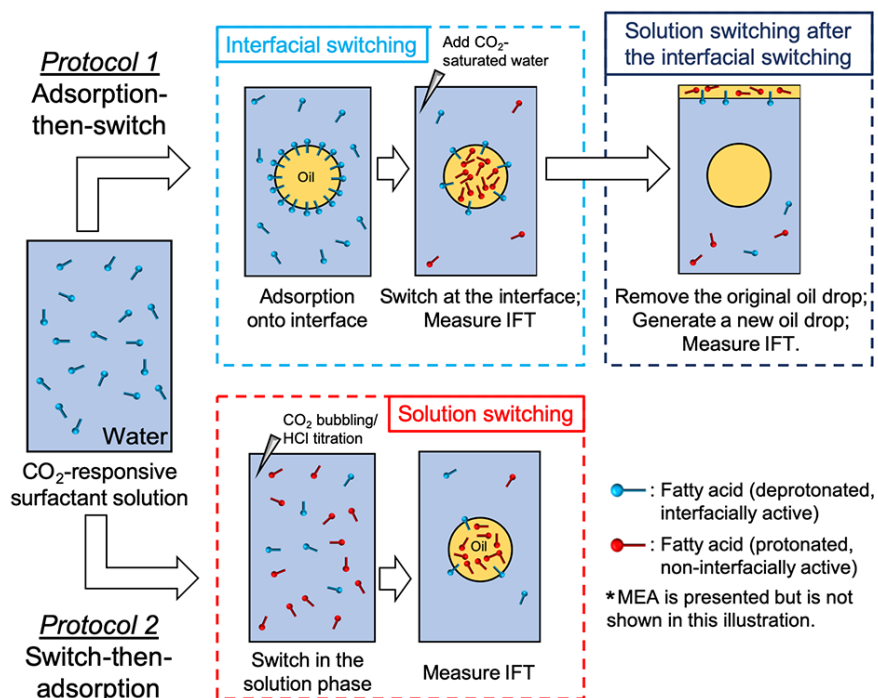


Figure 4.3. Two protocols were designed to distinguish switching mechanisms of MEA-LCFA surfactants at the oil/water interface and in bulk solution by CO₂ addition: *Protocol 1* represents interfacial switching while *Protocol 2* represents solution switching. Protocol 1 was further modified by removing the original drop and generating a new oil drop in the switched solution, representing the experiment of Protocol 1 followed by Protocol 2.

Two protocols of IFT measurements as illustrated in Figure 4.3 were designed to distinguish CO₂-responses of MEA-LCFA surfactants at the oil/water interface and in the solution phase. In the previous dynamic IFT measurements, the responses at the interface were probed by applying *Protocol 1* with an “adsorption-then-switch” strategy. Surfactants were first adsorbed and then switched at the interface. IFT changes were thereby the consequences of losing the surface activity at the interface or desorbing from the interface of surfactants due to CO₂ addition. On the other hand, a “switch-then-adsorption” strategy was conducted as *Protocol 2*, where solution pH was first manipulated to switch the surfactants in the solution phase, followed by generating the oil

drops in the switched surfactant solutions and measuring dynamic IFT. Furthermore, the dynamic IFT using a *modified Protocol 1* was measured to confirm our hypothesis. In this case, the original oil droplet at the end of the dynamic IFT experiment after CO₂ addition was removed and substituted by a fresh oil droplet. Under such circumstance, IFT values represent interfacial activity of MEA-LCFA surfactants remaining in the solution phase. Therefore, the IFTs measured here would match values obtained by Protocol 2 under similar solution conditions.

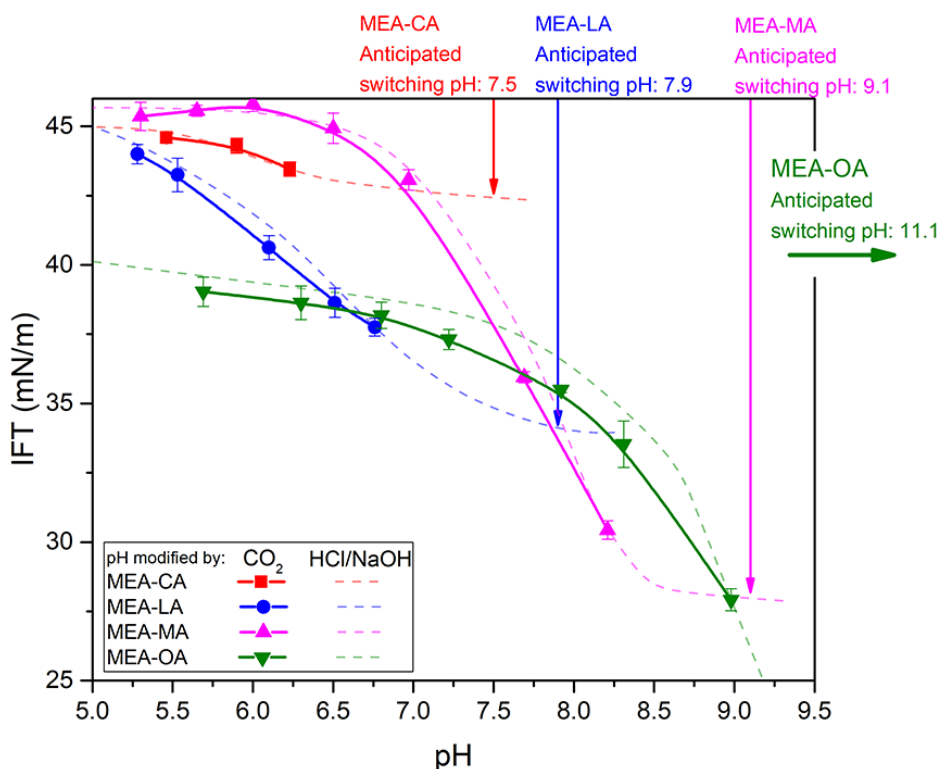


Figure 4.4. Solution responses of MEA-LCFA surfactants obtained using solution switching protocol described in Figure 4.3. pH of the surfactant solutions was modified either by gentle CO₂ bubbling (solid lines) or by HCl/NaOH titration (dash lines) at the heptane/water interface.

Solution responses of MEA-LCFA surfactants were examined by Protocol 2. The results in Figure 4.4 show no difference in measured IFT by changing the solution pH through gentle CO₂ bubbling (solid lines) or by HCl/NaOH titration (dash lines). There is no doubt that the CO₂-responses of MEA-LCFAs originate from the protonation of fatty acids, where CO₂ alone acts as a pH modifier. The switching pH of solution responses matched well with the anticipated switching pH calculated from apparent pK_a values. This finding suggests that the switching pH of MEA-LCFA surfactants correlates well with the apparent pK_a values of their acid components. However, these correlations are valid only for solution responses.

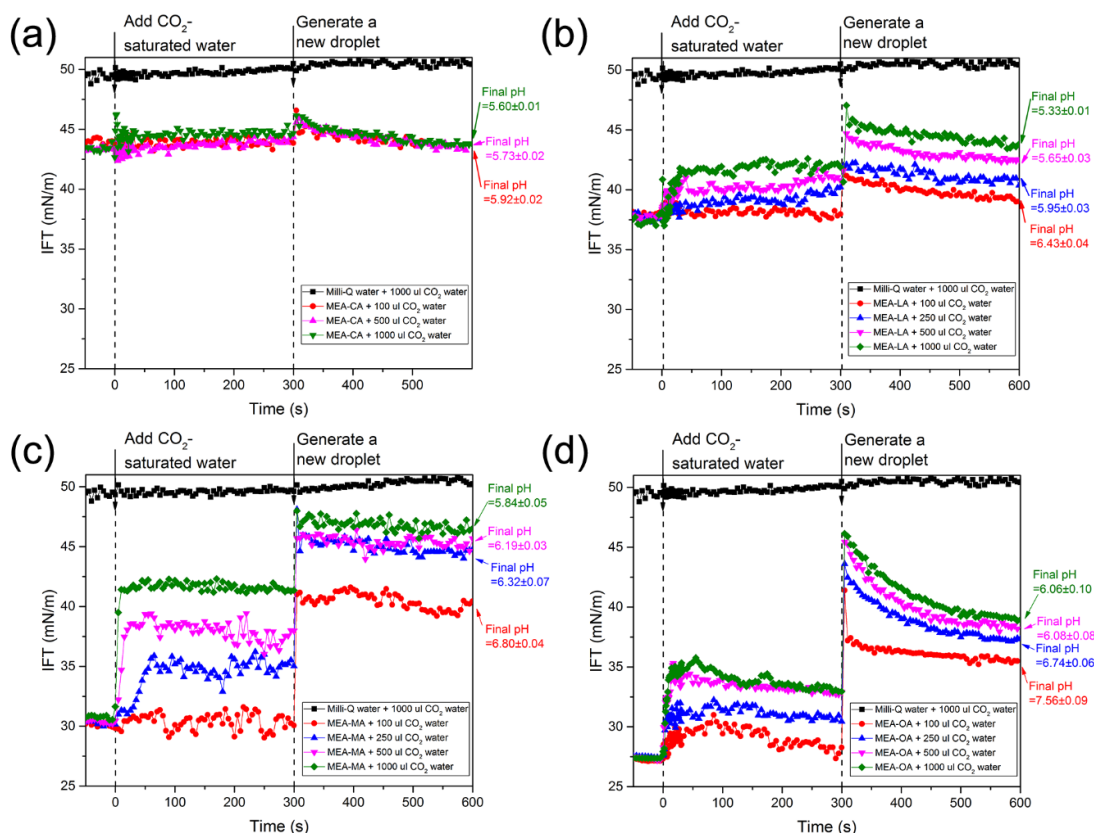


Figure 4.5. Dynamic IFT experiments following modified Protocol 1 at the heptane/water interface: (a) MEA-C; (b) MEA-LA; (c) MEA-MA; and (d) MEA-OA.

The subsequent Protocol 1 tests revealed that the CO₂-responses of MEA-LCFA surfactants at the interface were not identical to that in solutions (Figure 4.5). The tests using modified Protocol 1 always resulted in higher IFT values than that obtained using the original Protocol 1. The difference between these two protocols is that Protocol 1 monitors interfacial changes exclusively, while the modified Protocol 1 probes changes in solution. Furthermore, the equilibrium IFTs measured in the modified Protocol 1 are comparable to the values obtained using Protocol 2 at similar pH values. Therefore, it can be concluded that both results represent solution responses of MEA-LCFA surfactants to CO₂ addition or pH change.

Finally, the CO₂-responses of MEA-LCFA surfactants at the heptane/water interface and in bulk solution are both summarized in Figure 4.6. The switching at the oil/water interface is not identical to that in the bulk solution, arising from a different state of interfacial activity after switching. More importantly, there are two different switching pHs that activate the responses at the interface and in solution. As indicated early, the switching pH could be predicted by the apparent pK_a of the acid component only for solution switching (Figure 4.4). Furthermore, MEA-LCFA surfactants displayed a weaker IFT change when switched at the interface by CO₂ addition. However, it should be noted that there is always an excess amount of surfactants present in bulk solutions in real applications of interfacial switching. In this case, the surfactants remained in the bulk solution would be switched off first at pH close to pK_a values of corresponding LCFAs before corresponding interfacial switching at a much lower pH as illustrated in Figure 4.6. To confirm this hypothesis, the interfacial switching experiments were conducted at three different MEA-OA bulk concentration of 1 mM, 1.61 mM and 2.18 mM. Despite a decrease in initial IFT of the system with increasing MEA-OA surfactant concentration, the interfacial switching was observed at

pH~7.6 for all three tested concentrations, further confirming the nature of interfacial switching being characteristics of surfactant system.

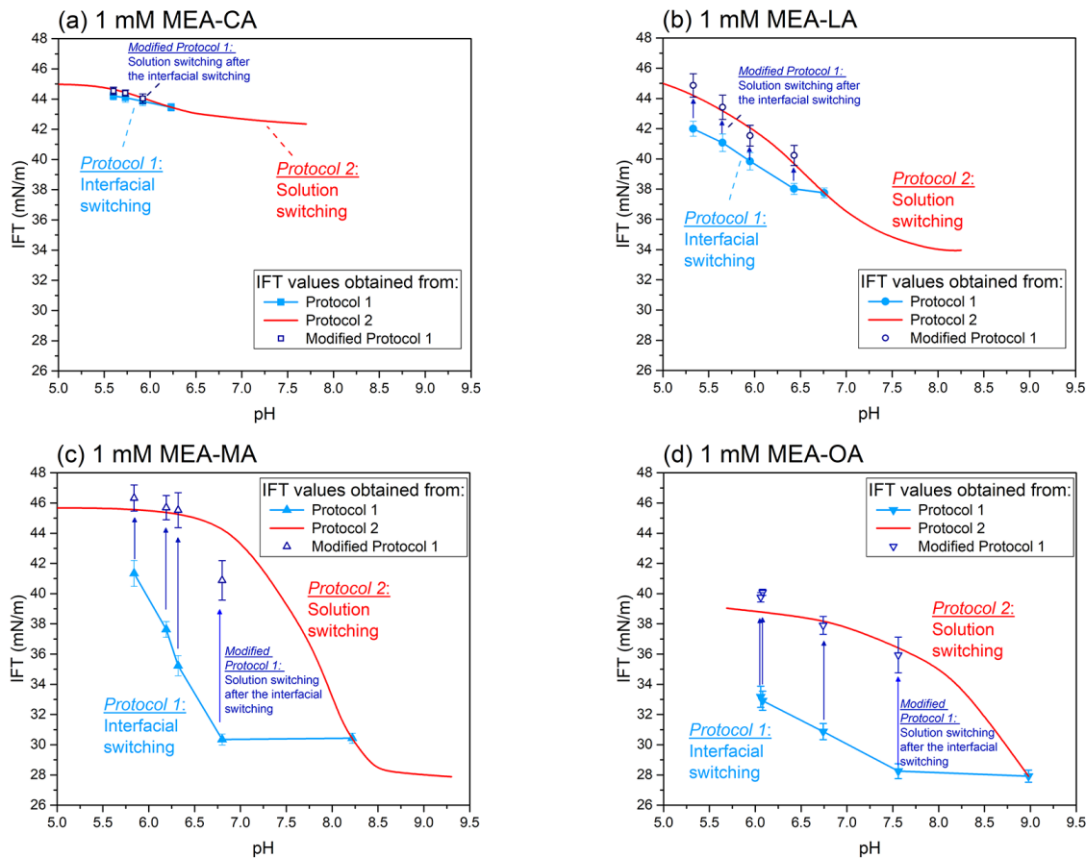


Figure 4.6. Responses at oil/water interface and in bulk solution of the MEA-LCFA surfactants to CO₂ addition: (a) 1mM MEA-CA; (b) 1mM MEA-LA; (c) 1mM MEA-MA; and (d) 1mM MEA-OA.

The difference between interfacial responses and solution responses of MEA-LCFA surfactants to CO₂ addition was further confirmed by the coalescence time between two heptane droplets in surfactant solutions. Coalescence time represents a minimum time required for two droplets in contact to become a single drop, which is of practical applications such as in demulsification. In general, a longer coalescence time refers to a more stable emulsion, which is more unlikely to be

demulsified. For instance, heptane droplets coalesced instantaneously in Milli-Q water, indicating a fast phase separation of heptane-in-water emulsions without any chemical treatment. In contrast, droplets soaked in MEA-OA solution remained separated even at an extended contact time, indicating a system of stable emulsions. More importantly, the setup of coalescence time measurement allows both “interfacial switching” and “solution switching” protocols to be probed (Figure 4.7a).

A significant difference in coalescence time was determined for two heptane droplets in MEA-OA solution treated by “interfacial switching” and “solution switching” protocols. In order to correlate the measured coalescence time with IFTs measured early in MEA-OA solutions, seven representative situations of the dynamic IFT measurements were considered in the coalescence time measurement, and the results were labeled accordingly (inset of Figure 4.7b). As shown in Figure 4.7b, heptane droplets were much harder to coalesce for the cases where MEA-OA were switched at the interface (cases #2, #3, #4). The coalescence of droplets was not observed in these scenarios unless the solution pH was decreased to be much lower than the interfacial switching pH determined by *in situ* probing methods. In contrast, the coalescence time became almost instantaneous if the MEA-OA solution was switched before the generation of heptane droplets (cases #5, #6, #7). Only a small change in solution pH was needed to decrease the coalescence time significantly. Figure 4.7c shows the images captured for different situations at the contact time of 10000 ms. Droplets in case #1 and case #2 did not coalesce, while droplets in case #4 became coalesced into a larger drop one after a long contact time.

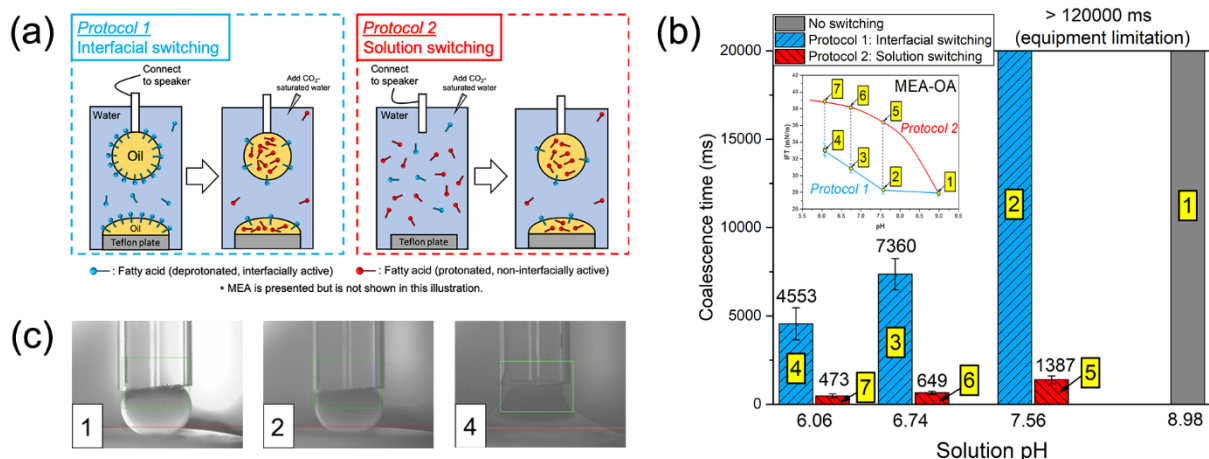


Figure 4.7. (a) Schematic drawings to show two experimental protocols of coalescence time measurement corresponding to Protocol 1 or Protocol 2 described in Figure 4.3; (b) Coalescence time of two heptane droplets measured in 1 mM MEA-OA solutions with the solution conditions and switching protocols being chosen from the previous IFT experiments and labelled in the inset; and (c) Images captured during coalescence experiments at the contact time of 10000 ms from Left (case #1), Mid (case #2) and Right (case #4) corresponding to no switching, switching at the interface, and further switching at the interface.

Results of droplet-droplet coalescence time are consistent with the previous analysis from IFT results. IFT measurements showed a weaker response of MEA-LCFA surfactants to CO₂ addition at the oil-water interface than in bulk solution, arising from less significant changes in interfacial activity after CO₂ addition and leading to a much lower switching pH value. The coalescence time of droplets obtained by Protocol 1 (i.e., interfacial switching) was found to be significantly longer than those by Protocol 2 (i.e., solution switching). In general, both IFT and coalescence time are not only correlated with the pH condition in the aqueous phase but also strongly dependent on whether the CO₂-response was activated at the interface or in bulk solutions.

Understanding the mechanism of shifting switching pH at the interface is essential to design appropriate responsive surfactants for desired applications. Initially, we attempted to correlate the switching pH to the apparent pKa of LCFAs reported in literature [23-27]. A brief summary of the reported pKa values is listed in Figure 4.8. However, most of the reported apparent pKa values were obtained from the acid/base titration technique, which is equivalent to the case of solution switching (Protocol 2). Hence, the calculation from these values is not appropriate for deriving interfacial responses.

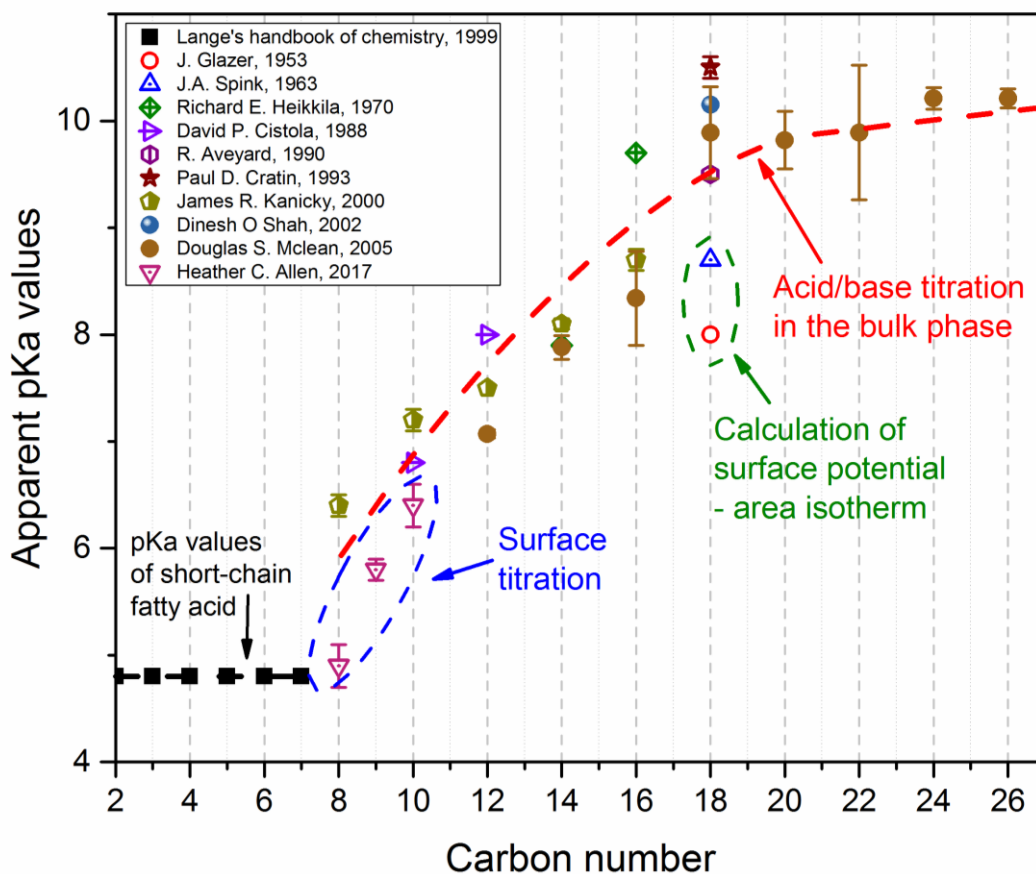


Figure 4.8. Apparent pKa values of LCFAs reported in literature [23-27, 40-46].

Meanwhile, there were few attempts conducting pKa determinations at an interfacial environment, all of which resulted in relatively lower apparent pKa values [27, 41, 42]. The “surface-pKa” of mid-chain fatty acid (C₈ – C₁₀) [27] was reported to be slightly lower than that obtained from the titration method of bulk solutions [23, 26]. Their methodology of “surface tension titration” is similar to our Protocol 1 (i.e., interfacial switching). The observed inconsistencies were attributed by these authors to the differences between measurement techniques [27]. We propose that the shift of switching pH to lower values could be attributed to the increase in intermolecular interactions of MEA-LCFA surfactants at the interface. Through a theoretical approaches using quantum chemical calculation, Sakurai et al. showed that the binding energy at the interface is amplified [47, 48]. The ion pair formed at the interface was found to have a potential minimum, where the separation or compression of counter-ions is energetically unfavorable. As a result, a significant energy barrier needs to be overcome for the dissociation of assembled molecules at the interface. The potential minimum is shallower for the ion pairs are formed in the bulk aqueous phase [47], suggesting a much easier dissociation of ion pairs in the bulk. Similar conclusions were reported by Eiseenthal et al., stressing a general trend of decreasing free energy of the system by neutralizing the charged species at the interface [49]. In fact, the enhancement of bindings at the interface is commonly seen in biological systems and known as molecular recognition. Such binding occurs typically at microscopic interfaces such as the bilayer of cell surfaces [50, 51]. Experimentally, Onda et al. reported a significantly enhanced hydrogen bonding and/or electrostatic interaction (around 10⁶ – 10⁷ times stronger) at the interface than in the aqueous phase [52]. Detected by second harmonic generation (SHG), Eiseenthal emphasized that the formation of acid/base pairs is strongly favored at the interface [53].

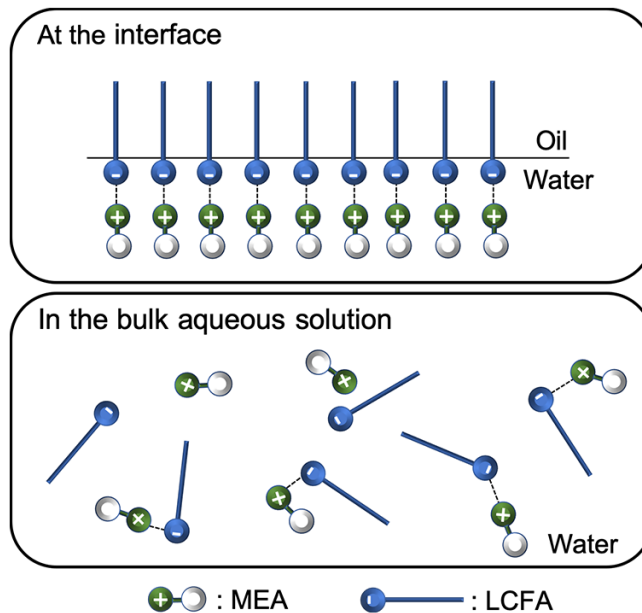


Figure 4.9. Schematic drawing of MEA-LCFA surfactants at the interface and in the bulk aqueous solution.

Others suggested the enhanced interactions at the interface probably because of the molecular ‘smoothness’ of the interface, which leads to a more organized orientation of surfactants at that interface [52, 54]. Figure 4.9 illustrates the proposed orientation of MEA-LCFA surfactants at the interface and in the bulk aqueous solutions. The microenvironment near the interface restricted the rotation of surfactants. The most reasonable placement of an ion pair at the interface was calculated to be the case where the hydrophobic moieties immerse in the low dielectric oil phase ($\epsilon = 2$) and the ionic binding sites remained in the aqueous phase ($\epsilon = 80$) [47]. The high interfacial excess of MEA-LCFA surfactants also places restrictions on the freedom of ion pairs moving at the interface. With these restrictions in the rotation and displacement, the probability of ion pair dissociation becomes less likely to occur. Considering these facts, one would expect a stronger electrostatic interaction between MEA^+ and LCFA^- at the interface than in the bulk solution, suppressing the

protonation of LCFA⁻ at the interface and hence showing a lower switching pH. Besides, this shift in switching pH is considered to be generally applicable regardless of the nature of the oil phase. Due to its low dielectric constant, the impact of oil type is relatively small.

4.3.4 Impacts on practical applications

In most practical applications, CO₂-responsive surfactants are switched at the interface. In a typical demulsification process, for example, MEA-LCFA surfactants are supposed to be interfacially active prior to the activation of their CO₂-responses. The switching pH of CO₂-responsive surfactants should therefore be determined through *in situ* probing of interfacial responses so that the results are more relevant and reliable. Although the switching pH values corresponding to solution responses of MEA-LCFA surfactants are much easier to derive from apparent pK_a values, they are less valuable in real applications. In the following part of this paper, two potential applications involving MEA-LCFA surfactants were considered to prove that the switching pH obtained from interfacial responses matched extremely well with macroscopic colloidal phenomena.

4.3.4.1 Switching of emulsion stability

Controlling emulsion stability is one of the most common and important applications of CO₂-responsive surfactants. Efficient demulsification requires the ability of surfactants to lose their surface activity and leave the oil-water interface, thus increasing the IFT and decreasing droplet-droplet coalescence time. The demulsification of heptane-in-water (H/W) emulsion stabilized by MEA-OA was first investigated. In order to correlate the results with the findings derived from probing interfacial properties, the pH conditions of emulsions were carefully titrated by bubbling CO₂ into the emulsion as a function of time. Visual observation of emulsion stability in Figure

4.10 shows an excellent agreement with the results of previous analysis on interfacial responses of MEA-LCFA surfactants. There is no change in emulsion stability with decreasing emulsion pH when the solution pH is higher than the interfacial switching pH. Once the switching pH of 7.60 determined using Protocol 1 was reached, the demulsification occurred gradually. Unfortunately, the lowest pH that can be obtained by CO₂ bubbling is not sufficient to switch off the interfacial activity of MEA-OA completely. Further acidification of the aqueous phase by HCl addition is needed to enhance the demulsification to a transparent oil phase at pH 3.04 as shown in Figure 4.10.

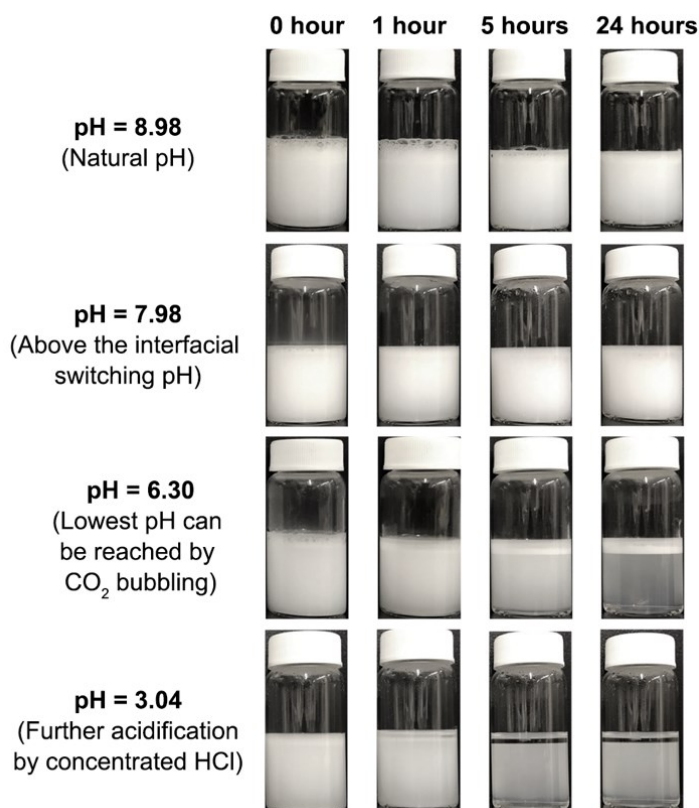


Figure 4.10. Visual observation of demulsifying heptane-in-water (v:v = 1:10) emulsions stabilized by MEA-OA by bubbling CO₂ up to pH 6.30 and then HCl addition to pH 3.04.

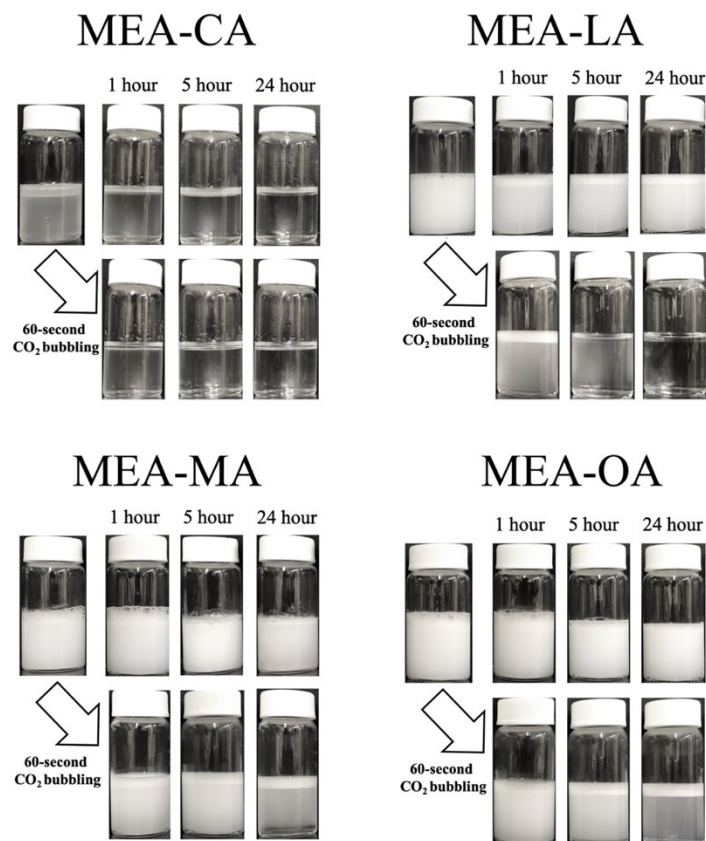


Figure 4.11. Demulsification efficiency was evaluated qualitatively by emulsion stability, where heptane-in-water (v:v = 1:10) emulsions were stabilized by different MEA-LCFA surfactants.

Other MEA-LCFA surfactants were also evaluated by their ability to demulsify stable emulsions as shown Figure 4.11. MEA-CA alone was not able to provide a strong interfacial activity to stabilize the H/W emulsion. H/W emulsion stabilized by MEA-LA are phase separated completely after CO₂ bubbling of the emulsion to pH 5.45, which is significantly lower than the switching pH of MEA-LA determined using Protocol 1. As for the MEA-MA and MEA-OA, demulsification occurred only marginally with the bubbling of CO₂ through the emulsions. It was noticed that the solution pH after CO₂ bubbling was only 6.21 in MEA-MA and 6.30 in MEA-OA. Based on the

results in Figure 4.2d, these were the pH range where the interfacial responses were just activated. These results confirm that the switching pH obtained by the *in-situ* probing method is more appropriate to predict the demulsification by turning off the surface activity of responsive surfactants through bubbling of CO₂ or/and acid addition.

4.3.4.2 Switching of physical properties at bitumen-water interfaces

The ability of CO₂-responsive surfactants to switch surface wettability of bitumen in water is shown in Figure 4.12. Bitumen was used as an example of extra heavy crude oil. The bitumen-air bubble attachment time, defined as the contact time at which 50% of air bubbles attach to the bitumen surface, is used as a measure of bitumen surface wettability, which is of great practical importance in heavy oil production [55]. Despite hydrophobic nature of oil, bitumen surfaces immersed in Milli-Q water exhibited a bitumen-air bubble attachment time of 1900 ms due to the presence of natural surfactants [1], showing a moderate hydrophobicity of the bitumen surface in water. These natural surfactants were not switchable, as shown by an almost unchanged attachment time of 1867 ms after CO₂ bubbling. Bitumen surfaces immersed in MEA-LCFA aqueous solutions became hydrophilic, demonstrated by their inability to attach to air bubbles within the experimental contact time of 5000 ms. This finding indicates a more surface-active nature of MEA-LCFA than natural surfactants in bitumen that they displaced to some degree the original surfactants at the bitumen-water interface.

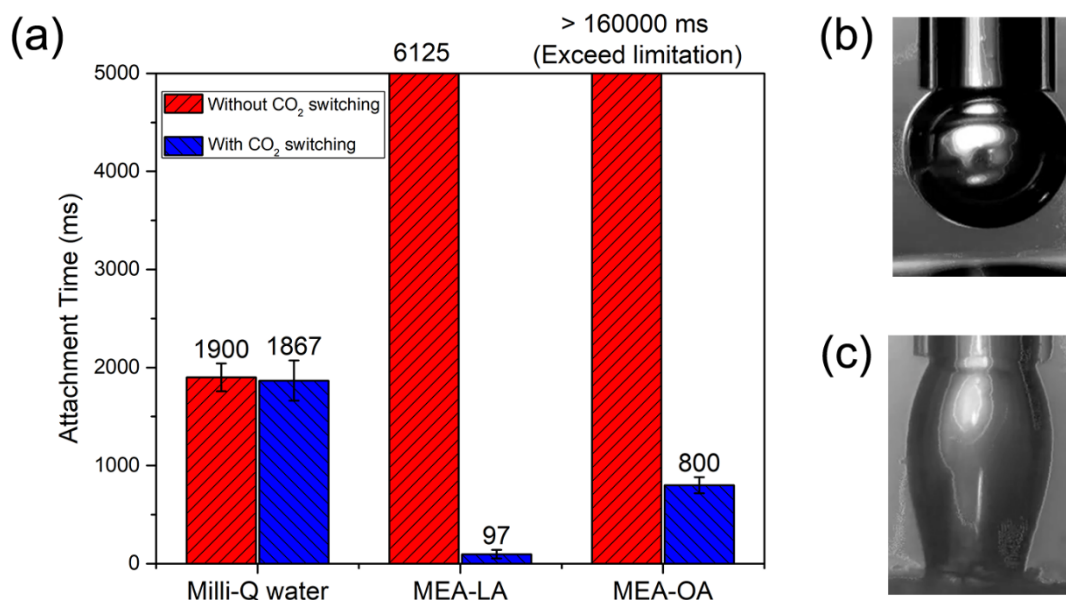


Figure 4.12. (a) Attachment time of an air bubble to a bitumen surface in MEA-LCFA surfactants with and without CO₂ bubbling; (b) Bitumen-air bubble contact in 1 mM MEA-LA solution for 1000 ms without CO₂ bubbling; and (c) Bitumen-air bubble contact in 1 mM MEA-LA solution for 100 ms with CO₂ bubbling.

More importantly, bitumen surfaces modified by MEA-LCFA aqueous solutions became more hydrophobic than natural bitumen after switching by CO₂ bubbling. The bitumen-air bubble attachment occurred at a contact time of 97 ms and 800 ms for MEA-LA and MEA-OA after CO₂ bubbling, respectively. After switching, MEA-LCFA became surface inactive and less hydrated than natural surfactants at bitumen-water interface, making the bitumen surface more hydrophobic and leading to an easier attachment to air bubbles as observed. The effectiveness of reducing attachment time by MEA-OA was not as strong as that by MEA-LA. Such difference between MEA-LA and MEA-OA matches well with the prediction on the interfacial responses of MEA-LCFA surfactants. The solution pH after CO₂ bubbling was 5.28 for MEA-LA solution and 6.13 for MEA-OA solution. According to the interfacial responses results (Figure 4.2d), MEA-LA is

much less surface active than MEA-OA at their corresponding pH conditions after being switched at the interface, i.e., a more hydrophobic interface is recovered by MEA-LA after switch. Nevertheless, both surfactants could enhance bitumen-air bubble attachment after CO₂ bubbling, which provides an effective avenue to separate or recovery heavy oil by flotation after the emulsification of heavy oil in reservoir using MEA-LCFA surfactants for production and subsequent switching by CO₂ bubbling of produced fluids at desired operating pHs.

4.4 Conclusions

In this work, a series of CO₂-responsive surfactants (MEA-LCFAs) were assembled by the non-covalent association between MEA and LCFAs. Compared with previous reports of CO₂-responsive surfactants [5, 8, 9, 19-21, 32], the switching pH of MEA-LCFA surfactants prepared in this study could be easily tuned by using different types of LCFAs, which provides a facile routine of customization towards varieties of applications. More importantly, the results from this study emphasize that the determination of switching pH should be proceeded carefully since the switching behaviors of MEA-LCFA surfactants at the oil-water interface were found to be significantly different from that in bulk solutions. Dynamic IFT and coalescence time measurements were both effective tools to distinguish interfacial switching and solution switching by applying “adsorption-then-switch” or “switch-then-adsorption” protocols, respectively. Switching pH for the oil-water interface was found to be lower than that in bulk solutions, which is the result of stronger molecular interactions of switching molecules at the oil-water interface. This colloidal phenomenon is consistent with theoretical calculations reported in literature [47, 48], and more broadly speaking, similar to the observations of enhanced molecular recognition at biological interfaces [50-52, 56]. In most applications, CO₂-responsive surfactants are switched at the interface. Therefore, it is more appropriate to determine the switching pH from interfacial

responses of MEA-LCFA surfactants to predict their performance in practical applications, such as demulsification of stable emulsions and switching wettability of crude oil surfaces.

Despite the fact that interfacial responses are relatively difficult to probe, while the solution responses correlate directly with the reported apparent pKa values [23-27], this study emphasizes the importance of understanding interfacial responses for accurate determination of switching pH and better bridging with application scenarios, especially when considering responsive surfactants with tunable switching conditions. It is however important to determine whether the findings in this study are applicable to other types of responsive surfactants (e.g., UV-responsive surfactants [57, 58], magneto-responsive surfactants [59], etc.). This study also provides a valuable guidance in developing responsive materials with enhanced robustness and versatility for potential applications, such as enhanced oil recovery (EOR), wastewater treatment, contaminated soil remediation, and controlled drug delivery.

4.5 References

1. Masliyah, J., J. Czarnecki, and Z. Xu, *Handbook on theory and practice of bitumen recovery from Athabasca oil sands: Vol. I. Theoretical basis*. 2010: Kingsley Knowledge Publishing.
2. Wang, J., et al., *CO₂-switchable foams stabilized by a long-chain viscoelastic surfactant*. *Journal of Colloid and Interface Science*, 2018. **523**: p. 65-74.
3. Lu, H.S., et al., *Application of CO₂-triggered switchable surfactants to form emulsion with Xinjiang heavy oil*. *Journal of Dispersion Science and Technology*, 2014. **35**(5): p. 655-662.
4. Liang, C., Q. Liu, and Z. Xu, *Surfactant-free switchable emulsions using CO₂-responsive particles*. *ACS Applied Materials & Interfaces*, 2014. **6**(9): p. 6898-904.
5. Chen, X., et al., *CO₂-responsive o/w microemulsions prepared using a switchable superamphiphile assembled by electrostatic interactions*. *Journal of Colloid and Interface Science*, 2018. **534**, p.595-604.
6. Cherukupally, P., et al., *Acid–base polymeric foams for the adsorption of micro-oil droplets from industrial effluents*. *Environmental Science & Technology*, 2017. **51**(15): p. 8552-8560.

7. Kwok, M.-h. and T. Ngai, *Chapter 4 Responsive particle-stabilized emulsions: Formation and applications*, in *Smart materials for advanced environmental applications*. 2016, The Royal Society of Chemistry. p. 91-138.
8. Ceschia, E., et al., *Switchable anionic surfactants for the remediation of oil-contaminated sand by soil washing*. RSC Advances, 2014. **4**(9): p. 4638-4645.
9. Chen, Q., et al., *A fatty acid solvent of switchable miscibility*. Journal of Colloid and Interface Science, 2017. **504**: p. 645-651.
10. Huang, J., et al., *pH-responsive gas-water-solid interface for multiphase catalysis*. Journal of the American Chemical Society, 2015. **137**(47): p. 15015-25.
11. Xie, C.-Y., et al., *Light and magnetic dual-responsive pickering emulsion micro-reactors*. Langmuir, 2017. **33**(49): p. 14139-14148.
12. Abbaspourrad, A., S.S. Datta, and D.A. Weitz, *Controlling release from pH-responsive microcapsules*. Langmuir, 2013. **29**(41): p. 12697-702.
13. Werner, J.r.G., et al., *Hydrogel microcapsules with dynamic pH-responsive properties from methacrylic anhydride*. Macromolecules, 2018. **51**(15): p. 5798-5805.
14. Li, J., et al., *Novel phthalocyanine and PEG-methacrylates based temperature-responsive polymers for targeted photodynamic therapy*. Polymer Chemistry, 2013. **4**(3): p. 782-788.
15. Mihut, A.M., et al., *Tunable adsorption of soft colloids on model biomembranes*. ACS Nano, 2013. **7**(12): p. 10752-10763.
16. Brown, P., et al., *CO₂-reactive ionic liquid surfactants for the control of colloidal morphology*. Langmuir, 2017. **33**(31): p. 7633-7641.
17. Jung, H.B., et al., *Stimuli-responsive/rheoreversible hydraulic fracturing fluids as a greener alternative to support geothermal and fossil energy production*. Green Chemistry, 2015. **17**(5): p. 2799-2812.
18. Barzagli, F., F. Mani, and M. Peruzzini, *A ¹³C NMR study of the carbon dioxide absorption and desorption equilibria by aqueous 2-aminoethanol and N-methyl-substituted 2-aminoethanol*. Energy & Environmental Science, 2009. **2**(3): p. 322-330.
19. Fameau, A.L., et al., *Smart foams: switching reversibly between ultrastable and unstable foams*. Angewandte Chemie International Edition, 2011. **50**(36): p. 8264-9.
20. Xu, P., et al., *Highly effective emulsification/demulsification with a CO₂-switchable superamphiphile*. Journal of Colloid and Interface Science, 2016. **480**: p. 198-204.
21. Dai, S., et al., *Controllable CO₂-responsiveness of o/w emulsions by varying the alkane carbon number of a tertiary amine*. Physical Chemistry Chemical Physics, 2018. **20**(16): p. 11285-11295.
22. Yin, H., et al., *Insights into the relationship between CO₂ switchability and basicity: examples of melamine and its derivatives*. Langmuir, 2014. **30**(33): p. 9911-9.
23. Kanicky, J., et al., *Cooperativity among molecules at interfaces in relation to various technological processes: Effect of chain length on the pK_a of fatty acid salt solutions*. Langmuir, 2000. **16**(1): p. 172-177.

24. Kanicky, J.R. and D.O. Shah, *Effect of degree, type, and position of unsaturation on the pK_a of long-chain fatty acids*. Journal of Colloid and Interface Science, 2002. **256**(1): p. 201-7.
25. Kanicky, J.R. and D.O. Shah, *Effect of premicellar aggregation on the pK_a of fatty acid soap solutions*. Langmuir, 2003. **19**(1): p. 2034-2038.
26. McLean, D.S., et al., *The colloidal pK_a of lipophilic extractives commonly found in *Pinus radiata**. Appita journal, 2005. **58**(5): p. 362-366.
27. Wellen, B.A., E.A. Lach, and H.C. Allen, *Surface pK_a of octanoic, nonanoic, and decanoic fatty acids at the air–water interface: Applications to atmospheric aerosol chemistry*. Physical Chemistry Chemical Physics, 2017. **19**(39): p. 26551-26558.
28. Fameau, A.L. and T. Zemb, *Self-assembly of fatty acids in the presence of amines and cationic components*. Advances in Colloid and Interface Science, 2014. **207**: p. 43-64.
29. Klein, R., D. Touraud, and W. Kunz, *Choline carboxylate surfactants: biocompatible and highly soluble in water*. Green Chemistry, 2008. **10**(4): p. 433-435.
30. Novales, B., et al., *Self-assembly of fatty acids and hydroxyl derivative salts*. Langmuir, 2008. **24**(1): p. 62-68.
31. Arnould, A., et al., *Impact of the molar ratio and the nature of the counter-ion on the self-assembly of myristic acid*. Journal of Colloid and Interface Science, 2018. **510**: p. 133-141.
32. Xu, W., et al., *CO_2 -controllable foaming and emulsification properties of the stearic acid soap systems*. Langmuir, 2015. **31**(21): p. 5758-66.
33. Wang, L., et al., *Measurement of interactions between solid particles, liquid droplets, and/or gas bubbles in a liquid using an integrated thin film drainage apparatus*. Langmuir, 2013. **29**(11): p. 3594-603.
34. Wang, L., Z. Xu, and J.H. Masliyah, *Dissipation of film drainage resistance by hydrophobic surfaces in aqueous solutions*. The Journal of Physical Chemistry C, 2013. **117**(17): p. 8799-8805.
35. Martínez-Balbuena, L., et al., *Applicability of the Gibbs Adsorption Isotherm to the analysis of experimental surface-tension data for ionic and nonionic surfactants*. Advances in Colloid and Interface Science, 2017. **247**: p. 178-184.
36. Eastoe, J., et al., *Interfacial properties of a catanionic surfactant*. Langmuir, 1996. **12**(11): p. 2706-2711.
37. Berg, J.C., *An introduction to interfaces & colloids: the Bridge to nanoscience*. 2010: World Scientific.
38. Lu, Y., et al., *CO_2 -responsive surfactants with tunable switching pH*. Journal of Colloid and Interface Science, 2019. **557**: p. 185-195.
39. Greenwood, N.N. and A. Earnshaw, *Chemistry of the elements*. 1984.
40. Dean, J.A., *Lange's handbook of chemistry*. 1999: New york; London: McGraw-Hill, Inc.
41. Glazer, J. and M.Z. Dogan, *Ionization of protein monolayers and related substances*. Transactions of the Faraday Society, 1953. **49**(0): p. 448-455.

42. Spink, J.A., *Ionization of monolayers of fatty acids from C₁₄ to C₁₈*. Journal of Colloid Science, 1963. **18**(6): p. 512-525.
43. Heikkila, R.E., D.W. Deamer, and D.G. Cornwell, *Solution of fatty acids from monolayers spread at the air-water interface: Identification of phase transformations and the estimation of surface charge*. Journal of Lipid Research, 1970. **11**(3): p. 195-200.
44. Cistola, D.P., et al., *Ionization and phase behavior of fatty acids in water: Application of the Gibbs phase rule*. Biochemistry, 1988. **27**(6): p. 1881-1888.
45. Aveyard, R., et al., *Stability of insoluble monolayers and ionization of Langmuir-Blodgett multilayers of octadecanoic acid*. Thin Solid Films, 1990. **188**(2): p. 361-373.
46. Cratin, P.D., *Mathematical modeling of some pH-dependent surface and interfacial properties of stearic acid*. Journal of Dispersion Science and Technology, 1993. **14**(5): p. 559-602.
47. Sakurai, M., et al., *Theoretical study of intermolecular interaction at the lipid-water interface: 1. Quantum chemical analysis using a reaction field theory*. The Journal of Physical Chemistry B, 1997. **101**(24): p. 4810-4816.
48. Tamagawa, H., et al., *Theoretical study of intermolecular interaction at the lipid-water interface: 2. Analysis based on the Poisson-Boltzmann equation*. The Journal of Physical Chemistry B, 1997. **101**(24): p. 4817-4825.
49. Zhao, X., S. Subrahmanyam, and K.B. Eisenthal, *Determination of pK_a at the air/water interface by second harmonic generation*. Chemical Physics Letters, 1990. **171**(5): p. 558-562.
50. Milani, S., et al., *Association of polynucleotides with nucleolipid bilayers driven by molecular recognition*. Journal of Colloid and Interface Science, 2011. **363**(1): p. 232-240.
51. G. Argudo, P., et al., *Folding of cytosine-based nucleolipid monolayer by guanine recognition at the air-water interface*. Journal of Colloid and Interface Science, 2019. **537**: p. 694-703.
52. Onda, M., et al., *Molecular recognition of nucleotides by the guanidinium unit at the surface of aqueous micelles and bilayers: A comparison of microscopic and macroscopic interfaces*. Journal of the American Chemical Society, 1996. **118**(36): p. 8524-8530.
53. Eisenthal, K.B., *Liquid interfaces probed by second-harmonic and sum-frequency spectroscopy*. Chemical Reviews, 1996. **96**(4): p. 1343-1360.
54. Ariga, K., et al., *Tunable pK_a of amino acid residues at the air-water interface gives an L-zyne (Langmuir Enzyme)*. Journal of the American Chemical Society, 2005. **127**(34): p. 12074-12080.
55. Gu, G., et al., *Effects of physical environment on induction time of air-bitumen attachment*. International Journal of Mineral Processing, 2003. **69**(1): p. 235-250.
56. Pan, F., et al., *Surface active complexes formed between keratin polypeptides and ionic surfactants*. Journal of Colloid and Interface Science, 2016. **484**: p. 125-134.
57. Chevallier, E., et al., *Pumping-out photo-surfactants from an air-water interface using light*. Soft Matter, 2011. **7**(17): p. 7866-7874.

58. Brown, P., C.P. Butts, and J. Eastoe, *Stimuli-responsive surfactants*. *Soft Matter*, 2013. **9**(8): p. 2365-2374.
59. Paul, B., et al., *Magnetic control over liquid surface properties with responsive surfactants*. *Angewandte Chemie International Edition*, 2012. **51**(10): p. 2414-2416.

Chapter 5. CO₂-Responsive Surfactants for Conventional Heavy Oil

Recovery

Properties of the interface between oil and water are of essential importance to various separation applications, such as heavy hydrocarbon recovery. Low interfacial tension (IFT) is more favorable to separate the heavy oil from solids by surfactant washing, while higher IFT benefits the later stage of oil-water separation. Ideally, if interfacial properties can be switched during the separation process, it would considerably improve the overall performance. Therefore, we investigate the use of CO₂-responsive surfactants in heavy hydrocarbon recovery, which allows the manipulation of interfacial activity through the bubbling of CO₂ gas. The performance of CO₂-responsive surfactants in the oil-solid separation stage was evaluated by contact angle measurements and liberation visualization. Meanwhile, the subsequent stage of oil-water separation was studied by demulsification tests and droplet-droplet coalescence. It was demonstrated that the surfactants with stronger interfacial activity exhibited a more pronounced enhancement to the separation of heavy oil from solids substrates into the aqueous phase, whereas the resulting stable heavy oil-in-water emulsions could also be easily demulsified after the activation of CO₂-responsiveness. Additionally, CO₂-responsive surfactants could be partially recycled to improve sustainability. In general, CO₂-responsive surfactants are considered to be the novel processing aids to enhance the heavy hydrocarbon recovery, since they could enhance both oil-solid and oil-water separation stages by switching their interfacial activity to the desired state.

5.1 Introduction

Separating oil from solids is a common process in our daily life, such as in dishwashing [1] and doing the laundry [2, 3]. It is also essential to many commercial applications, such as enhanced oil recovery [4-6], contaminated soil remediation [7-9], and emulsion polymerization [10]. Surfactant washing, consisting of washing the oil-solid mixture by a surfactant aqueous solution, is one of the most direct and effective methods to achieve successful separation. The introduction of surfactants could reduce the oil-water interfacial tension (IFT) efficiently, which leads to lower contact angle at the oil-water-solid three-phase contact line and better emulsification of oil components in aqueous washing fluid. Consequently, oil detaches from its solid substrate easier, and the solid surface can be cleaned. However, when the oil components are carried out by aqueous medium, they are in the form of oil-in-water (O/W) emulsion due to the low IFT and separating oil and water becomes the new issue. These emulsions may contain valuable products (e.g., enhanced oil recovery), cause environmental pollution (e.g., industrial laundry and soil remediation), or accumulate surfactants in eco-system [11]. In general, interfacial activity is only needed temporarily for the oil-solid separation during surfactant washing, which soon becomes problematic for oil-water separation.

Stimuli-responsive surfactants are one of the most promising candidates to resolve the above-mentioned problem. Responsive surfactants are capable of providing switchable interfacial activity that can be switched on and off by external stimuli, such as temperature [12, 13], pH [14], CO₂ gas [6, 15, 16], UV radiation [17], and magnetic field [14, 18, 19]. Hence, they usually serve as multi-functional materials and improve the process sustainability. From the separation perspective, the “switch-on” and “switch-off” features of responsive surfactant should benefit both oil-solid and oil-water separation. Responsive surfactants enhance oil detachment by providing the desired

interfacial activity. After that, their interfacial activity should be switched off by an external stimulus to facilitate oil-water separation. In an ideal scenario, clean solids would be filtered out in the first stage, while the oil and water components are separated in the following stage. Since one addition of responsive surfactants can serve multiple purposes, their successful implementation would have positive impacts on both economics and environments.

Although responsive surfactants possess great potential, there are still many considerable obstacles for their utilization. Responsive surfactants are usually more expensive than conventional surfactants, which results in economic barriers for commercialization [20]. On the other hand, triggering the switch of responsive surfactants may require extra energy input (e.g., changing temperature for thermal response), may produce secondary pollutant (e.g., salt accumulation for pH response), or may even be inefficient in harsh conditions (e.g., turbidity and opacity limits for UV response). In addition, the introduction of a switching mechanism would dramatically increase the difficulty of process design. Hence, responsive surfactants are mostly applied to well-designed small-scale chemical processes with high additional value such as controlled drug delivery system [21-23].

In an effort to bring these attractive chemicals into large-scale separation application, novel responsive surfactants should be easy-to-use, versatile and robust in various operating conditions. In our previous study, we developed a series of CO₂-responsive surfactants with tunable switching pH [15]. These CO₂-responsive surfactants were easily formed by mixing monoethanolamine (MEA) with long-chain fatty acids (LCFAs) in aqueous medium. Both compositions are commercially available at low prices, which alleviates the economic concerns. The tunability of switching pH permits the customization of surfactants regarding specific chemical processes, such that a suitable reagent could be readily selected according to requirements [15]. Furthermore, the

external stimulus, CO₂ gas, is also inexpensive, abundant in nature, and usually available onsite in the flue gas [11, 20, 24]. Hence, this series of MEA-LCFAs surfactants are promising to resolve the IFT conflicts between the oil-solid and oil-water separations.

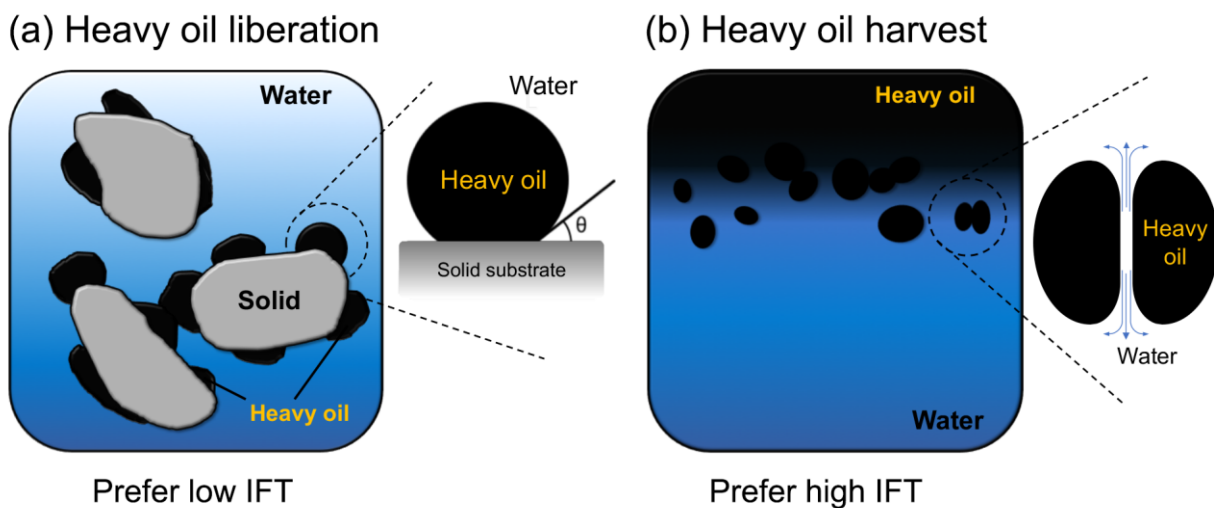


Figure 5.1. Schematic diagram of the two major stages in heavy oil recovery process: (a) Heavy oil liberation; and (b) Heavy oil harvest.

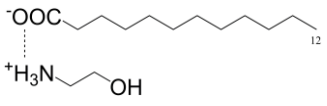
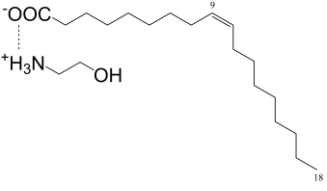
Due to our specific interest, we focused on the application of CO₂-responsive surfactants for enhancing heavy oil recovery, which is one of the most studied separation applications and is also remarkably large in scale. The primary goal for heavy oil recovery is to extract more hydrocarbon from the petroleum reservoir. Two major stages are considered in this process and are illustrated in Figure 5.1. The separation of heavy oil from solid substrate by surfactant washing is referred as the “*heavy oil liberation*”, whereas the subsequent stage of separating heavy oil from aqueous phase is denoted as the “*heavy oil harvest*”. As mentioned, the liberation stage would prefer low oil-water IFT, while the latter stage benefits from a high IFT. Successful enhancement of heavy oil recovery could only be achieved if both stages are significantly facilitated.

In this study, we investigated two representative CO₂-responsive surfactants from the MEA-LCFAs series by their performance in each stages of the heavy oil recovery process. The enhancement of heavy oil liberation was demonstrated by contact angle measurements on model system and liberation experiments on real petroleum ores. On the other hand, the effect of CO₂-responsive surfactants on heavy oil harvest was evaluated by demulsifying heavy oil-in-water emulsions and studying droplet-droplet coalescence. Furthermore, the recyclability of CO₂-responsive surfactants after the recovery process was also explored by analyzing both heavy oil products and aqueous tailings water.

5.2 Material and Methods

Lauric acid (LA) (99%, Fisher Scientific), oleic acid (OA) (> 95%, Fisher Scientific), monoethanolamine (MEA) (> 99%, Sigma-Aldrich) and toluene (> 99.5%, Fisher) were used as received without further purification. CO₂ gas (medical grade, Praxair) was also used as received. Details of the investigated surfactants are given in Table 5.1.

Table 5.1. Molecular structures and key properties of the CO₂-responsive surfactants

Full name	Abbrev.	Molecular structure	Molecular weight (g/mol)	Natural pH	Switching pH at the interface
Monoethanolamine – Lauric acid	MEA-LA		261.39	~ 6.76	~ 6.4 [15]
Monoethanolamine – Oleic acid	MEA-OA		334.55	~ 8.98	~ 7.6 [15]

The contact angle in the aqueous phase was measured by the micropipette system as previous introduced in Section 3.3. Experimental details could also be found in previous reports [25, 26]. Herein, the measurement was initiated by placing the oil-covered silica surface into the surfactant solution and the dynamic contact angles in the aqueous phase were obtained by analyzing the sequence of recorded images

Heavy oil liberation from the petroleum ores was studied by the custom-designed liberation visualization cell system. Details on the experimental setup could be found elsewhere [27, 28]. In general, the heavy oil liberation process was monitored by a camera for a duration of 600 s starting from the addition of surfactant solution. The “*degree of heavy oil liberation (DOL)*” as a function of the run time was analyzed off-line by an image processing method also given in a previous report [28]. Each experimental condition was conducted at least three times.

Demulsification of heavy oil-in-surfactant aqueous solution emulsions was assessed by comparing their stability with and without CO₂ bubbling. Due to the high viscosity of the heavy oil samples (2.22×10^3 Pa·s), the heavy oil used in this part of the study was diluted by toluene (1 wt.% heavy oil in toluene). Diluted heavy oil (15 ml) was mixed with surfactant aqueous solution (5 mM, 15 ml) in a glass vial. The mixture was then homogenized by a homogenizer (VWR[®] 250) at 30,000 rpm for 60 s. The demulsification process was conducted by continuous bubbling of CO₂ into the emulsions for sufficient time until no visual change was observed (typically required ~ 120 s). Demulsification efficiency was evaluated by the volume of the black heavy oil in the upper layer.

The coalescence between two interacting toluene-diluted heavy oil droplets was studied by an integrated thin film drainage apparatus (ITFDA). Details of this instrument [29, 30] as well as the modified methodology used here [15] were given in Section 3.4. Generally, two diluted heavy oil

droplets were generated in the CO₂-responsive surfactant solution (5 mM, 15 ml). One droplet was placed at the bottom by coating onto a Teflon surface, while the other was suspended on the top at the tip of a glass tube. A sufficient aging time (~ 30 min) was given to ensure the equilibrium of surfactant adsorption. The interfacial response of the CO₂-responsive surfactants at the heavy oil-water interface was activated by adding CO₂-saturated water (3 ml) into the surfactant solution. The reason for using CO₂ water instead of CO₂ bubbling was to avoid issues that can increase experimental error, such as the environmental disturbance and the bubble attachment to oil droplets. Another equilibration time of 30 min was given to ensure the new equilibrium was reached after the interfacial switching. After that, the droplets were driven to touch each other for 120 s, and the process was recorded by a high-speed camera. The coalescence time was obtained by analyzing the video frame-by-frame. Experiments were conducted at least three times. The interfacial activity of the remaining aqueous solution was determined by T200 Theta Optical Tensiometer (Biolin Scientific) using the pendant drop method.

5.3 Results and Discussion

5.3.1 Effect of CO₂-responsive surfactants on heavy oil liberation

The effect of CO₂-responsive surfactants on heavy oil liberation can be preliminarily described by the change on the aqueous-phase contact angle (θ) at the heavy oil-water-solid three-phase contact line, as illustrated in the inset of Figure 5.1a. A smaller value of the contact angle indicates a weaker interaction between heavy oil and solid substrate [31, 32], and thereby allows heavy oil to be swept out more efficiently [33]. It is known that the contact angle, θ , is governed by Young's equation [34]:

$$\cos \theta = (\gamma_{os} - \gamma_{ws})/\gamma_{ow} \quad (5.1)$$

where γ_{os} , γ_{ws} , and γ_{ow} are the interfacial tensions (IFTs) of the oil-solid, water-solid, and oil-water interfaces, respectively. Adding surfactants decreases the oil-water IFT (γ_{ow}) and thereby reduces the contact angle in the aqueous phase, resulting in the enhancement of heavy oil liberation.

The interfacial activity of CO₂-responsive surfactants at the oil-water interface has been described in our previous study [15]. In general, both MEA-LA and MEA-OA are capable of decreasing the oil-water IFT efficiently. MEA-OA is slightly more interfacially active when its concentration in the aqueous phase ranges from 0.1 mM to 20 mM, whereas MEA-LA is more active at concentrations above 20 mM. It has also been demonstrated that the interfacial behavior of surfactants is independent of the nature of the oil phase [15, 35], that means, such interfacial activity is generally applicable to the heavy oil-water interface.

The recession of the droplet in the presence of CO₂-responsive surfactants was studied in a model system using the micropipette technique. A spherical silica cap was initially covered by high viscous model oil. As soon as the oil-covered silica cap was submersed into the aqueous phase, the oil drop started to recede on the solid surface spontaneously (Figure 5.2a), which simulates the liberation of heavy oil on the solid substrate during surfactant washing. The temporal evolution of the contact angles in the aqueous phase is exhibited in Figure 5.2b. It was found that the addition of both CO₂-responsive surfactants would slow down the receding rates initially, but ended up in smaller static contact angles. MEA-OA had a more pronounced impact on slowing down the receding rate, as well as on decreasing the contact angle. Meanwhile, the values of static contact angles were obtained when the change of dynamic contact angle became negligible over time. It is shown that the static contact angles gradually reduced with increasing surfactant concentration

(Figure 5.2c). The contact angles measured in MEA-OA solutions were always slightly lower than those in MEA-LA solutions at the same concentration, which is consistent with MEA-OA being more interfacially active than MEA-LA at low concentration (< 20 mM) [15]. When treated with 5 mM MEA-OA solution, the oil drop would detach from the silica surface even before equilibrium was reached, which was caused by the buoyance force. Nevertheless, these results of contact angle measurements suggest that heavy oil would become much easier to be liberated from the solid substrates with the aid of CO₂-responsive surfactants.

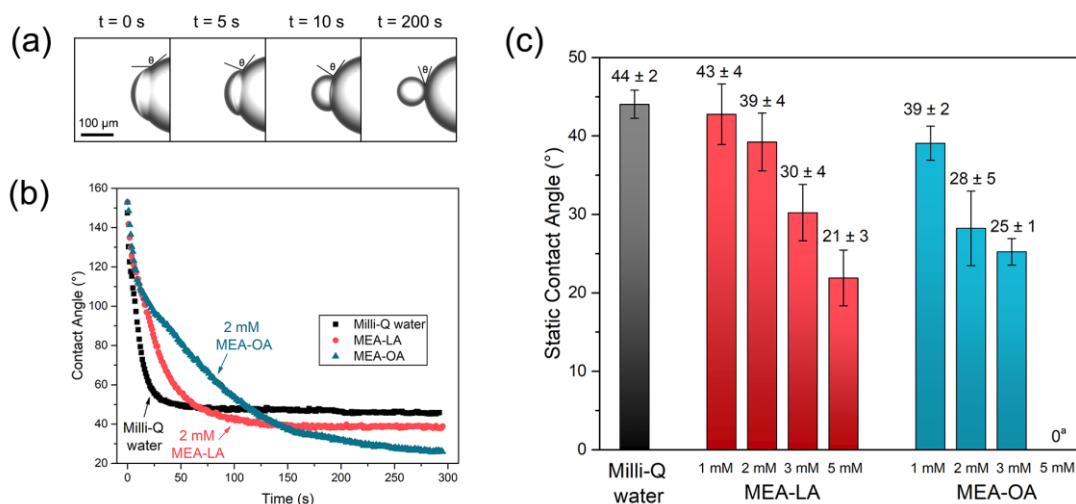


Figure 5.2. (a) Snapshots of the high viscosity oil droplet receding on a silica surface in Milli-Q water; (b) Dynamic contact angle in the first 300 s; and (c) Static contact angles in different aqueous solutions. ^a The oil drop detached from the silica surface in 5 mM MEA-OA solution, thus showing a contact angle with zero degree.

The heavy oil liberation process on real petroleum ores was investigated by a house-made heavy oil liberation visualization cell system. The liberation cell was explicitly designed to monitor heavy oil liberation [27]. Figure 5.3a shows snapshot images obtained from the experiments. At first

glance, there is a significant reduction of “dark” areas on the ore surfaces after being immersed in the aqueous solution for 600 s. Such a phenomenon illustrates the release of heavy oil from their host surfaces. Furthermore, ores treated by CO₂-responsive surfactant solutions appears to be “brighter” than that treated by Milli-Q water at t = 600 s, which readily implies the enhancement of heavy oil liberation by adding CO₂-responsive surfactants.

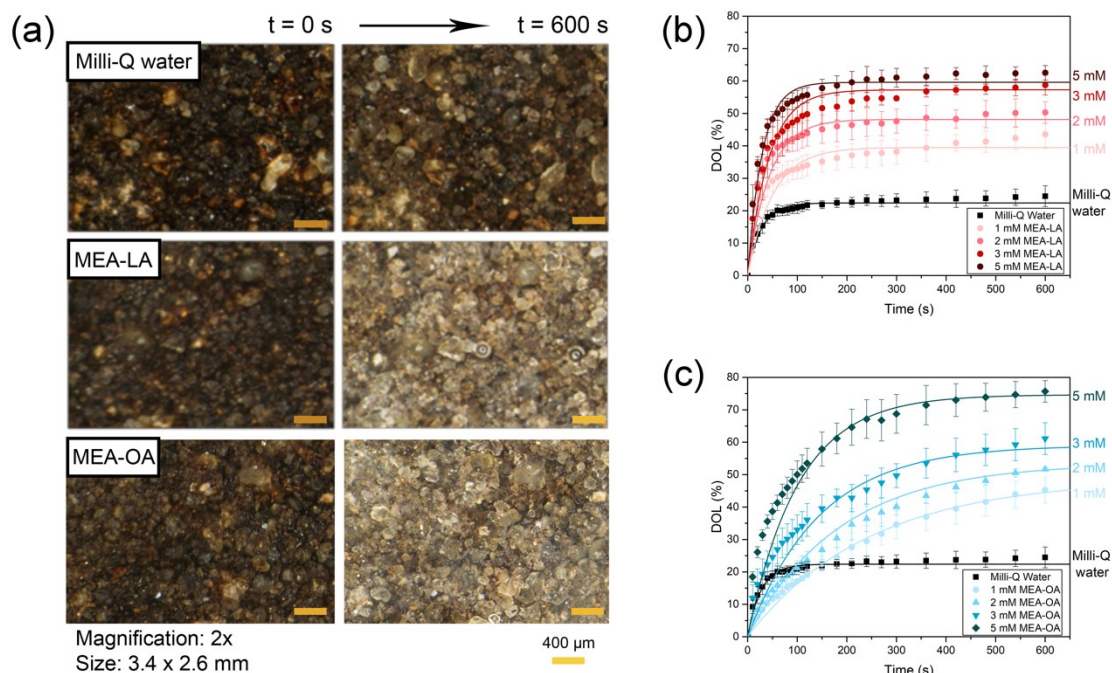


Figure 5.3. (a) Typical images from the house-made heavy oil liberation visualization cell system; Temporary evolution of heavy oil liberation for the petroleum ores treated by MEA-LA solution (b) and MEA-OA solution (c).

Details of the heavy oil liberation process were elucidated by analyzing the degree of heavy oil liberation (DOL). DOL values were calculated from the real-time images in liberation cell experiments using the image processing method previously reported [28]. Experimental results are given as the scatter points in Figures 5.3b & 5.3c. In an effort to understand the kinetics of heavy

oil liberation, one could consider the liberation process as a first order reaction, i.e., the liberation rate is proportional to sand areas covered by bitumen and the rate of reverse process be negligible. With the DOL values being the percentage of sand areas that is free of bitumen, a simple approach of kinetics analysis is to fit the dynamic liberation data by the first-order kinetics model with an exponential expression as following [36]:

$$\text{DOL (\%)} = A[1 - \exp(-kt)] \quad (5.2)$$

where A (%) refers to the ultimate DOL and k (s^{-1}) represents the rate constant of heavy oil liberation. In Eq. 5.2, a zero DOL value is given at the initial point ($t = 0$ s), representing no heavy oil liberation. On the other hand, the ultimate DOL is defined as when the ores are treated by the aqueous solution for a sufficiently long time. Approaching the limit of $t \rightarrow \infty$ would result in $\text{DOL}|_{t \rightarrow \infty} = A[1 - \exp(-kt)]|_{t \rightarrow \infty} = A$. Finally, a higher value of k refers to a faster increase of the DOL value, thus considering as a faster rate of heavy oil liberation. Obviously, it is preferable of have a higher value of both ultimate DOL (A) and liberation rate (k).

Both MEA-LA and MEA-OA boosted the ultimate DOL values (A) but also slow down the liberation rate (k) at the same time. The values of the fitting parameters are summarized in Table 5.2 for each liberation condition. CO_2 -responsive surfactants have a dramatic impact on the ultimate DOL due to their strong interfacial activity, resulting in more than threefold enhancements using 5 mM MEA-OA solution. MEA-OA addition was slightly more effective than MEA-LA addition at the same bulk concentration, since MEA-OA is more interfacially active [15]. In fact, there appears to be a clear relationship between the ultimate DOL and the surfactant interfacial activity (Figure 5.4). This relationship supports our hypothesis that reducing the oil-water IFT is key to enhancing heavy oil liberation. On the other hand, CO_2 -responsive surfactants also slowed

down the value of k_i . Indeed, such phenomena correspond well with the dynamic contact angle results (Figure 5.2b). Ores treated by MEA-LA solutions exhibited a slightly slower liberation rate than in Milli-Q water, whereas the hindrance caused by MEA-OA solutions was more severe. The reduction of the liberation rate is unfavorable in the heavy oil industry since that longer residence time would be needed to approach the ultimate DOL value. Fortunately, these side effects on the liberation kinetics start to diminish as the ultimate DOL becomes high enough.

Table 5.2. Fitting parameters in Eq. 5.2 for the real-time heavy oil liberation experiments.

Group		Fitting parameters		
		A (%)	k ($\times 10^{-2} \text{ s}^{-1}$)	R^2
Milli-Q water		22.38 ± 0.04	3.73 ± 0.25	0.9122
MEA-LA	1 mM	39.51 ± 0.68	1.98 ± 0.15	0.8503
	2 mM	48.17 ± 0.42	2.32 ± 0.12	0.9396
	3 mM	57.29 ± 0.26	2.35 ± 0.14	0.9591
	5 mM	59.60 ± 0.76	3.42 ± 0.21	0.9284
MEA-OA	1 mM	48.68 ± 0.70	0.41 ± 0.01	0.9975
	2 mM	53.54 ± 0.94	0.54 ± 0.03	0.9911
	3 mM	59.08 ± 1.44	0.69 ± 0.04	0.9422
	5 mM	74.67 ± 0.54	0.98 ± 0.03	0.9756

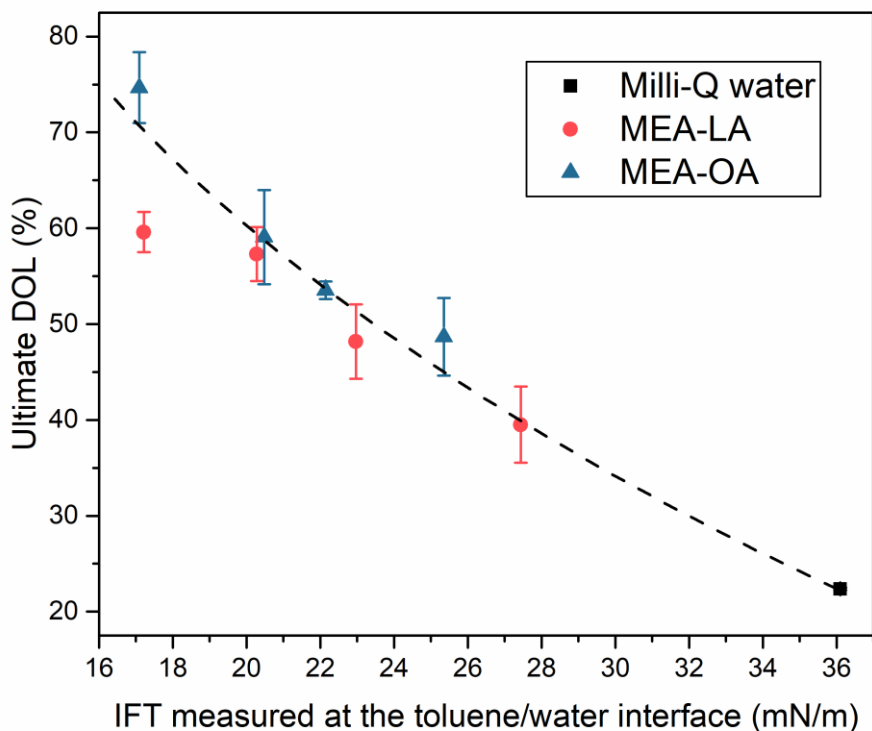


Figure 5.4. Relationships between the ultimate DOL and the interfacial activity of the corresponding surfactant at the toluene/water interface.

5.3.2 Effect of CO₂-responsive surfactants on heavy oil harvest

After being released from solid substrates, heavy oil is carried out by the aqueous washing fluid in the form of heavy oil-in-water (HO/W) emulsions, which are usually very stable and inseparable. Unfortunately, these emulsions contain a considerable amount of heavy oil products. Besides, they turn into tailings water if untreated, which are hazardous to the near animals and environment. In general, surfactants with strong interfacial activity become detrimental to the downstream operations where heavy oil needs to be separated and harvested from the emulsions.

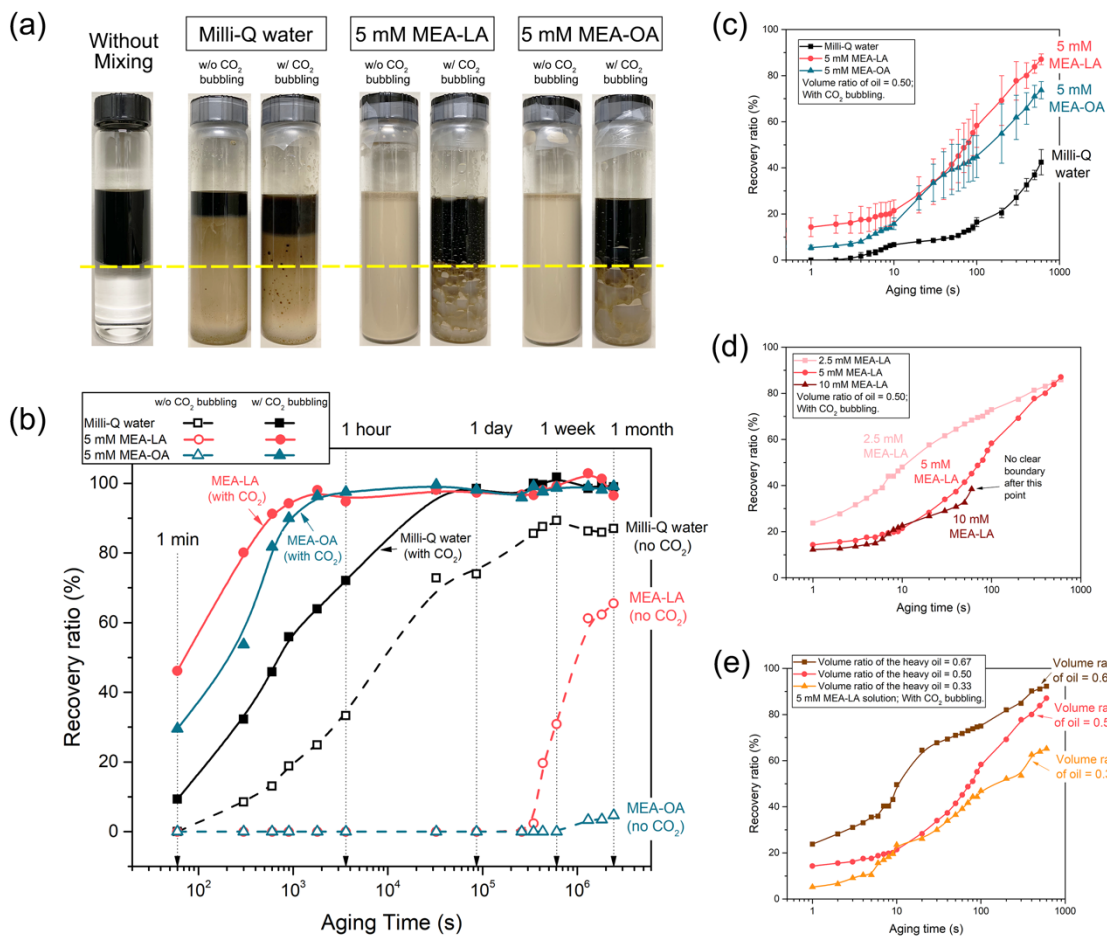


Figure 5.5. (a) Demulsification of the stable heavy oil-in-water (HO/W) emulsions stabilized by CO₂-responsive surfactants with and without CO₂ bubbling (aging time = 1 hour); Evolution of the heavy oil recovery ratio in a storage time of 1 month (b), as well as in the first 600 s after CO₂ bubbling in the cases of different surfactant types (c), different MEA-LA concentration (d), and different volume ratio of the heavy oil (e).

In this study, CO₂-responsive surfactants are designed to overcome such disadvantages of conventional surfactants in the heavy oil harvest stage. CO₂-responsive surfactants feature switchable interfacial activity, i.e., their interfacial activity can be switched off by CO₂ gas. Hence, emulsions stabilized by CO₂-responsive surfactants could be easily demulsified by bubbling of

CO₂ gas. As a consequence, the heavy oil product would be phase-separated spontaneously. Meanwhile, the amount of tailings water could also be reduced, thereby enhancing sustainability. The interfacial switching behavior of MEA-LA and MEA-OA had been studied in detail previously [15]. Briefly speaking, both CO₂-responsive surfactant solutions increases the IFT at the oil/water interface after CO₂ addition. MEA-LA possesses a more pronounced CO₂ switchability than MEA-OA. Namely, the oil/water interface occupied by MEA-LA recovers to a higher IFT value than that by MEA-OA after the activation of CO₂ responsiveness, indicating a more complete depletion of surfactants from the interface.

Visual observations of the HO/W emulsion stability were conducted to evaluate the effectiveness of CO₂-responsive surfactants in the heavy oil harvest stage. It is first noticed that HO/W emulsions were readily stable even without surfactant addition (Milli-Q water group in Figure 5.5a), which is attributed to the existence of natural surfactants in the heavy oil [37]. Only a small amount of heavy oil was phase-separated within an aging time of 1 hour. This is considered a demonstration that most of the heavy oil product was still unrecoverable in the emulsion. Bubbling of CO₂ slightly enhanced the phase separation process in the Milli-Q water group. This can be explained by the fact that natural surfactants in heavy oil are mostly composed of acids [37, 38], e.g., naphthenic acids, which could be protonated during the pH decrease upon CO₂ solvation and partially lose their interfacial activity.

Emulsions stabilized by CO₂-responsive surfactants exhibit dramatic differences with or without CO₂ bubbling. With the addition of surfactants but no switching, emulsions appeared to be extremely stable. There were no signs of phase separation being observed for days (Figure 5.6). Undoubtedly, such ultra-stable emulsions are severe problems for the harvesting of heavy oil and should be eliminated in the industrial scenarios. After the direct bubbling of CO₂ gas into the

emulsions, a fast and near-complete demulsification could be easily achieved in the groups with CO₂-responsive surfactants. It is shown that most of the heavy oil product was readily recovered within 1 hour, which is promising from the industrial perspective. This result also proves that CO₂-responsive surfactants are more interfacially active than natural surfactants. The interfacial properties of the heavy oil/water interface are fully governed by the CO₂-responsive surfactants, and thereby the precise switching of emulsion stability at a desired stage becomes accessible.

Demulsification efficiency was qualitatively estimated by the recovery ratio of heavy oil from the emulsions. The recovery ratio was generated by counting the volume of “black” heavy oil in a sequence of images using the following equation:

$$\text{Recovery ratio} = \frac{\text{Volume of harvested heavy oil}}{\text{Volume of emulsion} \times \text{Volume ratio of heavy oil}} \times 100\% \quad (5.3)$$

The volume measurements were calculated using heights, and the volume ratio of the heavy oil was readily known according to the preparation procedures. The evolution of heavy oil recovery ratio upon a storage time of 1 month is shown in Figure 5.5b. Similar to the visual observations, the demulsification in Milli-Q water was rather inefficient and incomplete. CO₂ treatment into Milli-Q water made the phase separation occur slightly faster. With CO₂-responsive surfactants but no switching, emulsions were ultra-stable. Emulsions stabilized by MEA-OA had no sign of phase separation for at least 1 month. The demulsification processes in both surfactant solutions were extremely rapid and efficient after CO₂ switching. The recovery ratios of heavy oil were nearly 100% within 30 minutes.

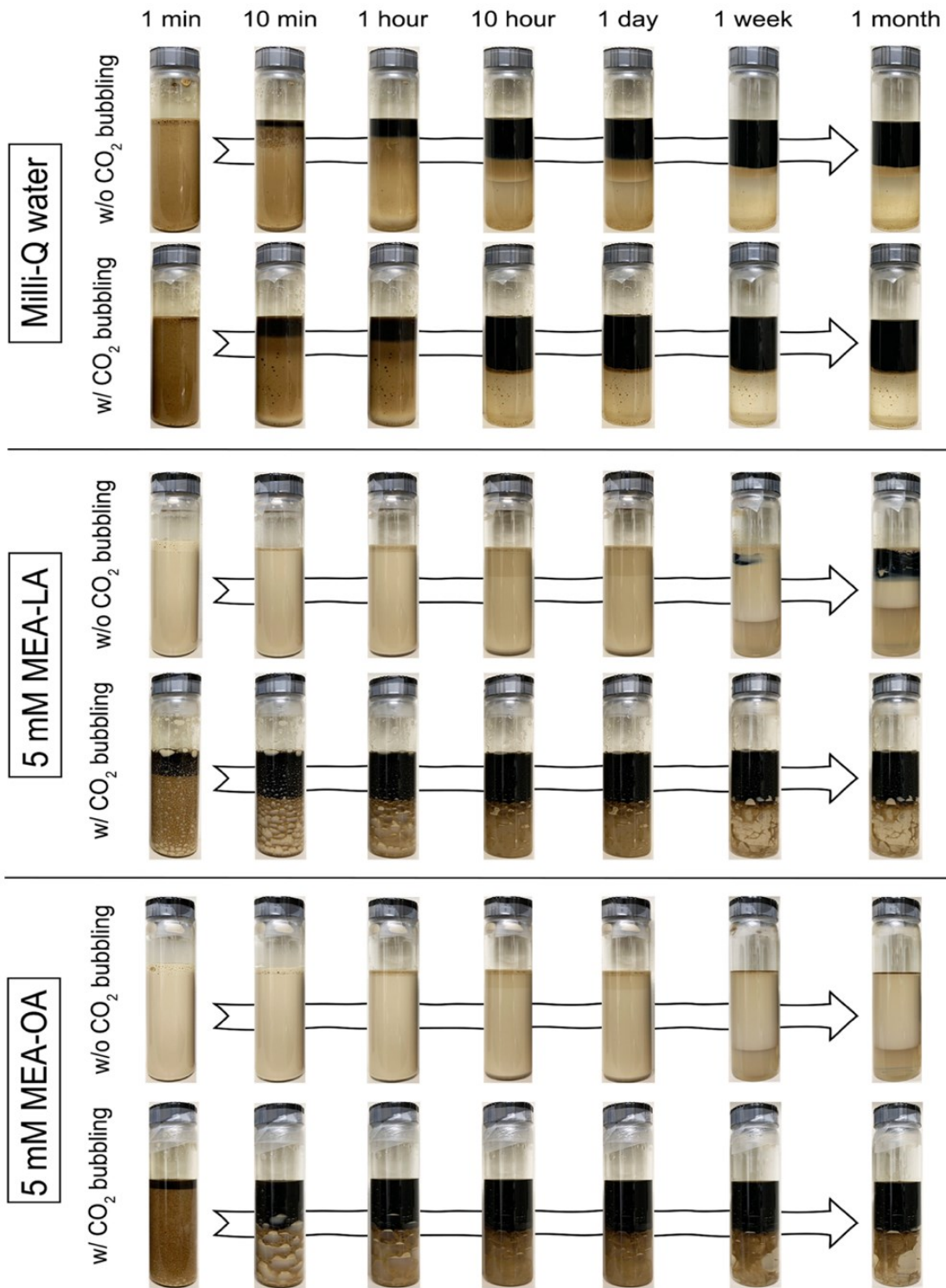


Figure 5.6. Long term storage of heavy oil-in water emulsions.

The demulsification efficiency was further investigated by focusing on the recovery ratio evolution in the first 600 s. Results are provided in Figures 5.5c – 5.5e, where all results corresponded to the cases after CO₂ bubbling. The phase separation in MEA-LA solution was slightly faster than that in MEA-OA solution, both of which were significantly stronger than in Milli-Q water (Figure 5.5c). As demonstrated previously, MEA-LA surfactants could be depleted from the oil/water interface more completely than MEA-OA after switching [15]. Hence, it is not surprising that MEA-LA emulsions were easier to phase separate after CO₂ bubbling. Besides, lower surfactant concentration and higher volume ratio of the heavy oil results in better demulsification efficiency (Figures 5.5d & 5.5e). These results also follow the intuition that it is always favorable to use less surfactants and operate in oil-rich reservoirs.

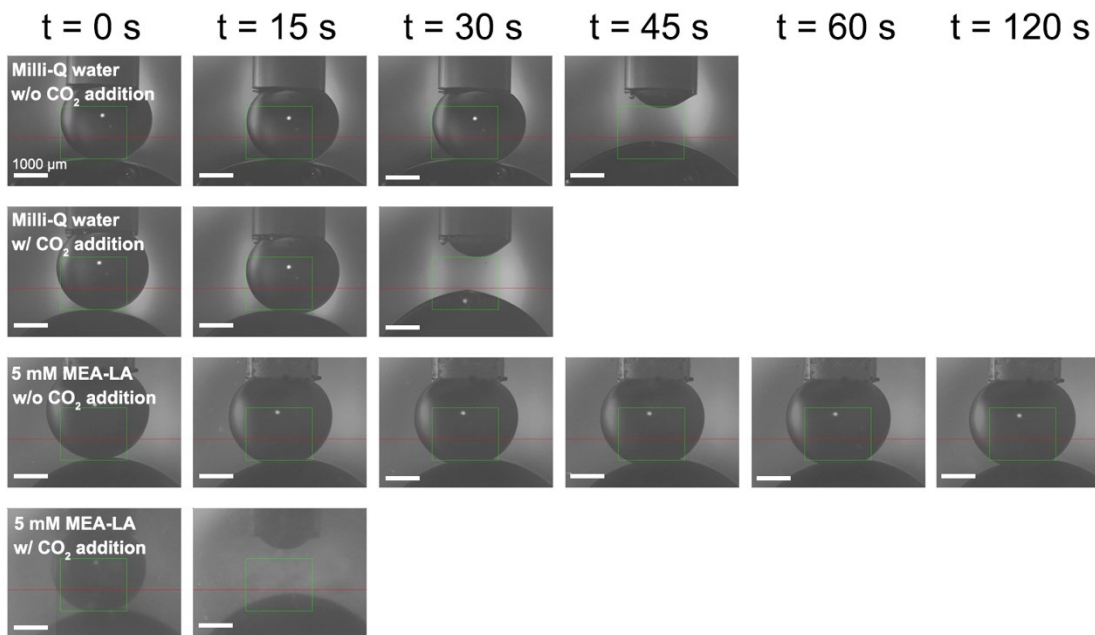


Figure 5.7. Images for the coalescence process of toluene-diluted heavy oil droplets in CO₂-responsive surfactant solutions without and with the activation of interfacial CO₂ switching.

Table 5.3. Coalescence time of toluene-diluted heavy oil stabilized by different aqueous solutions with or without CO₂ addition.

Group		Coalescence time (s)
Milli-Q water	Without CO ₂ addition	33 ± 5
	With CO ₂ addition	27 ± 5
5 mM MEA-LA	Without CO ₂ addition	NA*
	With CO ₂ addition	11 ± 1
5 mM MEA-OA	Without CO ₂ addition	NA*
	With CO ₂ addition	19 ± 5

* No droplets coalescence was observed within the contact time of 120 s, which is the limitation of the instrument.

Further insights into the demulsification process were obtained by understanding the coalescence between two toluene-diluted heavy oil droplets immersed in the aqueous medium. The coalescence time was defined as the average time for two oil droplets to coalesce and merge into one drop upon contact. Generally, a shorter coalescence time represents a higher change of the coalescence to occur, thus suggesting a faster phase separation. Snapshots of the measurements are shown in Figure 5.7, while the results of coalescence time are given in Table 5.3. In Milli-Q water, the average time for two diluted heavy oil droplets to coalesce was 33 ± 5 s. This coalescence time was slightly reduced with CO₂ addition. In the cases of CO₂-responsive surfactants but without CO₂ addition, no droplet coalescence could be found within the contact time of 120 s, suggesting the formation of ultra-stable emulsions. In contrast, when the CO₂ switching was activated in surfactant solutions, coalescence occurred within a much shorter contact time. Once again, it is the switch-off of surfactants interfacial activity, which recovers the hydrophobic nature of oil surfaces, that promotes the droplet-droplet coalescence. It could be concluded that CO₂-responsive surfactants dramatically enhance the demulsification efficiency of heavy oil from emulsions once

their interfacial activity was switched off by CO₂ bubbling. Hence, they are capable of facilitating the harvest of heavy oil product after the heavy oil liberation stage.

5.3.3 Life cycle of CO₂-responsive surfactants

In the previous sections, we have demonstrated that CO₂-responsive surfactants could facilitate the heavy oil liberation, as well as the heavy oil harvest after switching. With the goal of recycling tailings water and reinforce process sustainability, we investigated the life cycle of these CO₂-responsive surfactants after the heavy oil recovery process. This section is directly related to the recyclability of these CO₂-responsive surfactants.

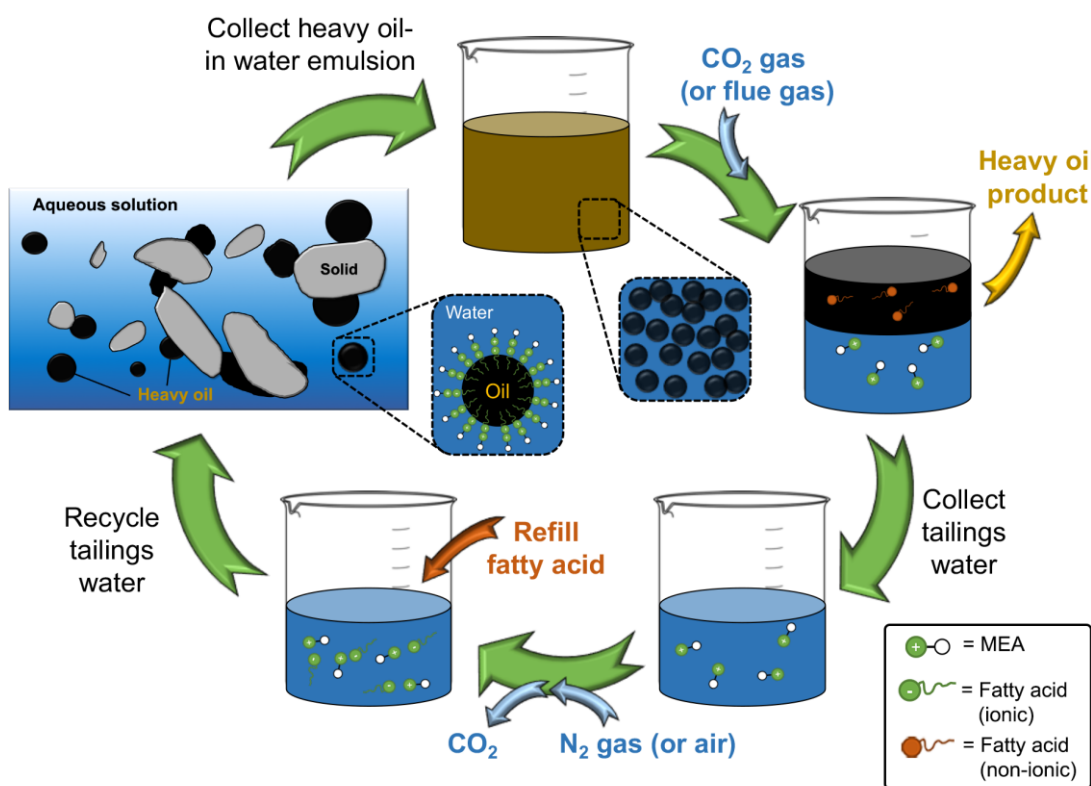


Figure 5.8. CO₂-responsive surfactants in the heavy oil recovery process.

The proposed life cycle of MEA-LCFA surfactants is illustrated in Figure 5.8. It is hypothesized that fatty acid components would partition into the heavy oil phase after the switch and become part of the product, whereas MEA prefers to stay in the aqueous phase. Such prediction is based on their corresponding distribution coefficient values ($\log D$). Distribution coefficient is the ratio of the compound (both ionic species and non-ionic species) in the organic phase to that in the aqueous phase [39, 40]:

$$\log D_{o/w} = \log \left(\frac{[\text{solute}]_{\text{oil}}^{\text{non-ionized}} + [\text{solute}]_{\text{oil}}^{\text{ionized}}}{[\text{solute}]_{\text{water}}^{\text{non-ionized}} + [\text{solute}]_{\text{water}}^{\text{ionized}}} \right) \quad (5.4)$$

where $[\text{solute}]_{\text{oil}}^{\text{non-ionized}}$ is the concentration of the non-ionic form of the solute in the oil phase and so on. From this definition, the value of $\log D$ represents the concentration distribution of the compound in a binary system at equilibrium. When $\log D > 0$, the compound prefers to stay in the organic phase, whereas when $\log D < 0$, the compound prefers the aqueous phase. The structure property predictions and calculations were conducted using Calculator Plugins (v.19.17, ChemAxon Ltd.) and the results are shown in Figure 5.9 in the Supplementary Materials. The distribution coefficient is greatly influenced by the aqueous pH values for all species in this study, because their solubility in both oil and water phases are affected by their degree of protonation. Since we are most interested in the compound distribution after the heavy oil harvest stage, clean aqueous solutions were collected at the bottom layer from the demulsification tests after CO₂ bubbling. The pH value of these aqueous solutions was measured to be ~ 5.16 . Consequently, $\log D$ values were calculated to be -4.34, 4.15, and 6.48 for MEA, LA, and OA, respectively. According to Eq. 5.4, MEA should be $\sim 20,000$ times more concentrated in water than in the organic phase, referring to a strong preference of staying in the aqueous phase. Similarly, fatty acids are mostly partitioned into the oil phase after CO₂ switching.

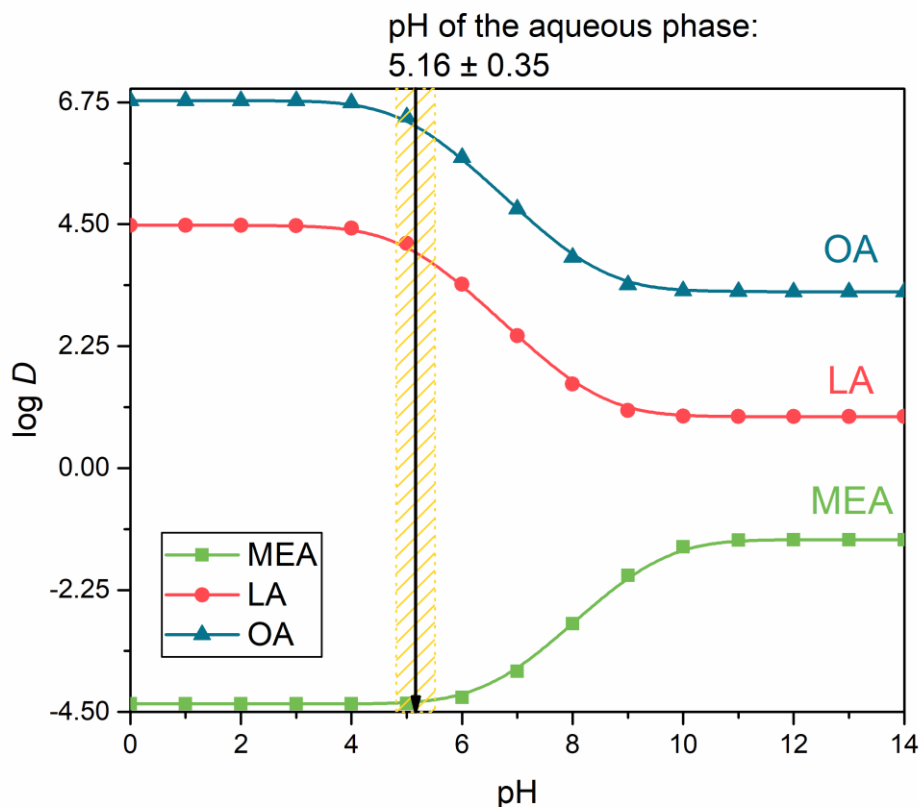


Figure 5.9. Distribution coefficient of MEA, LA and OA when the pH value of the aqueous phase is 5.16 ± 0.35 .

The fate of CO₂-responsive surfactants after switching was determined experimentally by analyzing the extracted heavy oil from the demulsification experiments using FTIR spectroscopy. In general, the main purpose of this FTIR experiment was to characterize whether MEA and fatty acids entered the heavy oil phase after switching. Meantime, it was also attempted to estimate the concentration of a known type of fatty acid in the heavy oil phase after switching. Although FTIR spectroscopy is usually considered as a semi-quantitative characterization method, it is still a practical tool to determine the concentration of a target compound in a known system. For example, the only possible changes in the extracted heavy oil from 5 mM MEA-LA group are the raise of

MEA and LA concentration, if compared to the original toluene-diluted heavy oil without any treatment. Hence, the changes in the corresponding FTIR spectra must be associated with MEA and LA.

Standard samples were first prepared by dissolving a certain concentration of fatty acid into toluene-diluted heavy oil. It was shown that the presence of fatty acids led to the growth of a characteristic peak at $\sim 1714 \text{ cm}^{-1}$ in the FTIR spectrum (Figure 5.10), which corresponds to the stretching of C=O in the carboxylic acid. Moreover, the concentration of fatty acid exhibited strong correlations with the integrated area of FTIR patterns between 1700 cm^{-1} to 1720 cm^{-1} , as presented in Figure 5.11. Thereby, these correlations could be used to calculate the fatty acid concentration in the diluted heavy oil. The extracted heavy oil samples were collected from the upper layer of the heavy oil after the demulsification tests. FTIR analysis was conducted for the heavy oil samples, while the values of the integrated area were then interpolated into the corresponding calibration curves in Figure 5.11. It was found that the heavy oil harvested from the MEA-LA group contained $5.4 \pm 1.1 \text{ mM}$ of LA, whereas that from the MEA-OA group had an OA concentration of $4.1 \pm 1.0 \text{ mM}$. Considering the fact that the initial concentration of anionic fatty acid in the aqueous phase was 5 mM , as well as that the volume of oil and water was the same during preparation, one could say that fatty acids were almost completely partitioned into the oil phase after CO_2 switching process. Unfortunately, this FTIR method was not appropriate to identify the MEA concentration in diluted heavy oil. There was no characteristic peak can be observed for MEA in the toluene-diluted heavy oil.

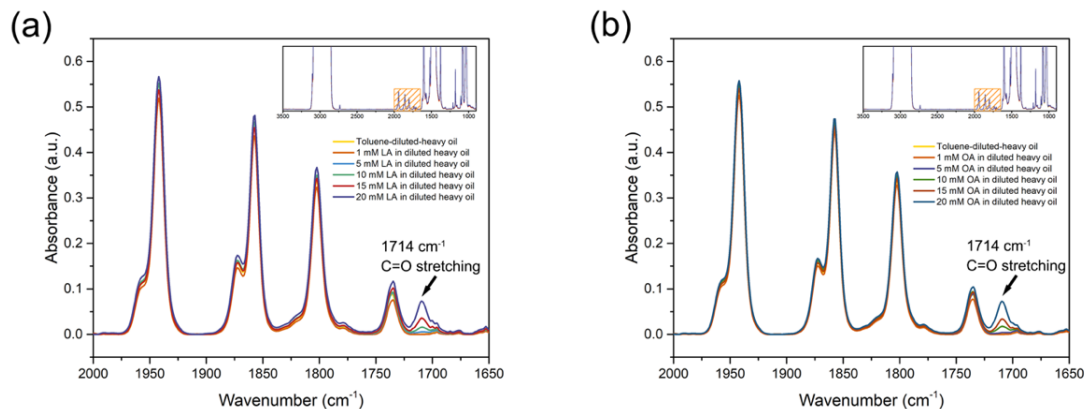


Figure 5.10. FTIR spectrum of the toluene-diluted heavy oil containing a certain concentration of LA (a) and OA (b). The full spectra are given as insets, whereas the characteristic peak of carboxylic group in fatty acids at the wavenumber of 1714 cm^{-1} is emphasized by zooming in the region from wavenumber 2000 cm^{-1} to 1650 cm^{-1} .

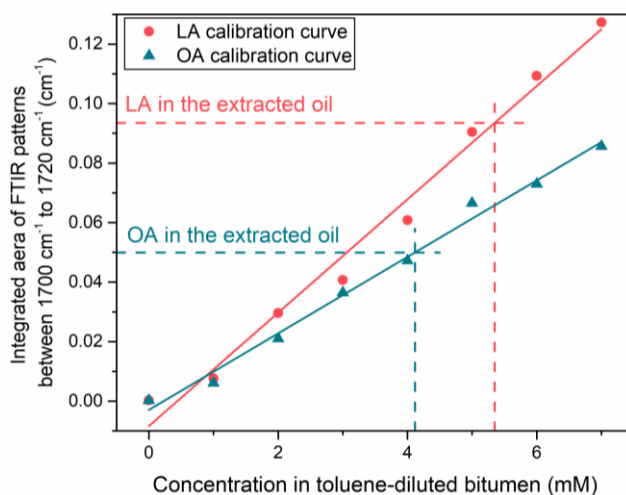


Figure 5.11. Calibration curves for the fatty acids in toluene-diluted heavy oil. Concentrations of LA and OA in the extracted heavy oil samples were obtained by interpolating the values of the integrated area of FTIR patterns on the calibration curves.

Finally, the recyclability of CO₂-responsive surfactants was investigated by the regeneration of interfacial activity in the tailings water. Originally, the IFT values at the toluene/water interface were measured to be 19.40 ± 0.07 mN/m or 18.84 ± 0.04 mN/m, when the aqueous solution was 5 mM MEA-LA or 5 mM MEA-OA, respectively. These CO₂-responsive surfactant solutions were brought to the demulsification experiments, where HO/W emulsions were generated and then demulsified by bubbling CO₂. Clear tailings water was collected from the bottom layers in demulsification tests. These aqueous samples were evaluated by their bulk pH and their ability to reduce toluene/water IFT. The results are given in Figure 5.12. It is shown that interfacial activities were completely switched off in bulk solutions after CO₂ bubbling, indicated by high IFT at the interface. N₂ bubbling into the aqueous phase purged the dissolved CO₂, showing as the increase in the bulk pH. However, there was no change to the oil-water IFT. The reason is the absence of fatty acids, which had transferred into the organic phase in the demulsification process and were removed together with the heavy oil products, as demonstrated previously. In order to regenerate the interfacial activity and recycle tailings water, the addition of a molar equivalent amount of the corresponding fatty acid is required. It is assumed that all MEA stayed in the aqueous phase after CO₂ bubbling based on the calculation of $\log D$ values (Figure 5.9), i.e., MEA concentration should equal to 5 mM in the aqueous phase. Correspondingly, the tailings water was refilled with 5 mM of fatty acids and mixed sufficiently. Interfacial activities were successfully brought back to comparable values as that in the original surfactant solutions. Hence, these recycled tailings water should be readily available for use in the next cycle. There were only negligible differences from the perspective of IFT after three cycles. Such phenomena also suggest that MEA was maintained in the aqueous phase during cycles. Any loss of MEA to the organic phase during cycles would have caused gradual attenuation of the interfacial activity.

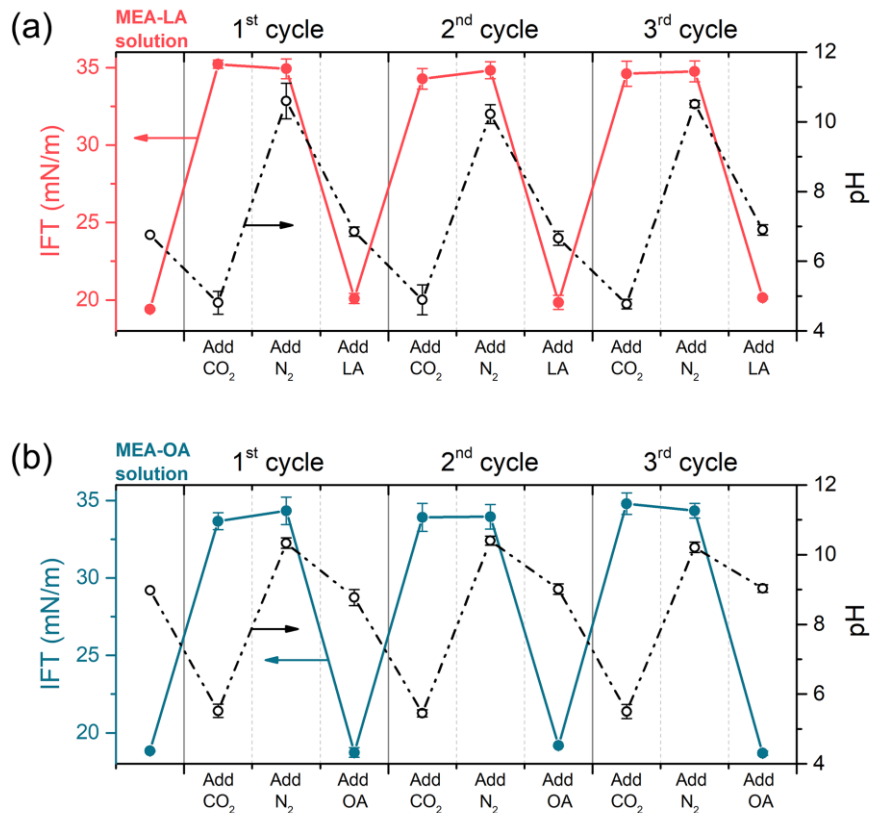


Figure 5.12. Evaluation of the tailings water collected from the demulsification experiments by their bulk pH and interfacial activity at the toluene/water interface throughout three cycles: (a) 5 mM MEA-LA; and (b) 5 mM MEA-OA.

5.4 Conclusions

In this study, two CO₂-responsive surfactants were investigated to enhance heavy oil recovery by utilizing their interfacial activity and switchability. Compared with most conventional surfactants, CO₂-responsive surfactants possess significant advantages, in which their interfacial activity can be switched off by CO₂ bubbling at the desired stage. Hence, they are capable of performing as surfactants to enhance the oil-solid separation in the liberation stage, and then switch to demulsifiers to facilitate the oil-water separation in the harvest stage. The enhancement of heavy

oil liberation by CO₂-responsive surfactants was confirmed throughout contact angle measurements in a model system and the liberation visualization cell on the real petroleum ores. The addition of both surfactants boosted the degree of heavy oil liberation (DOL), although they also slowed down the initial liberation rate. On the other hand, the results from demulsification tests indicated that significantly more heavy oil could be harvested in the groups of CO₂-responsive surfactants along with CO₂ bubbling treatment. Coalescence time provided further evidence that the improvement in demulsification efficiency was directly related to the CO₂ switchability at the interface, which decreased the droplet-droplet coalescence time dramatically. Additionally, it is also viable to recycle the MEA component together with the tailing water after treatments. Since more heavy oil is swept out from the petroleum reservoir by CO₂-responsive surfactant washing, as well as that the harvest of heavy oil from the HO/W emulsions becomes more efficient after activating the CO₂ switching, these novel CO₂-responsive surfactants should be promising additives to enhance the heavy oil recovery process.

We anticipate that this study will provide valuable guidance in developing responsive materials for various large-scale separation applications, such as household cleaning, contaminated soil remediation, and oil spill management. Both MEA and fatty acids are common chemicals that are commercially available at affordable prices, which offers scale-up possibilities. Besides, the versatility of this group of CO₂-responsive is also readily involved in their design. Their interfacial activity and switchability could be easily modified by changing the types of amines and fatty acids, such that CO₂-responsive surfactants could be customized for specific requirements.

5.5 References

1. Falbe, J., *Surfactants in consumer products: Theory, technology and application*. 2012: Springer Science & Business Media.
2. Nicolaidis, C. and I. Vyrides, *Closing the water cycle for industrial laundries: An operational performance and techno-economic evaluation of a full-scale membrane bioreactor system*. *Resources Conservation and Recycling*, 2014. **92**: p. 128-135.
3. Janpoor, F., A. Torabian, and V. Khatibikamal, *Treatment of laundry waste-water by electrocoagulation*. *Journal of Chemical Technology and Biotechnology*, 2011. **86**(8): p. 1113-1120.
4. Hirasaki, G., C.A. Miller, and M. Puerto, *Recent advances in surfactant EOR*. *SPE Journal*, 2011. **16**(04): p. 889-907.
5. Raffa, P., A.A. Broekhuis, and F. Picchioni, *Polymeric surfactants for enhanced oil recovery: A review*. *Journal of Petroleum Science and Engineering*, 2016. **145**: p. 723-733.
6. Lu, Y., et al., *Pseudo-gemini biosurfactants with CO₂ switchability for enhanced oil recovery (EOR)*. *Tenside Surfactants Detergents*, 2019. **56**(5): p. 407-416.
7. dos Santos, E.V., et al., *Treatment of ex-situ soil-washing fluids polluted with petroleum by anodic oxidation, photolysis, sonolysis and combined approaches*. *Chemical Engineering Journal*, 2017. **310**: p. 581-588.
8. Bai, X., et al., *Remediation of phenanthrene contaminated soil by coupling soil washing with Tween 80, oxidation using the UV/S₂O₈²⁻ process and recycling of the surfactant*. *Chemical Engineering Journal*, 2019. **369**: p. 1014-1023.
9. Quinlan, P.J. and K.C. Tam, *Water treatment technologies for the remediation of naphthenic acids in oil sands process-affected water*. *Chemical Engineering Journal*, 2015. **279**: p. 696-714.
10. Xiang, B.X., et al., *Tailoring CO₂-responsive polymers and nanohybrids for green chemistry and processes*. *Industrial & Engineering Chemistry Research*, 2019. **58**(33): p. 15088-15108.
11. Yang, Z., et al., *Recent advances of CO₂-responsive materials in separations*. *Journal of CO₂ Utilization*, 2019. **30**: p. 79-99.
12. Li, Z.F., W. Richtering, and T. Ngai, *Poly(N-isopropylacrylamide) microgels at the oil-water interface: temperature effect*. *Soft Matter*, 2014. **10**(33): p. 6182-6191.
13. Li, Z.F., et al., *Poly(N-isopropylacrylamide) microgels at the oil-water interface: adsorption kinetics*. *Soft Matter*, 2013. **9**(41): p. 9939-9946.
14. Yan, T., et al., *A magnetic pH-induced textile fabric with switchable wettability for intelligent oil/water separation*. *Chemical Engineering Journal*, 2018. **347**: p. 52-63.
15. Lu, Y., et al., *CO₂-responsive surfactants with tunable switching pH*. *Journal of Colloid and Interface Science*, 2019. **557**: p. 185-195.

16. Sui, H., et al., *Understanding the roles of switchable-hydrophilicity tertiary amines in recovering heavy hydrocarbons from oil sands*. Chemical Engineering Journal, 2016. **290**: p. 312-318.
17. Chevallier, E., et al., *Pumping-out photo-surfactants from an air–water interface using light*. Soft Matter, 2011. **7**(17): p. 7866-7874.
18. He, X., et al., *Magnetically responsive Janus nanoparticles synthesized using cellulosic materials for enhanced phase separation in oily wastewaters and water-in-crude oil emulsions*. Chemical Engineering Journal, 2019. **378**: p. 122045.
19. Xu, H., et al., *Novel and recyclable demulsifier of expanded perlite grafted by magnetic nanoparticles for oil separation from emulsified oil wastewaters*. Chemical Engineering Journal, 2018. **337**: p. 10-18.
20. Jessop, P.G., S.M. Mercer, and D.J. Heldebrant, *CO₂-triggered switchable solvents, surfactants, and other materials*. Energy & Environmental Science, 2012. **5**(6): p. 7240-7253.
21. Abbaspourrad, A., S.S. Datta, and D.A. Weitz, *Controlling release from pH-responsive microcapsules*. Langmuir, 2013. **29**(41): p. 12697-702.
22. Werner, J.r.G., et al., *Hydrogel microcapsules with dynamic pH-responsive properties from methacrylic anhydride*. Macromolecules, 2018. **51**(15): p. 5798-5805.
23. Mihut, A.M., et al., *Tunable adsorption of soft colloids on model biomembranes*. ACS Nano, 2013. **7**(12): p. 10752-10763.
24. Darabi, A., P.G. Jessop, and M.F. Cunningham, *CO₂-responsive polymeric materials: Synthesis, self-assembly, and functional applications*. Chemical Society Reviews, 2016. **45**(15): p. 4391-4436.
25. Li, R., et al., *Spontaneous displacement of high viscosity micrometer size oil droplets from a curved solid in aqueous solutions*. Langmuir, 2019. **35**(3): p. 615-627.
26. Yeung, A., et al., *On the interfacial properties of micrometre–sized water droplets in crude oil*. Proceedings of the Royal Society of London. Series A: Mathematical, Physical and Engineering Sciences, 1999. **455**(1990): p. 3709-3723.
27. Srinivasa, S., et al., *Study of bitumen liberation from oil sands ores by online visualization*. Energy & Fuels, 2012. **26**(5): p. 2883-2890.
28. He, L., et al., *Image analysis of heavy oil liberation from host rocks/sands*. The Canadian Journal of Chemical Engineering, 2015. **93**(6): p. 1126-1137.
29. Wang, L., et al., *Measurement of interactions between solid particles, liquid droplets, and/or gas bubbles in a liquid using an integrated thin film drainage apparatus*. Langmuir, 2013. **29**(11): p. 3594-603.
30. Wang, L., Z. Xu, and J.H. Masliyah, *Dissipation of film drainage resistance by hydrophobic surfaces in aqueous solutions*. The Journal of Physical Chemistry C, 2013. **117**(17): p. 8799-8805.
31. He, L., et al., *Interfacial sciences in unconventional petroleum production: from fundamentals to applications*. Chemical Society Reviews, 2015. **44**(15): p. 5446-94.

32. Masliyeh, J., J. Czarnecki, and Z. Xu, *Handbook on theory and practice of bitumen recovery from Athabasca oil sands: Vol. I. Theoretical basis*. 2010: Kingsley Knowledge Publishing.
33. Tangparitkul, S., et al., *Interfacial and colloidal forces governing oil droplet displacement: Implications for enhanced oil recovery*. *Colloids and Interfaces*, 2018. **2**(3): p. 30.
34. Young, T., III. *An essay on the cohesion of fluids*. *Philosophical Transactions of the Royal Society of London*, 1805(95): p. 65-87.
35. Sakurai, M., et al., *Theoretical study of intermolecular interaction at the lipid–water interface: 1. Quantum chemical analysis using a reaction field theory*. *The Journal of Physical Chemistry B*, 1997. **101**(24): p. 4810-4816.
36. He, L., et al., *Enhancing bitumen liberation by controlling the interfacial tension and viscosity ratio through solvent addition*. *Energy & Fuels*, 2014. **28**(12): p. 7403-7410.
37. Schramm, L.L., *Surfactants : Fundamentals and applications in the petroleum industry*. 2000, Cambridge University Press: Cambridge, UK.
38. Ashrafizadeh, S., E. Motaei, and V. Hoshyargar, *Emulsification of heavy crude oil in water by natural surfactants*. *Journal of Petroleum Science and Engineering*, 2012. **86**: p. 137-143.
39. Scherrer, R.A. and S.M. Howard, *Use of distribution coefficients in quantitative structure-activity relations*. *Journal of Medicinal Chemistry*, 1977. **20**(1): p. 53-58.
40. Leo, A. and D. Hoekman, *Exploring QSAR*. 1995: American Chemical Society.

Chapter 6. CO₂-Responsive Surfactants for the Enhancement of *Ex-Situ* Oil Sands Extraction: A Bench-Scale Demonstration

6.1 Introduction

Oil sands, the crude bitumen and mineral solids matrix, are considered to be one of the most important non-conventional petroleum resources in the world. The largest oil sands deposits are located in the northern areas of Alberta, Canada, containing about 1.7 to 2.5 trillion barrels of bitumen [1-3]. The current production of crude oil is reported as ~ 236 million liters per day (ML/day), which provides for 56% of total Canadian oil output [4, 5]. The oil production from oil sands is forecasted to grow up to 620 ML/day by 2030 [1].

In the oil sands industry, open-pit mining followed by Clark hot/warm water extraction (CHWE) is one of the most developed and commercialized technologies. Figure 6.1a illustrates the typical process of CHWE operation. Mineable oil sands ores are first collected by shovels and trucks, then crushed into pieces, conditioned by process water, and become oil sands slurries. These slurries are introduced into hydrotransport pipelines, where the *oil sands extraction* process begins. Within the pipelines, bitumen is liberated and dispersed into the aqueous medium spontaneously (Figure 6.1b), since the sand grains in northern Alberta are of hydrophilic natures [3]. This process is referred to the '*bitumen liberation*'. Meanwhile, streams of air are injected to aerate and collect the dispersed bitumen in the aqueous phase via bitumen-air bubble attachment. This is known as the stage of '*bitumen aeration*' (Figure 6.1c). After that, the mixture of aerated bitumen, process water, and solid wastes would enter gravitational separation vessels, including primary separation vessel (PSV) and secondary separation vessel (SSV), where further bitumen liberation and aeration

takes place. Finally, the bitumen-concentrated froth is harvested from the top stream and goes into the froth treatment process, while the bottom streams of slurries are deposited to tailing ponds for tailing management. Both froth treatment and tailings management processes are beyond our scope of oil sands extraction in this study, although they are essential to the industry.

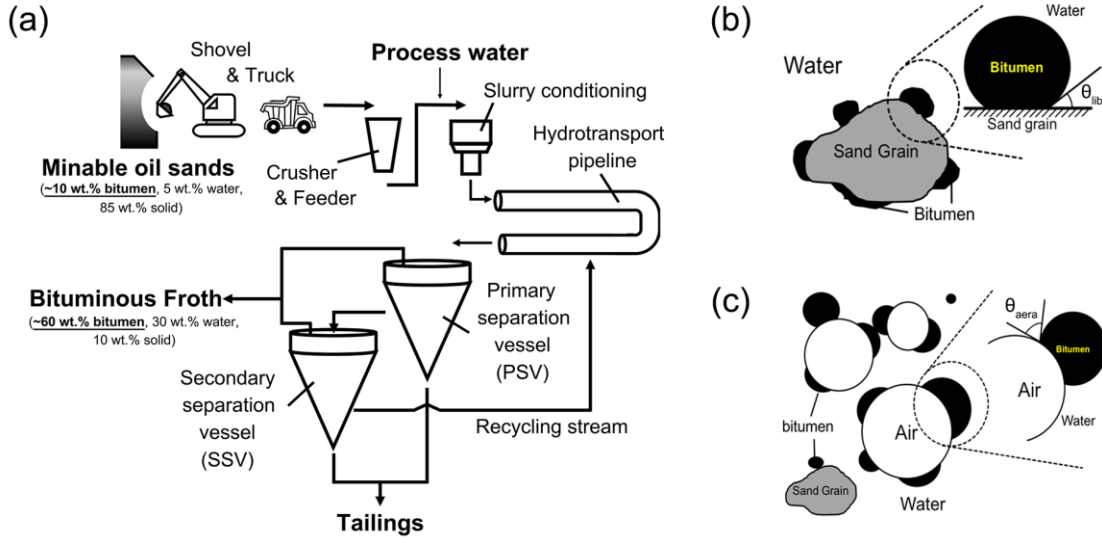


Figure 6.1. (a) Schematic graph of typical CHWE process; (b) Bitumen liberation from sand grains with inset illustrating the liberation contact angle (θ_{lib}); and (c) Bitumen-air bubble attachment with inset illustrating the aeration contact angle (θ_{aera}).

In order to enhance the oil sands extraction and achieve higher bitumen recovery, major improvements are expected to be obtained from both bitumen liberation and aeration stages. Unfortunately, these two stages appear to be conflictive with each other from the perspective of water-bitumen interfacial tensions (IFTs, γ_{WB}). In the bitumen liberations stage, a low value of γ_{WB} is preferable [6, 7]. A lower value of γ_{WB} results in smaller liberation contact angle (θ_{lib} , inset of Figure 6.1b), which means more efficient removal of bitumen from their host solids could be achieved. On the other hand, decreasing γ_{WB} not only leads to the formation of stable bitumen-in-

water emulsions, but also reflects as small aeration contact angle (θ_{aera}), which represents weak interactions between bitumen and air bubble [8]. Neither is favorable in the bitumen aeration stage. In common practices, the enhancement of bitumen recovery is often optimized by compromise strategies. For instance, “caustics” additions (e.g., sodium hydroxide, ammonium hydroxide) are often used in the CHWE process as the processing aids to increase the bitumen recovery [1, 4, 9]. The addition of caustics releases natural surfactants and decreases the γ_{WB} . The maximum bitumen recovery can thereby be achieved by controlling the pH of the process water at ~ 8.0 , where bitumen liberation is greatly facilitated while the hindrance for bitumen aeration is acceptable [1].

Responsive surfactants are believed to be promising candidates to resolve such IFT paradox in the oil sands extraction process, attributed to their switchable characters. Their interfacial activity is capable of being switched off throughout the presence of external stimuli. Hence, responsive surfactants possess the potential to enhance both bitumen liberation and aeration stages together without compromise. Ideally, responsive surfactants are introduced with the process water and provide a desired interfacial activity, and thereby enhance the bitumen liberation stage. More importantly, these interfacial activities could be switched off prior to the bitumen aeration stage. Consequently, the bitumen surfaces recover their hydrophobic nature, and the attachment to air bubbles would become much easier.

There are several attempts being made to develop thermo-responsive polymeric surfactants for the oil sands extraction process [10-12]. It is known that thermo-responsive polymers exhibit coil-globule transition as the environment temperature increases above its lower critical solution temperature (LCST) [13], where they transform from water-soluble to water-insoluble. Hence, polymeric surfactants could be designed as the block copolymer that is composed of a thermal-responsive block and another balancing block. The interfacial activity of polymeric surfactants

becomes switchable when the thermo-responsive block performs its LCST transition behavior, which breaks the natural amphiphilicity balance. Although these approaches are of great scientific importance, as well as open avenues for responsive materials, the use of thermal response is economically unfavorable because of the enormous energy consumption to change bulk temperature, especially when considering the large scale of oil sands industry. Besides, the costs for precise copolymerization are often expensive as well.

Recently, our group developed a series of CO₂-responsive surfactants with tunable switching pH for large-scale applications [14]. One of the most critical concepts involved in our design was that responsive surfactants should be feasible and affordable for large-scale applications with less technical and economic barriers. Following such spirit, CO₂ was selected as the external stimuli because the switching behavior could be easily activated by the bubbling of CO₂ gas, which is inexpensive and easy-to-operate with negligible energy input [15-17]. Besides, CO₂ gas is accessible from the flue gas in near utilities, which may have an impact on reducing carbon footprint. From the materials perspective, CO₂-responsive surfactants were assembled by the non-covalent interaction between monoethanolamine (MEA) and long-chain fatty acid (LCFA) in the aqueous phase, both of which are commercially available at low prices. These novel CO₂-responsive surfactants had been successfully applied to enhance conventional heavy oil recovery during surfactant washing in the previous chapter. They exhibited exceptional performance on facilitating the heavy oil liberation from the petroleum ores, as well as on harvesting more heavy oil from oil-in-water (O/W) emulsions after CO₂ switching.

In this study, we further investigated these CO₂-responsive surfactants in the Canadian oil sands extraction process to enhance the ultra-heavy oil (bitumen) recovery. Compared to the conventional heavy oil recovery, the biggest difference in the oil sands extraction is that air bubble-

assisted flotation was used to harvest the liberated bitumen instead of spontaneous phase separation. Hence, CO₂-responsive surfactants were first assessed by their effects on the bitumen-air bubble attachment. More importantly, the investigated CO₂-responsive surfactants were applied to bench-scale oil sands extraction experiments using real oil sands ores at ambient temperature. Bitumen recovery could be significantly improved by CO₂-responsive surfactants, whereas the enhancement was confirmed to be a direct consequence of the CO₂-responsiveness.

6.2 Materials and Methods

Lauric acid (LA) (99%, Fisher Scientific), oleic acid (OA) (> 95%, Fisher Scientific), monoethanolamine (MEA) (> 99%, Sigma-Aldrich) and toluene (> 99.5%, Fisher) were used as received without further purification. Hydrochloride (HCl) (1 N solution, RICCA Chemical Company) and sodium hydroxide (NaOH) (1 N solution, Fisher Scientific) were diluted before being used. CO₂ gas (medical grade, Praxair) was also used as received. Milli-Q water was supplied by ThermoFischer Barnstead Nanopure ultrapure water purification system (resistivity > 18 MΩ·cm). CO₂-responsive surfactants were prepared by mixing the fatty acid with MEA in the aqueous phase at 1:1 molar ratio for at least 48 hours before use. The details of surfactant information are provided in Section 3.1 & Section 5.2.

Oil sands ores (Athabasca, site AC, 2016) in this study were provided by Syncrude Canada Ltd. The ores contained 11.4 wt.% of bitumen, 3.7 wt.% of water and 84.9 wt.% of solids. The ore composition was determined by the Dean Stark apparatus and was consistent with the previous reports [18, 19]. The solid particles less than 44 µm in size, which is also known as the fines, had a content of 22.0 wt.% of total solids in this oil sands ores. Bitumen samples was collected from

the predominantly fed to the vacuum distillation unit and was also obtained from Syncrude Canada Ltd. The process water used was from the Aurora process water on September 2016.

Bitumen-air bubble attachment was studied by determining the induction time of bitumen-air bubble attachment in aqueous solutions [20]. Details of the experimental setup can be found in previous studies [20, 21] and are also described in Section 3.7. In general, bitumen surface was treated by CO₂-responsive surfactants with or without the bubbling of CO₂. An air bubble (d = 2 mm) was generated in the solution and then moved downwards towards the bitumen surface. Air bubble was in contact with the bitumen surface for a controlled period of time, and the state of attaching or no attaching was recorded. Each contact time was repeated for 50 times for a certain bitumen surface.

Bitumen recovery experiments were carried out in a modified bitumen extraction unit (M-BEU). M-BEU consisted of a 1-L stainless steel cell modified with water jacket, an impeller, an adjustable AC motor (KBAC series, NEMA 4X/IP65, equipped with a tachometer from Jone™) and a mass flow controller (AALBORG® GFC17). Circulating water at constant temperature of 23 ± 1 °C from a thermal water bath was pumped through the water jacket to ensure ambient temperature condition. The operation procedure is summarized in Table 3.1. Briefly speaking, the oil sands extraction contained three continuous stages: slurry condition, primary flotation and secondary flotation, which mimicked the oil sands ores in hydrotransport pipeline, PSV and SSV, respectively. Each stage was operated for 10 minutes. In the slurry condition stage, 500 ± 1 g of thawed oil sands ores were added into the M-BEU cell, which contained 150 g of surfactant solution. The mixing speed was set as 600 rpm while the external air flow was set as 150 ml/min. In the primary flotation stage, another 900 g surfactant solution was added. The agitator was kept running at 600 rpm, but the air flow was turned off. The primary bituminous froth was collected

and weighted in a cellulose Soxhlet extraction thimble (Whatman™ 2800432, single wall). At last, in the secondary flotation stage, the mixing speed was raised up to 800 rpm, while CO₂ flow was input at the flow rate of 50 ml/min. The secondary froth was also collected and weighted in another thimble. The bitumen recovery ratio and froth quality were analyzed by the Dean-Stark apparatus using toluene as the refluxing solvent [22].

6.3 Results and Discussion

CO₂-responsive surfactants had been demonstrated to have promising performances on the enhancement of heavy oil recovery in the previous chapter. It is of our specific interest to utilize these novel processing aids in the oil sands extraction process and to evaluate their effectiveness in bench-scale operations. Compared to the conventional heavy oil recovery process where the oil products are harvested after phase separation, the oil sands extraction process collects the ultra-heavy oil (bitumen) in aqueous phase by the flotation technique, where air bubbles are used to capture the liberated bitumen. The aerated bitumen floats to the top spontaneously in the form of bituminous froth, which will then be collected. Obviously, the bitumen recovery during the oil sands extraction process heavily relies on the efficiency of bitumen-air bubble attachment.

6.3.1 Bitumen-air bubble attachment

The effects of the CO₂-responsive surfactants on bitumen aeration were investigated by measuring the induction time of an air bubble attaching to a bitumen surface, which was soaked in the CO₂-responsive surfactant solution. The bubbling of CO₂ gas was conducted to trigger the switching behavior at the bitumen-water interface after soaking, and the results are compared to the groups without switching. The induction time is defined as the contact time at which 50% of air bubbles attach to the bitumen surface [23, 24]. Generally, a shorter induction time refers to a more efficient

bitumen-air bubble attachment. The results of induction time are shown in Figure 6.2. At first glance, the induction time of the bitumen surface treated with Milli-Q water was not affected by the CO₂ bubbling. The induction times were both around 1900 ms at ambient temperature. This finding indicates that there exist natural surfactants that could adsorb onto the bitumen-water interface and make the interface less hydrophobic. These natural surfactants are not responsive to the CO₂ bubbling, resulting in unchanged induction time.

The bitumen surface treated by CO₂-responsive surfactants exhibited completely opposite behaviors with and without the CO₂ bubbling, which must be correlated to the switching behavior. Bitumen-air bubble attachment barely occurred in the surfactant solutions without switching. In fact, the air bubble never attached to the bitumen surfaces treated by CO₂-responsive surfactant solution even when the contact time exceeded the limitation of the induction timer (16000 ms). The only exception was the 1 mM MEA-LA group, where the introduced interfacial activity was still weak at this surfactant concentration as demonstrated in Figure 4.1a [14]. Nevertheless, the induction time is still significantly longer if compared to the bitumen surfaces treated by Milli-Q water. More importantly, the induction time was greatly reduced for the bitumen surface first treated by the CO₂-responsive surfactants then experienced CO₂ bubbling. The induction time after the CO₂ bubbling was as low as 97 ms for 1 mM MEA-LA treated bitumen surface, indicating an instantaneous air bubble attachment. Similarly, the induction time was 800 ms for 1 mM MEA-OA after the CO₂ bubbling. Besides, it was documented that the bitumen surfaces treated by MEA solutions could not exhibit the same low induction time after CO₂ bubbling (Figure 6.3). Hence, the dramatic change of bitumen-air bubble interaction from no attaching to instantaneous attaching must be attributed to the switchable characters of the CO₂-responsive surfactants.

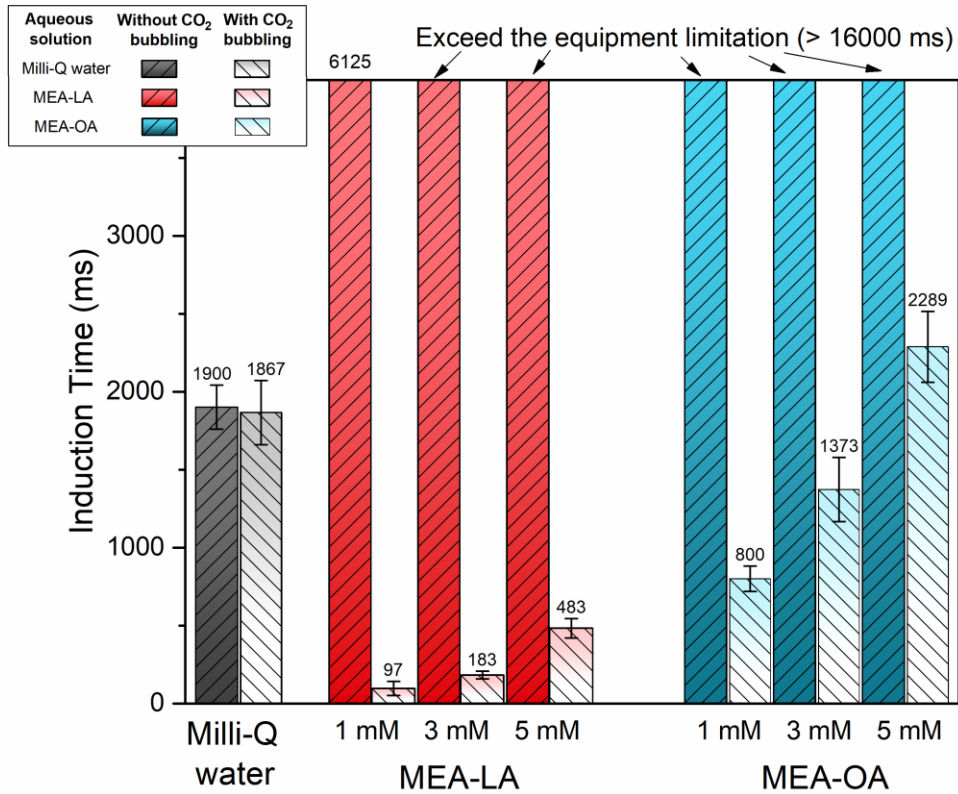


Figure 6.2. Induction time of air bubble attachment to bitumen surface treated by CO₂-responsive surfactants with and without the CO₂ bubbling.

It is further recognized that the induction time after CO₂ bubbling was affected by the surfactant concentration and the type of the CO₂-responsive surfactants. For the same type of surfactant, the induction time gradually raised up with increasing surfactant concentration. It had been confirmed that the adsorption of these CO₂-responsive surfactants onto the interface becomes much stronger with the increase of their bulk concentration within the investigated concentration range (1 mM to 5 mM) [14]. Hence, it becomes more difficult to recover a surfactant-free interface by CO₂ bubbling, especially at higher surfactant concentration. Even a trace amount of the adsorbed surfactant could have a considerable impact on the bitumen-air bubble attachment [25]. On the

other hand, the induction time of the MEA-LA group was significantly lower than that of the MEA-OA group at the same concentration after CO₂ bubbling. This is also consistent with the previous findings that MEA-LA could desorb from the oil-water interface more completely than MEA-OA after CO₂ bubbling, resulting in a much higher IFT value (Figure 4.2d). For example, the IFT value at the heptane-water interface was measured to be 42.0 mN/m for 1 mM MEA-LA after switching, which was 33.2 mN/m for 1 mM MEA-OA after switching. Accordingly, the bitumen surface was more hydrophobic in the MEA-LA group, and it was easier to have the air bubbles attached.

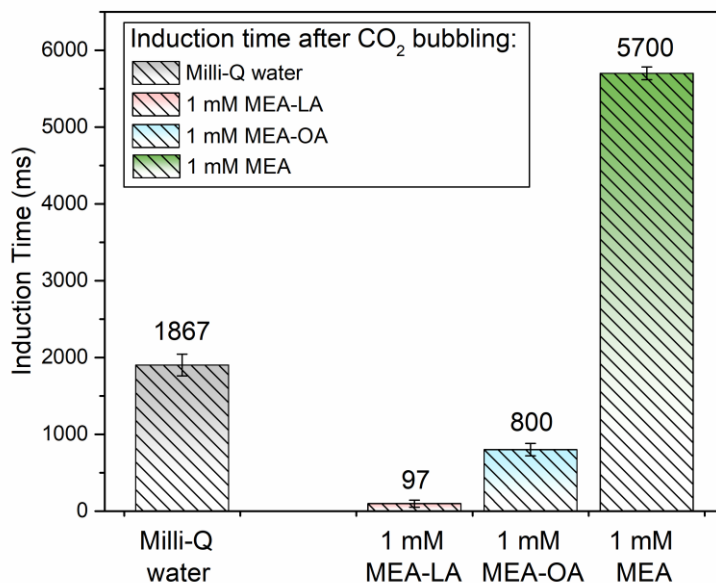


Figure 6.3. Induction time of air bubble attaching to bitumen surface treated by CO₂-responsive surfactants or MEA solution after the bubbling of CO₂ gas.

It is also worth noting that most bitumen surfaces treated by the CO₂-responsive surfactants had a much lower induction time than that in the Milli-Q water after CO₂ bubbling. This phenomenon indicates that the CO₂-responsive surfactants governed the interfacial property, and the effect of

natural surfactants became almost negligible. Otherwise, the induction time should be comparable to that in the Milli-Q water, which was around 1900 ms.

In general, experimental results evidenced our hypothesis that the CO₂-responsive surfactants can enhance the bitumen-air bubble attachment, utilizing their ability to switch interfacial activities. In reality, the CO₂ bubbling deactivates the interfacial activities of the surfactants, thereby increases the bitumen-water IFT and increases the aeration contact angle (θ_{aera}). Since both the air bubble and the bitumen surfaces recover their hydrophobicity, the attachment is much easier to occur. MEA-LA treated bitumen exhibited the shortest time for the air bubbles getting attached to the bitumen surface, while MEA-OA treated bitumen displayed relatively longer induction time.

6.3.2 Bitumen recovery

Bench-scale oil sands extraction experiments were conducted at ambient temperature in a custom-modified bitumen extraction unit (M-BEU) using Canadian oil sands ores. Details of the operation procedure are given in the experimental section and were designed to mimic the industrial operations in Figure 6.1a. CO₂-responsive surfactants were dissolved in the aqueous solutions and added together with the water. More importantly, CO₂ was used as the flotation gas in the secondary flotation stage to activate the switching behavior. It is also worth mentioning that the extraction experiments in this study were conducted at room temperature (23 ± 1 °C), which is notably lower than the current industrial operating temperature (~ 35 °C [2]). The solubility of CO₂ gas in the aqueous phase gradually decreases with elevating temperature [26]. The lack of CO₂ in water could become a potential restriction on the activation of switching behaviors. Furthermore, the industry prefers the operations at ambient temperature because of the significant reductions in energy input as well as on carbon footprint.

CO₂-responsive surfactant successfully improved the bitumen recovery in bench-scale oil sands extraction demonstrations. Figure 6.4a shows the images of the bituminous froth harvested on the top of the M-BEU cell. With the addition of 3 mM MEA-LA, both primary flotation and secondary flotation stages presented significant increases on the froth quantity, indicating the enhancement of bitumen recovery. These images also suggest that the most pronounced difference between the Milli-Q water and the MEA-LA solution came from the secondary flotation stage, where CO₂ gas was applied to activate the switching behavior. Dean-Stark apparatus was used to analyze these bituminous froths, and the results of total bitumen recovery are given in Figure 6.4b. It is first recognized that the enhancement of bitumen recovery was not attained by the MEA solution. MEA solution had been patented to facilitate the oil sands extraction from high-grade ores (34.5 wt.% bitumen) at high pH, NaOH addition, and elevated temperature [27]. However, the MEA solution did not help in extracting more bitumen under our conditions. The addition of MEA-LA improved the total bitumen recovery from 15.0 % up to 50.4 %, illustrating a threefold enhancement. An optimum concentration of MEA-LA addition was found to be around 3 mM, where an overdose of surfactant decreased bitumen recovery. This overdosing effect should be attributed to the increasing induction time at high surfactant concentrations (Figure 6.2).

Surprisingly, the bitumen recovery ratio was only slightly affected by the MEA-OA solution. It is readily known that MEA-OA exhibited better performance than MEA-LA in bitumen liberation stage as discussed the previous chapter (Figure 5.3c), but much less efficient on facilitating the bitumen-air bubble attachment (Figure 6.2). It is most likely that the liberated bitumen was still dispersed in the process water due to the poor air bubble capture efficiency. Results from the oil sands extraction experiments suggest that the aeration became a limiting step for the final bitumen

recovery ratio after bitumen is liberated, although the liberation stage is a prerequisite condition that determines how much bitumen could have been harvested.

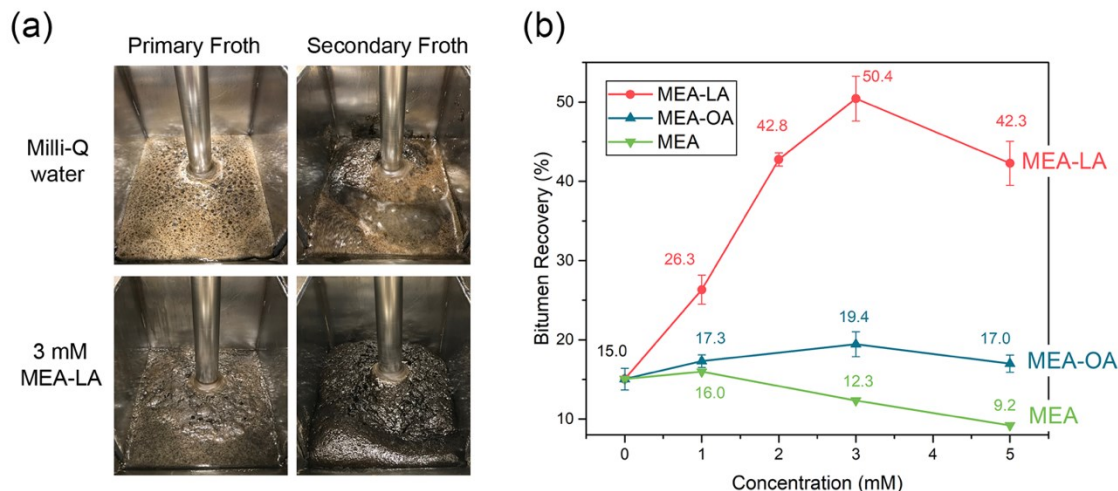


Figure 6.4. (a) Comparison of the bituminous froth in Milli-Q water and in 3 mM MEA-LA; and (b) Total bitumen recovery in bench-scale oil sands extraction experiments using CO₂-responsive surfactants as the processing aid and using CO₂ gas as the secondary flotation gas.

Since the MEA-LA addition exhibited a more promising enhancement on bitumen recovery, we are now focusing on this specific compound to understand its mechanisms in the oil sands extraction process. Bitumen recovery from the MEA-LA group was analyzed in the primary froth and the secondary froth separately. The results are shown in Figure 6.5. In the primary froth, there was a steady but marginal bitumen recovery enhancement as the MEA-LA concentration increased. It needs to be mentioned that CO₂ had not been introduced into the system yet when collecting the primary froth. Hence, MEA-LA acted as a conventional surfactant in the primary flotation stage. Although more bitumen could be washed out from the host solids with the addition of CO₂-responsive surfactant in the previous chapter, the liberated bitumen would be dispersed in the aqueous phase due to the low bitumen-water IFT. On the other hand, the major enhancement

of bitumen recovery was obtained in the secondary froth, when CO₂ gas was used as the secondary flotation gas and the responsiveness of MEA-LA was activated. The maximum bitumen recovery in secondary froth was found at the optimum MEA-LA concentration (3 mM), where 42.8% of bitumen contained in the oil sands ores was collected. Overdosing MEA-LA resulted in a drawback in the bitumen recovery in the secondary froth, corresponding to the increase of induction time (Figure 6.2).

In order to prove the concept that CO₂-responsive surfactants serve as better processing aids due to their ability to control the water-bitumen interfacial tension, a set of control groups was conducted using air instead of CO₂ as the secondary flotation gas, while all the other conditions were kept the same. MEA-LA could be considered as a conventional surfactant if its responsiveness was not activated. The results are exhibited in Figure 6.6. Without the addition of MEA-LA, using CO₂ as the secondary flotation gas was actually a hindrance to the oil sands extraction process. The bitumen recovery in the secondary froth was only 12.5% when using CO₂, which became 20.4% when using air. CO₂, as an acidic gas, decreases the bulk pH and diminishes the bitumen liberation from the oil sands ores [1]. Quite oppositely, with the addition of 3 mM MEA-LA, a better oil sands extraction performance was obtained when using CO₂ as the secondary flotation gas instead of air. The differences were found in the secondary flotation stage. The bitumen recovery in the secondary froth was 42.9% when using CO₂, which decreased down to 34.4% when using air. Obviously, this enhancement should be credited to the CO₂ switching behavior of MEA-LA at the bitumen-water interface, which permits the “switch-off” of interfacial activity and thereby benefits the bitumen-air bubble attachment upon the introduction of CO₂.

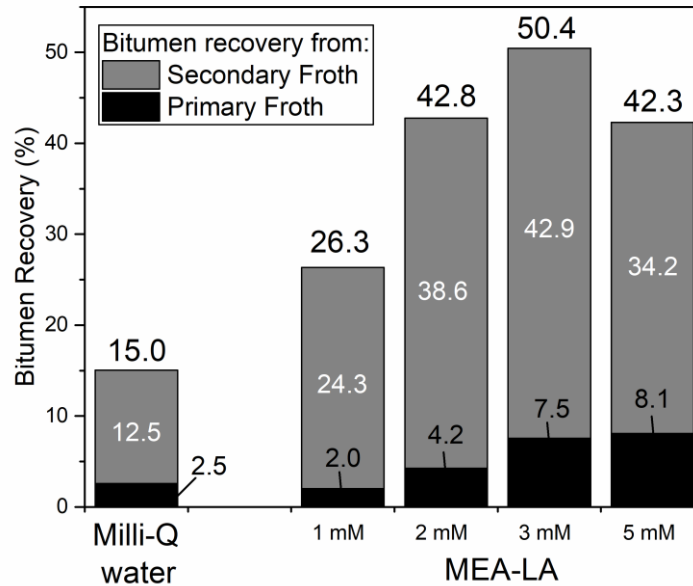


Figure 6.5. Comparison of bitumen recovery from the primary froth and the secondary froth in the cases of MEA-LA solution at different concentrations.

Interestingly, it was also found that the use of 10-minute CO₂ flow in the secondary flotation stage was more than necessary to activate the responsiveness of MEA-LA. As shown in Figure 6.6, when employing 3 mM MEA-LA as the processing aid, the total bitumen recovery did not change much if the duration of CO₂ flow was reduced to from 10 minutes to 5 minutes. Another 5-minute airflow was applied to compensate for the flotation duration for the latter case. The result suggests that using pure CO₂ flow as the secondary flotation gas is superabundant to switch off the interfacial activity of MEA-LA and achieve higher bitumen recovery. Instead, there is plenty of room to reduce the amount of CO₂ by using CO₂-air mixture, such as flue gas, without harming the effectiveness of MEA-LA, which is also of more practical implications.

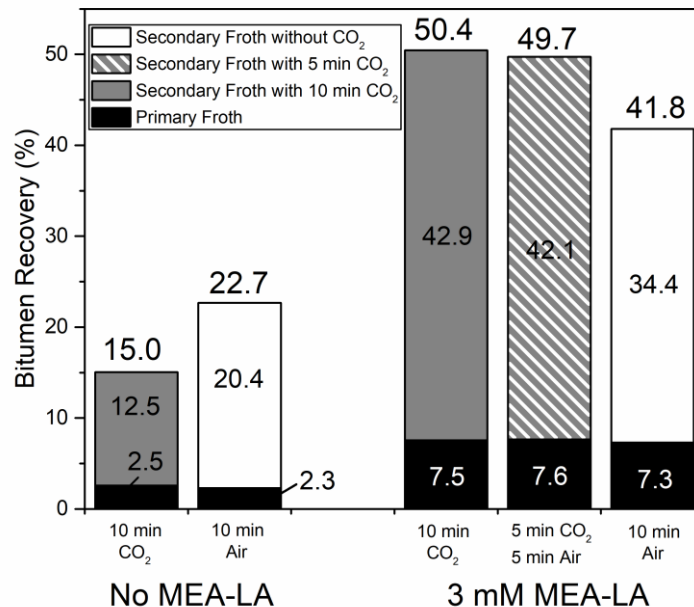


Figure 6.6. Comparison of bitumen recovery using CO₂ or air as the secondary flotation gas, in the cases of no MEA-LA addition and 3 mM MEA-LA addition.

6.3.3 Froth quality

Quality of the bituminous froth is another critical consideration in the oil sands extraction process. Despite bitumen content, the froth contains undesired compositions such as mineral solids and water, both of which are corrosive for the upgraders and cause serious problems. Ideally, the froth should contain as more bitumen as it can, meanwhile fewer solids and water as possible. The froth quality discussed in this section is determined by froth composition, including bitumen, water, and solid, as well as the bitumen-to-solid ratio (B/S) and bitumen-to-water ratio (B/W). Higher values of B/S and B/W refer to a better quality of the bituminous froth. The first glance of froth quality was determined by the visual observation during oil sands extraction operation. The first impression of the froth quality was readily shown by the images in Figure 6.4a. Both primary and

secondary froths were “darker” in color with the addition of 3 mM MEA-LA, which visually demonstrated that the froth quality had been improved.

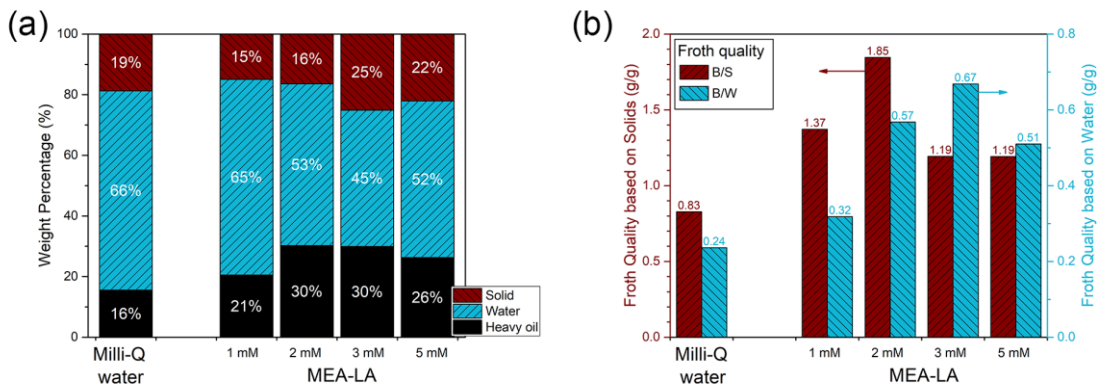


Figure 6.7. Evaluation of the froth quality by (a) froth composition; and by (b) bitumen-to-solid (B/S) ratio and bitumen-to-water (B/W) ratio.

Further froth quality analysis was accomplished by quantifying the froth composition. In Figure 6.7a, the weight percentage of bitumen was steadily enhanced with increasing concentration of MEA-LA until the optimum concentration was reached. Although more solids were collected in the froth with MEA-LA addition, the corresponding B/S and B/W ratios were higher than that in the Milli-Q water group, as illustrated in Figure 6.7b. The maximum B/S value was found at 2 mM MEA-LA addition, while the best B/W ratio was observed at 3 mM MEA-LA addition. Besides, the froth quality became worse when MEA-LA concentration rose up to 5 mM. This is caused by the reduction of recovered bitumen and the increasing amount of entrained water at the same time. Therefore, it can be concluded that overdosing CO₂-responsive surfactants harms not only the bitumen recovery but also the froth quality.

6.3.4 Salt effects

In the previous sections, we have successfully validated that CO₂-responsive surfactants are capable of enhancing bitumen recovery in bench-scale oil sands extraction operations. In order to prove this novel concept, the system was simplified by using Milli-Q water such that the salt effects were eliminated. In reality, however, the process water contains a variety of dissolved ions, which could play essential roles in the extraction process [20, 21]. Therefore, some tests were conducted to investigate the performance of MEA-LA on enhancing bitumen recovery under the process water conditions.

Table 6.1. Major ions and their concentrations in the process water.

Ion type	F ⁻	Cl ⁻	NO ₃ ⁻	SO ₄ ²⁻	Na ⁺	K ⁺	Mg ²⁺	Ca ²⁺
Concentration (ppm)	11.1	455.6	44.4	500.0	833.4	21.1	16.7	27.8

The major ions and their concentrations in the process water were detected by ion chromatography (IC). Results are summarized in Table 6.1 and are consistent with the previous reports [18, 19]. When dissolving MEA-LA into the process water, it is first recognized that some precipitates would appear, which implies the formation of insoluble ion-surfactant complexes. These precipitates were centrifuged and filtered out, while the clear supernatant fluids were used as the aqueous solutions in further investigation.

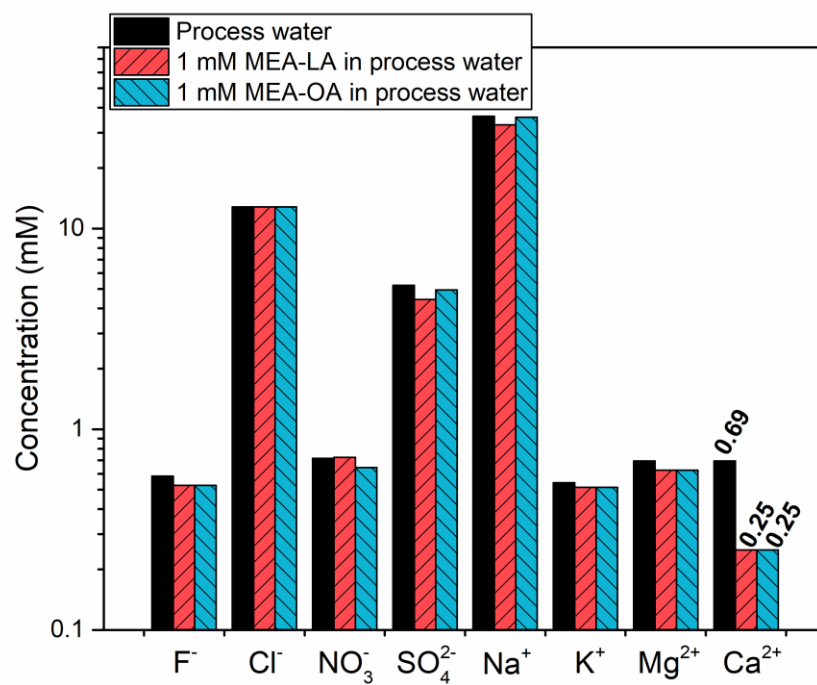


Figure 6.8. Ion concentration in the supernatant fluids, which were filtered from the mixture of CO₂-responsive surfactants and process water.

The formation of undesired precipitates is most likely to be the consequence of calcium ions in the process water, which weakens the ability to reduce oil-water IFT. The ion concentrations were further analyzed in the supernatant fluids. Calcium ions suffered a dramatic decrease in their concentration, whereas other types of ions only exhibited negligible changes (Figure 6.8). Hence, the precipitates are considered to be the insoluble complexes formed by the strong affinity between calcium ions and anionic fatty acids [28]. The results also elucidate that the presence of 1 mM calcium ion could react with approximate 2 mM of fatty acid. The most direct consequence of the precipitate formation is that a considerable amount of the CO₂-responsive surfactants was consumed by the calcium ions. Hence, their ability to decrease the oil-water IFT would be

weakened (Figure 6.9). Such phenomena are unfavorable to the oil sands extraction process because the interfacial activity is of critical importance to the bitumen liberation stage. On the other hand, however, calcium ions are also known as the major issue causing the “slime coating”, which inhibits the bitumen-air bubble attachment [1, 20]. Reducing calcium concentration in the process water has some positive impacts on the bitumen recovery. At this point, one has to admit that it is rather difficult to predict the performance of CO₂-responsive surfactants dissolved in the process water on the oil sands extraction operations.

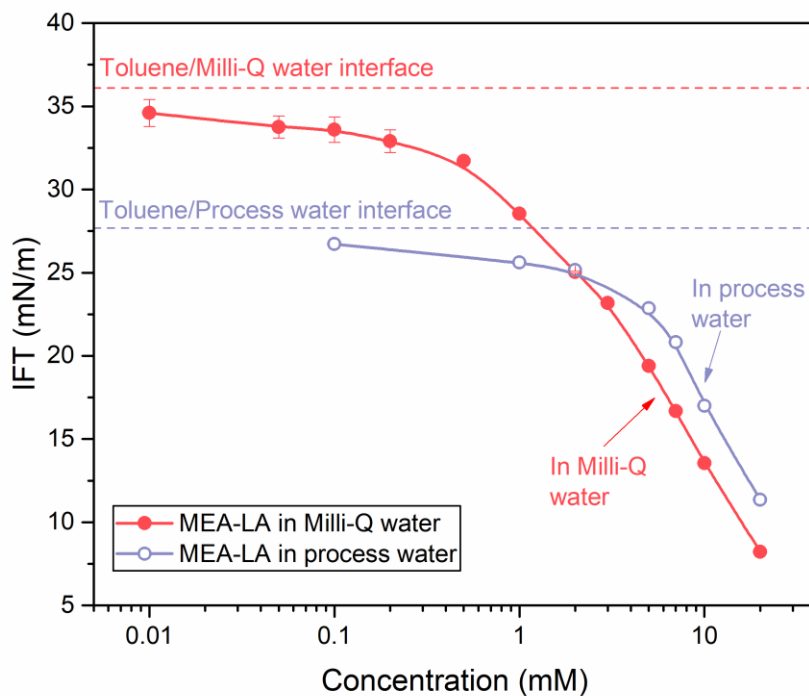


Figure 6.9. IFT measured at the toluene/aqueous interface of MEA-LA in the Milli-Q water or in the process water.

Nevertheless, experiments demonstrated that MEA-LA was capable of enhancing the total bitumen recovery when dissolved in the process water but less efficient than in Milli-Q water (Figure 6.10).

Without surfactant addition, the bitumen recovery was even worth in the process water due to the presence of calcium ions. With the help of MEA-LA addition, there still displayed a considerable improvement in the total bitumen recovery ratio, indicating the robustness of MEA-LA in the process water conditions. MEA-LA in the process water required roughly 2 mM higher concentration to achieve a similar bitumen recovery ratio as that in the Milli-Q water. Further investigations are needed to obtain a more comprehensive understanding of the mechanism involved. Besides, CO₂-responsive surfactants with better calcium tolerance are anticipated to have exceptional potentials in the fields of oil sands extraction process.

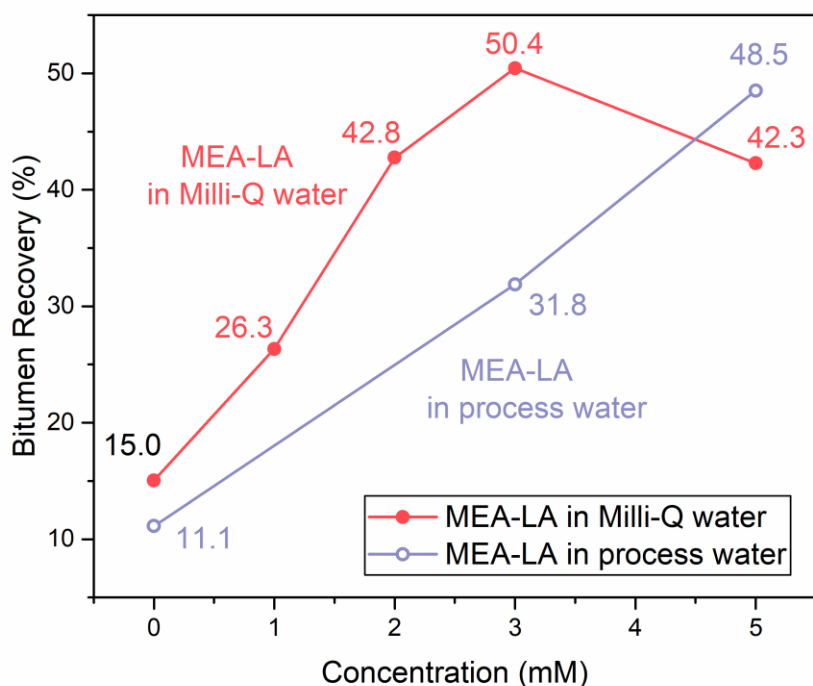


Figure 6.10. Comparison of the bitumen recovery using MEA-LA as the processing aid in Milli-Q water and process water.

6.4 Conclusion

In this study, two CO₂-responsive surfactants were applied to the bench-scale oil sands extraction process. MEA-LA was found to successfully enhance the total bitumen recovery at ambient temperature, whereas unfortunately, the improvement from MEA-OA was rather weak. Results indicated that MEA-LA has a more significant impact on the bitumen aeration stage after CO₂ switching, whereas MEA-OA possesses the advantages in the bitumen liberation stage. It is then concluded that the harvest of bitumen from the aqueous medium is the limiting step for the enhancement of final bitumen recovery, although the bitumen liberation stage is also necessary as a prerequisite condition. There existed an optimum concentration of MEA-LA where overdosage could cause a decrease of bitumen recovery. The major improvement was obtained after the activation of CO₂-responsiveness, which strongly supports the advantages of using these novel responsive surfactants. Using air instead of CO₂ as the secondary flotation gas reduced the effectiveness of MEA-LA, which further demonstrated the importance of CO₂ switching. It was possible to use the flue gas instead without harming the bitumen recovery, which is of more practical implications. The froth quality was also improved by MEA-LA addition. Both B/S and B/W ratios were increased with the treatment of CO₂-responsive surfactants. Besides, MEA-LA was still capable of enhancing bitumen recovery in the process water condition, although its efficiency was impeded due to the formation of insoluble complexes with calcium ions.

6.5 References

1. Masliyah, J., et al., *Understanding water- based bitumen extraction from Athabasca oil sands*. The Canadian Journal of Chemical Engineering, 2004. **82**(4): p. 628-654.
2. Masliyah, J., J. Czarnecki, and Z. Xu, *Handbook on theory and practice of bitumen recovery from Athabasca oil sands: Vol. I. Theoretical basis*. 2010: Kingsley Knowledge Publishing.

3. Mossop, G.D., *Geology of the Athabasca oil sands*. Science, 1980. **207**(4427): p. 145-152.
4. Chen, T., et al., *Impact of salinity on warm water-based mineable oil sands processing*. The Canadian Journal of Chemical Engineering, 2017. **95**(2): p. 281-289.
5. *Alberta mineable oil sands plant statistics monthly supplement*. 2016, Alberta Energy Regulator.
6. He, L., et al., *Interfacial sciences in unconventional petroleum production: From fundamentals to applications*. Chemical Society Reviews, 2015. **44**(15): p. 5446-5494.
7. He, L., et al., *Enhancing bitumen liberation by controlling the interfacial tension and viscosity ratio through solvent addition*. Energy & Fuels, 2014. **28**(12): p. 7403-7410.
8. He, L., et al., *Effect of solvent addition on bitumen-air bubble attachment in process water*. Chemical Engineering Science, 2015. **137** p. 31-39.
9. Flury, C., et al., *Effect of caustic type on bitumen extraction from Canadian oil sands*. Energy & Fuels, 2014. **28**(1): p. 431-438.
10. Long, J., et al., *Improving oil sands processability using a temperature-sensitive polymer*. Energy & Fuels, 2011. **25**(2): p. 701-707.
11. Han, C., *Design and synthesis of temperature switchable non-ionic block copolymers for application to oil sands extraction*. 2016, University of Alberta.
12. Yang, B. and J. Duhamel, *Extraction of oil from oil sands using thermoresponsive polymeric surfactants*. ACS Applied Materials & Interfaces, 2015. **7**(10): p. 5879-5889.
13. Tiktopulo, E.I., et al., *Domain coil-globule transition in homopolymers*. Macromolecules, 1995. **28**(22): p. 7519-7524.
14. Lu, Y., et al., *CO₂-responsive surfactants with tunable switching pH*. Journal of Colloid and Interface Science, 2019. **557**: p. 185-195.
15. Jessop, P.G., S.M. Mercer, and D.J. Heldebrant, *CO₂-triggered switchable solvents, surfactants, and other materials*. Energy & Environmental Science, 2012. **5**(6): p. 7240-7253.
16. Yang, Z., et al., *Recent advances of CO₂-responsive materials in separations*. Journal of CO₂ Utilization, 2019. **30**: p. 79-99.
17. Darabi, A., P.G. Jessop, and M.F. Cunningham, *CO₂-responsive polymeric materials: Synthesis, self-assembly, and functional applications*. Chemical Society Reviews, 2016. **45**(15): p. 4391-4436.
18. Zhu, Y., et al., *Biodiesel-assisted ambient aqueous bitumen extraction (BA³BE) from Athabasca oil sands*. Energy & Fuels, 2018.
19. Lu, Y., et al., *Pseudo-Gemini biosurfactants with CO₂ switchability for enhanced oil recovery (EOR)*. Tenside Surfactants Detergents, 2019. **56**(5): p. 407-416.
20. Gu, G., et al., *Effects of physical environment on induction time of air-bitumen attachment*. International Journal of Mineral Processing, 2003. **69**(1): p. 235-250.

21. Chen, T., et al., *Impact of salinity on warm water-based mineable oil sands processing*. Canadian Journal of Chemical Engineering, 2017. **95**(2): p. 281-289.
22. Bulmer, J. and J. Starr, *Syncrude analytical methods for oil sand and bitumen processing*. AOSTRA, Edmonton, 1979.
23. Yoon, R.-H. and J.L. Yordan, *Induction time measurements for the quartz—amine flotation system*. Journal of Colloid and interface Science, 1991. **141**(2): p. 374-383.
24. Ye, Y., S.M. Khandrika, and J.D. Miller, *Induction-time measurements at a particle bed*. International Journal of Mineral Processing, 1989. **25**(3-4): p. 221-240.
25. Schramm, L.L. and R.G. Smith, *The influence of natural surfactants on interfacial charges in the hot-water process for recovering bitumen from the Athabasca oil sands*. Colloids and Surfaces, 1985. **14**(1): p. 67-85.
26. Dean, J.A., *Lange's handbook of chemistry*. 1999: New York; London: McGraw-Hill, Inc.
27. Klimpel, R.R. and B.S. Fee, *Recovery of petroleum from tar sands*. 1992, The Dow Chemical Company, Midland, Mich: US.
28. Jandacek, R.J., *The solubilization of calcium soaps by fatty acids*. Lipids, 1991. **26**(3): p. 250-253.

Chapter 7. Conclusions and Future Perspectives

7.1 Conclusions

A series of CO₂-responsive surfactants (MEA-LCFAs) were assembled by the non-covalent association between MEA and LCFAs. The switching pH of MEA-LCFA surfactants could be easily tuned by using different types of LCFAs, which provides a facile route of customization towards varieties of applications. More importantly, it is emphasized that the determination of switching pH should be proceeded carefully since the switching behaviors of MEA-LCFA surfactants at the oil-water interface were found to be significantly different from that in bulk solutions. Dynamic IFT and coalescence time measurements were both effective tools to distinguish interfacial switching and solution switching by applying “adsorption-then-switch” or “switch-then-adsorption” protocols. Switching pH for the oil-water interface was found to be lower than that in bulk solutions, which is the result of stronger molecular interactions of switching molecules at the oil-water interface. This colloidal phenomenon is consistent with theoretical calculations reported in literature, and more broadly speaking, similar to the observations of enhanced molecular recognition at biological interfaces. In most applications, CO₂-responsive surfactants are switched at the interface. Therefore, it is more appropriate to determine the switching pH from interfacial responses of MEA-LCFA surfactants to predict their performance in practical applications.

Two representative CO₂-responsive surfactants from the MEA-LCFAs series were investigated to enhance conventional heavy oil recovery. Compared with most traditional surfactants, CO₂-responsive surfactants possess significant advantages, in which their interfacial activity can be

switched off by CO₂ bubbling at the desired stage. Hence, they are capable of performing as surfactants to enhance the oil-solid separation in the liberation stage and then switch to demulsifiers to facilitate the oil-water separation in the harvest stage. Additionally, it is also viable to recycle the MEA component together with the tailing water after treatments.

Finally, CO₂-responsive surfactants were applied to the bench-scale oil sands extraction process. MEA-LA was found to successfully enhance the total bitumen recovery at ambient temperature, whereas unfortunately, the improvement from MEA-OA was rather weak. Results indicate that MEA-LA has a more significant impact on the bitumen aeration after CO₂ bubbling, whereas MEA-OA possesses the advantages in the bitumen liberation stage. It is concluded that the harvest of bitumen from the aqueous medium is the predominant factor for increasing final bitumen recovery, although the bitumen liberation stage is as a prerequisite condition.

7.2 Future perspectives

We anticipate that this project provides valuable guidance in developing responsive materials for various large-scale applications, such as household cleaning, contaminated soil remediation, and oil spill management. Both MEA and fatty acids are common chemicals that are commercially available at affordable prices, which offers scale-up possibilities. The versatility of this group of CO₂-responsive is also readily involved in their design. Their interfacial activity and switchability could be easily modified by changing the types of amines and fatty acids, such that CO₂-responsive surfactants could be customized for specific requirements.

Future works of this project are proposed in the following directions:

- It has been indicated in Chapter 4 that the type of fatty acids decides the switching pH of the CO₂-responsive surfactants. Further studies should be performed to understand the role of amines in the CO₂-responsive surfactants. There are results showing that using multi-valent amines instead of MEA⁺ could significantly improve the interfacial activity by forming the pseudo-Gemini structures at the interface, whereas the switching pH remains unchanged. It would be interesting to study the effect of amines by their valency, topology, and affinity to different fatty acids.
- Chapter 5 and Chapter 6 prove the concept that CO₂-responsive surfactants could enhance the heavy oil/bitumen recovery by switching their interfacial properties. In an effort to recover more hydrocarbon resources, CO₂-responsive surfactants could be integrated with the novel aqueous-nonaqueous hybrid extraction process in the oil sands extraction. Most recent results have shown that bitumen recovery could be improved from 74.3 % to 88.6 % with industrial process water and at the ambient temperature. Further optimization of this approach is needed to unleash the ultimate potential of CO₂-responsive surfactants.
- CO₂-responsive surfactants are anticipated to be expanded to broader aspects of applications, including oil spill treatment, oil-contaminated soil remediation, and enhanced oil recovery (EOR).

Bibliography

- Abbaspourrad, Alireza, Sujit S. Datta, and David A. Weitz. 2013. 'Controlling release from pH-responsive microcapsules', *Langmuir*, 29: 12697-702.
- Afolabi, Richard O., Gbenga F. Oluyemi, Simon Officer, and Johnson O. Ugwu. 2019. 'Hydrophobically associating polymers for enhanced oil recovery – Part A: A review on the effects of some key reservoir conditions', *Journal of Petroleum Science and Engineering*, 180: 681-98.
- Agista, Madhan Nur, Kun Guo, and Zhixin Yu. 2018. 'A state-of-the-art review of nanoparticles application in petroleum with a focus on enhanced oil recovery', *Applied Sciences*, 8: 871.
- Ahmed, Shehzad, Khaled Abdalla Elraies, Isa M. Tan, and Mudassar Mumtaz. 2017. "A review on CO₂ foam for mobility control: Enhanced oil recovery." In *ICIPEG 2016* (pp. 205-215). Springer, Singapore.
- Al-Anssari, Sarmad, Ahmed Barifcani, Shaobin Wang, Lebedev Maxim, and Stefan Iglauer. 2016. 'Wettability alteration of oil-wet carbonate by silica nanofluid', *Journal of Colloid and Interface Science*, 461: 435-42.
- Al-shehri, Abdullah A., Erika S. Ellis, Jesus M. Felix Servin, Dmitry V. Kosynkin, Mazen Y. Kanj, and Howard K. Schmidt. 2013. "Illuminating the reservoir: Magnetic NanoMappers." In *SPE Middle East Oil and Gas Show and Conference*, 10. Manama, Bahrain: Society of Petroleum Engineers.
- Regulator, A.E. 2016 "Alberta mineable oil sands plant statistics monthly supplement." *Alberta Energy Regulator*
- Araujo, Elmo, Yahya Rharbi, Xiaoyu Huang, Mitchell A. Winnik, David R. Bassett, and Richard D. Jenkins. 2000. 'Pyrene excimer kinetics in micellelike aggregates in a C₂₀-HASE associating polymer', *Langmuir*, 16: 8664-71.
- Ariga, Katsuhiko, Takashi Nakanishi, Jonathan P. Hill, Makoto Shirai, Minoru Okuno, Takao Abe, and Jun-ichi Kikuchi. 2005. 'Tunable pK_a of amino acid residues at the air–water interface

- gives an L-zyne (Langmuir Enzyme)', *Journal of the American Chemical Society*, 127: 12074-80.
- Arnould, Audrey, Fabrice Cousin, Léa Chabas, and Anne-Laure Fameau. 2018. 'Impact of the molar ratio and the nature of the counter-ion on the self-assembly of myristic acid', *Journal of Colloid and Interface Science*, 510: 133-41.
- Ashrafizadeh, SN, and M Kamran. 2010. 'Emulsification of heavy crude oil in water for pipeline transportation', *Journal of Petroleum Science and Engineering*, 71: 205-11.
- Ashrafizadeh, SN, E Motaeae, and V Hoshyargar. 2012. 'Emulsification of heavy crude oil in water by natural surfactants', *Journal of Petroleum Science and Engineering*, 86: 137-43.
- Aveyard, R., B. P. Binks, N. Carr, and A. W. Cross. 1990. 'Stability of insoluble monolayers and ionization of Langmuir-Blodgett multilayers of octadecanoic acid', *Thin Solid Films*, 188: 361-73.
- Bai, Xinxin, Yan Wang, Xin Zheng, Kangmeng Zhu, Anhua Long, Xiaogang Wu, and Hui Zhang. 2019. 'Remediation of phenanthrene contaminated soil by coupling soil washing with Tween 80, oxidation using the UV/S₂O₈²⁻ process and recycling of the surfactant', *Chemical Engineering Journal*, 369: 1014-23.
- Barzagli, Francesco, Fabrizio Mani, and Maurizio Peruzzini. 2009. 'A ¹³C NMR study of the carbon dioxide absorption and desorption equilibria by aqueous 2-aminoethanol and N-methyl-substituted 2-aminoethanol', *Energy & Environmental Science*, 2: 322-30.
- Berg, John C. 2010. *An introduction to interfaces & colloids: the bridge to nanoscience* (World Scientific).
- Bokias, G., D. Hourdet, I. Iliopoulos, G. Staikos, and R. Audebert. 1997. 'Hydrophobic interactions of poly(N-isopropylacrylamide) with hydrophobically modified poly(sodium acrylate) in aqueous solution', *Macromolecules*, 30: 8293-97.
- Brown, Paul, Craig P. Butts, and Julian Eastoe. 2013. 'Stimuli-responsive surfactants', *Soft Matter*, 9: 2365-74.
- Brown, Paul, Vishnu Sresht, Burak H. Eral, Andrew Fiore, César de la Fuente-Núñez, Marcus O'Mahony, Gabriel P. Mendes, William T. Heller, Patrick S. Doyle, Daniel Blankschtein,

- and T. Alan Hatton. 2017. 'CO₂-reactive ionic liquid surfactants for the control of colloidal morphology', *Langmuir*, 33: 7633-41.
- Brown, Paul, Matthew J. Wasbrough, Burcu E. Gurkan, and T. Alan Hatton. 2014. 'CO₂-responsive microemulsions based on reactive ionic liquids', *Langmuir*, 30: 4267-72.
- Bulmer, JT, and J Starr. 1979. 'Syn crude analytical methods for oil sand and bitumen processing', *AOSTRA, Edmonton*.
- Cates, M. E., D. Andelman, S. A. Safran, and D. Roux. 1988. 'Theory of microemulsions: Comparison with experimental behavior', *Langmuir*, 4: 802-06.
- Ceschia, Elize, Jitendra R. Harjani, Chen Liang, Zahra Ghoshouni, Tamer Andrea, R. Stephen Brown, and Philip G. Jessop. 2014. 'Switchable anionic surfactants for the remediation of oil-contaminated sand by soil washing', *RSC Advances*, 4: 4638-45.
- Chen, I, Cengiz Yegin, Ming Zhang, and Mustafa Akbulut. 2014. 'Use of pH-responsive amphiphilic systems as displacement fluids in enhanced oil recovery', *SPE Journal*, 19: 1,035-1,46.
- Chen, Qianqian, Lei Wang, Gaihan Ren, Qian Liu, Zhenghe Xu, and Dejun Sun. 2017. 'A fatty acid solvent of switchable miscibility', *Journal of Colloid and Interface Science*, 504: 645-51.
- Chen, Quansheng, Yu Wang, Zhiyong Lu, and Yujun Feng. 2013. 'Thermoviscosifying polymer used for enhanced oil recovery: Rheological behaviors and core flooding test', *Polymer Bulletin*, 70: 391-401.
- Chen, Tong, Feng Lin, Bauyrzhan Primkulov, Lin He, and Zhenghe Xu. 2017b. 'Impact of salinity on warm water-based mineable oil sands processing', *The Canadian Journal of Chemical Engineering*, 95: 281-89.
- Chen, Xiangyu, Xinrui Ma, Ci Yan, Dejun Sun, Tony Yeung, and Zhenghe Xu. 2018. 'CO₂-responsive o/w microemulsions prepared using a switchable superamphiphile assembled by electrostatic interactions', *Journal of Colloid and Interface Science*, 534: 595-604

- Cherukupally, Pavani, Edgar J. Acosta, Juan P. Hinestroza, Amy M. Bilton, and Chul B. Park. 2017. 'Acid–base polymeric foams for the adsorption of micro-oil droplets from industrial effluents', *Environmental Science & Technology*, 51: 8552-60.
- Chevallier, E., A. Mamane, H. A. Stone, C. Tribet, F. Lequeux, and C. Monteux. 2011. 'Pumping-out photo-surfactants from an air–water interface using light', *Soft Matter*, 7: 7866-74.
- Christie, Michael A, James Glimm, John W Grove, David M Higdon, David H Sharp, and Merri M Wood-Schultz. 2005. 'Error analysis and simulations of complex phenomena', *Los Alamos Science*, 29.
- Cistola, David P, James A Hamilton, David Jackson, and Donald M Small. 1988. 'Ionization and phase behavior of fatty acids in water: Application of the Gibbs phase rule', *Biochemistry*, 27: 1881-88.
- Cratin, Paul D. 1993. 'Mathematical modeling of some pH-dependent surface and interfacial properties of stearic acid', *Journal of Dispersion Science and Technology*, 14: 559-602.
- Czarnecki, Jan, and Kevin Moran. 2005. 'On the stabilization mechanism of water-in-oil emulsions in petroleum systems', *Energy & Fuels*, 19: 2074-79.
- Dai, S., K.C. Tam, R.D. Jenkins, and D.R. Bassett. 2000. 'Light scattering of dilute hydrophobically modified alkali-soluble emulsion solutions: Effects of hydrophobicity and spacer length of macromonomer', *Macromolecules*, 33: 7021-28.
- Dai, Shanshan, Yuxin Suo, Dongfang Liu, Peiyao Zhu, Jihe Zhao, Jiang Tan, and Hongsheng Lu. 2018. 'Controllable CO₂-responsiveness of o/w emulsions by varying the alkane carbon number of a tertiary amine', *Physical Chemistry Chemical Physics*, 20: 11285-95.
- Darabi, A., P. G. Jessop, and M. F. Cunningham. 2016. 'CO₂-responsive polymeric materials: synthesis, self-assembly, and functional applications', *Chemical Society Reviews*, 45: 4391-436.
- De Gennes, P. G., and C. Taupin. 1982. 'Microemulsions and the flexibility of oil/water interfaces', *The Journal of Physical Chemistry*, 86: 2294-304.
- Dean, John Aurie. 1999. *Lange's handbook of chemistry* (New york; London: McGraw-Hill, Inc.).

- dos Santos, Elisama Vieira, Cristina Sáez, Pablo Cañizares, Djalma Ribeiro da Silva, Carlos A. Martínez-Huitle, and Manuel A. Rodrigo. 2017. 'Treatment of *ex-situ* soil-washing fluids polluted with petroleum by anodic oxidation, photolysis, sonolysis and combined approaches', *Chemical Engineering Journal*, 310: 581-88.
- Dreiss, Cécile A. 2017. 'Chapter 1. Wormlike micelles: an Introduction.' in, *Wormlike micelles: Advances in systems, characterisation and applications* (The Royal Society of Chemistry).
- Eastoe, Julian, James Dalton, Philippe Rogueda, Donal Sharpe, Jinfeng Dong, and John R. P. Webster. 1996. 'Interfacial properties of a catanionic surfactant', *Langmuir*, 12: 2706-11.
- Eisenthal, K. B. 1996. 'Liquid interfaces probed by second-harmonic and sum-frequency spectroscopy', *Chemical Reviews*, 96: 1343-60.
- English, Robert J., Jonathan H. Laurer, Richard J. Spontak, and Saad A. Khan. 2002. 'Hydrophobically modified associative polymer solutions: Rheology and microstructure in the presence of nonionic surfactants', *Industrial & Engineering Chemistry Research*, 41: 6425-35.
- Falbe, Jürgen. 2012. *Surfactants in consumer products: Theory, technology and application* (Springer Science & Business Media).
- Fameau, A. L., A. Saint-Jalmes, F. Cousin, B. Houinsou Houssou, B. Novales, L. Navailles, J. Emile, F. Nallet, C. Gaillard, F. Boue, and J. P. Douliez. 2011. 'Smart foams: Switching reversibly between ultrastable and unstable foams', *Angewandte Chemie, International Edition in English*, 50: 8264-9.
- Fameau, A. L., and T. Zemb. 2014. 'Self-assembly of fatty acids in the presence of amines and cationic components', *Advances in Colloid and Interface Science*, 207: 43-64.
- Fanchi, John R. 2018. 'Chapter 6. Fluid properties and model initialization.' in John R. Fanchi (ed.), *Principles of Applied Reservoir Simulation (Fourth Edition)* (Gulf Professional Publishing).
- Feng, Yujun, Zonglin Chu, and Cécile A. Dreiss. 2015. 'Applications of smart wormlike micelles.' in, *Smart wormlike micelles: Design, characteristics and applications* (Springer Berlin Heidelberg: Berlin, Heidelberg).

- Flury, Christopher, Artin Afacan, Marjan Tamiz Bakhtiari, Johan Sjoblom, and Zhenghe Xu. 2014. 'Effect of caustic type on bitumen extraction from canadian oil sands', *Energy & Fuels*, 28: 431-38.
- G. Argudo, Pablo, Eulogia Muñoz, Juan José Giner-Casares, María Teresa Martín-Romero, and Luis Camacho. 2019. 'Folding of cytosine-based nucleolipid monolayer by guanine recognition at the air-water interface', *Journal of Colloid and Interface Science*, 537: 694-703.
- Glazer, J., and M. Z. Dogan. 1953. 'Ionization of protein monolayers and related substances', *Transactions of the Faraday Society*, 49: 448-55.
- Greenwood, Norman Neill, and Alan Earnshaw. 1984. 'Chemistry of the elements'.
- Gu, Guoxing, Zhenghe Xu, Kumar Nandakumar, and Jacob Masliyah. 2003. 'Effects of physical environment on induction time of air-bitumen attachment', *International Journal of Mineral Processing*, 69: 235-50.
- Guo, Y., J. Hu, X. Zhang, R. Feng, and H. Li. 2016. 'Flow behavior through porous media and microdisplacement performances of hydrophobically modified partially hydrolyzed polyacrylamide', *SPE Journal*, 21: 688-705.
- Halland, Eva K, Jasminka Mujezinovic, Fridtjof Riis, A Bjørnstad, IM Meling, IT Gjeldvik, IM Tappel, M Bjørheim, RS RØD, and VTH Pham. 2014. 'CO₂ storage atlas: Norwegian continental shelf', *Norwegian Petroleum Directorate*.
- Hammond, Paul S., and Evren Unsal. 2011. 'Spontaneous imbibition of surfactant solution into an oil-wet capillary: wettability restoration by surfactant-contaminant complexation', *Langmuir*, 27: 4412-29.
- Han, Chao. 2016. 'Design and synthesis of temperature switchable non-ionic block copolymers for application to oil sands extraction', University of Alberta.
- He, Lin, Feng Lin, Xingang Li, Zhenghe Xu, and Hong Sui. 2014. 'Enhancing bitumen liberation by controlling the interfacial tension and viscosity ratio through solvent addition', *Energy & Fuels*, 28: 7403-10.

- . 2015. 'Effect of solvent addition on bitumen-air bubble attachment in process water', *Chemical Engineering Science*, 137: 31-39.
- He, Lin, Feng Lin, Xingang Li, Hong Sui, and Zhenghe Xu. 2015. 'Interfacial sciences in unconventional petroleum production: from Fundamentals to applications', *Chemical Society Reviews*, 44: 5446-94.
- He, Lin, Yile Zhang, Feng Lin, Zhenghe Xu, Xingang Li, and Hong Sui. 2015. 'Image analysis of heavy oil liberation from host rocks/sands', *The Canadian Journal of Chemical Engineering*, 93: 1126-37.
- He, Xiao, Chen Liang, Qingxia Liu, and Zhenghe Xu. 2019. 'Magnetically responsive Janus nanoparticles synthesized using cellulosic materials for enhanced phase separation in oily wastewaters and water-in-crude oil emulsions', *Chemical Engineering Journal*, 378: 122045.
- Heikkila, Richard E., David W. Deamer, and David G. Cornwell. 1970. 'Solution of fatty acids from monolayers spread at the air-water interface: identification of phase transformations and the estimation of surface charge', *Journal of Lipid Research*, 11: 195-200.
- Hendraningrat, Luky, Shidong Li, and Ole Torsæter. 2013. 'A coreflood investigation of nanofluid enhanced oil recovery', *Journal of Petroleum Science and Engineering*, 111: 128-38.
- Hirasaki, George, Clarence A. Miller, and Maura Puerto. 2011. 'Recent advances in surfactant EOR', *SPE Journal*, 16: 889-907.
- Holland, Amy, Dominik Wechsler, Anjali Patel, Brian M. Molloy, Alaina R. Boyd, and Philip G. Jessop. 2012. 'Separation of bitumen from oil sands using a switchable hydrophilicity solvent', *Canadian Journal of Chemistry*, 90: 805-10.
- Hourdet, D, F L'alloret, and R Audebert. 1994. 'Reversible thermo-thickening of aqueous polymer solutions', *Polymer*, 35: 2624-30.
- Huang, Jianping, Fangqin Cheng, Bernard P. Binks, and Hengquan Yang. 2015. 'pH-responsive gas-water-solid interface for multiphase catalysis', *Journal of the American Chemical Society*, 137: 15015-25.

- Jahagirdar, Shruti Ravindra. 2008. "Oil-microbe detection tool using nano optical fibers." In *SPE Western Regional and Pacific Section AAPG Joint Meeting*, 7. Bakersfield, California, USA: Society of Petroleum Engineers.
- Jandacek, R. J. 1991. 'The solubilization of calcium soaps by fatty acids', *Lipids*, 26: 250-53.
- Janpoor, Fatemeh, Ali Torabian, and Vahid Khatibikamal. 2011. 'Treatment of laundry wastewater by electrocoagulation', *Journal of Chemical Technology and Biotechnology*, 86: 1113-20.
- Jessop, Philip G., David J. Heldebrant, Xiaowang Li, Charles A. Eckert, and Charles L. Liotta. 2005. 'Reversible nonpolar-to-polar solvent', *Nature*, 436: 1102-02.
- Jessop, Philip G., Sean M. Mercer, and David J. Heldebrant. 2012. 'CO₂-triggered switchable solvents, surfactants, and other materials', *Energy & Environmental Science*, 5: 7240-53.
- Jessop, Philip G., Lam Phan, Andrew Carrier, Shona Robinson, Christoph J. Dürr, and Jitendra R. Harjani. 2010. 'A solvent having switchable hydrophilicity', *Green Chemistry*, 12: 809-14.
- Jia, Weihong, Sili Ren, and Bin Hu. 2013. 'Effect of water chemistry on zeta potential of air bubbles', *International Journal of Electrochemical Science*, 8: 5828-37.
- Jung, H. B., K. C. Carroll, S. Kabilan, D. J. Heldebrant, D. Hoyt, L. Zhong, T. Varga, S. Stephens, L. Adams, A. Bonneville, A. Kuprat, and C. A. Fernandez. 2015. 'Stimuli-responsive/rheoreversible hydraulic fracturing fluids as a greener alternative to support geothermal and fossil energy production', *Green Chemistry*, 17: 2799-812.
- Kamal, Muhammad Shahzad, Abdullah S. Sultan, Usamah A. Al-Mubaiyedh, Ibelwaleed A. Hussein, and Yujun Feng. 2015. 'Rheological properties of thermoviscosifying polymers in high-temperature and high-salinity environments', *The Canadian Journal of Chemical Engineering*, 93: 1194-200.
- Kanicky, J. R., and D. O. Shah. 2002. 'Effect of degree, type, and position of unsaturation on the pK_a of long-chain fatty acids', *Journal of Colloid and Interface Science*, 256: 201-7.
- . 2003. 'Effect of premicellar aggregation on the pK_a of fatty acid soap solutions', *Langmuir*, 19: 2034-38.

- Kanicky, JR, AF Poniatowski, NR Mehta, and DO Shah. 2000. 'Cooperativity among molecules at interfaces in relation to various technological processes: Effect of chain length on the pK_a of fatty acid salt solutions', *Langmuir*, 16: 172-77.
- Kim, Jaemyung, Laura J. Cote, Franklin Kim, Wa Yuan, Kenneth R. Shull, and Jiaying Huang. 2010. 'Graphene oxide sheets at interfaces', *Journal of the American Chemical Society*, 132: 8180-86.
- Klein, R., D. Touraud, and W. Kunz. 2008. 'Choline carboxylate surfactants: biocompatible and highly soluble in water', *Green Chemistry*, 10: 433-35.
- Klimpel, R.R., and B.S. Fee. 1992. "Recovery of petroleum from tar sands." In. US Patent: The Dow Chemical Company, Midland, Mich.
- Ko, Saebom, Valentina Prigiobbe, Chun Huh, Steven Lawrence Bryant, Martin Vad Bennetzen, and Kristian Mogensen. 2014. "Accelerated oil droplet separation from produced water using magnetic nanoparticles." In *SPE Annual Technical Conference and Exhibition*, 14. Amsterdam, The Netherlands: Society of Petroleum Engineers.
- Kwok, Man-hin, and To Ngai. 2016. 'Chapter 4. Responsive particle-stabilized emulsions: Formation and applications.' in, *Smart materials for advanced environmental applications* (The Royal Society of Chemistry).
- L'alloret, F, P Maroy, D Hourdet, and R Audebert. 1997. 'Reversible thermoassociation of water-soluble polymers', *Revue de l'Institut Français du Pétrole*, 52: 117-28.
- Leo, Albert, and DH Hoekman. 1995. *Exploring QSAR* (American Chemical Society).
- Li, Dexiang, Bo Ren, Liang Zhang, Justin Ezekiel, Shaoran Ren, and Yujun Feng. 2015. 'CO₂-sensitive foams for mobility control and channeling blocking in enhanced WAG process', *Chemical Engineering Research and Design*, 102: 234-43.
- Li, Dexiang, Shaoran Ren, Panfeng Zhang, Liang Zhang, Yunjun Feng, and Yibin Jing. 2017. 'CO₂-sensitive and self-enhanced foams for mobility control during CO₂ injection for improved oil recovery and geo-storage', *Chemical Engineering Research and Design*, 120: 113-20.

- Li, J., W. D. Zhang, Z. J. Hu, X. J. Jiang, T. Ngai, P. C. Lo, W. Zhang, and G. J. Chen. 2013. 'Novel phthalocyanine and PEG-methacrylates based temperature-responsive polymers for targeted photodynamic therapy', *Polymer Chemistry*, 4: 782-88.
- Li, Jing, and Meyya Meyyappan. 2011. "Real time oil reservoir evaluation using nanotechnology." In. U.S. Patent 7,875,455..
- Li, Rui, Rogerio Manica, Anthony Yeung, and Zhenghe Xu. 2019. 'Spontaneous displacement of high viscosity micrometer size oil droplets from a curved solid in aqueous solutions', *Langmuir*, 35: 615-27.
- Li, X. J., H. S. Lu, D. F. Liu, G. J. Yan, S. S. Dai, and Z. Y. Huang. 2019. 'Cleaner and sustainable approach of washing oil sands using CO₂-responsive composite switchable water (CSW) with lower volatility', *Journal of Cleaner Production*, 236.
- Li, Xian'e, Zhi Xu, Hongyao Yin, Yujun Feng, and Hongping Quan. 2017. 'Comparative studies on enhanced oil recovery: Thermoviscosifying polymer versus polyacrylamide', *Energy & Fuels*, 31: 2479-87.
- Li, Xian'e, Hong-Yao Yin, Ru-Sheng Zhang, Jia Cui, Jun-Wen Wu, and Yu-Jun Feng. 2019. 'A salt-induced viscosifying smart polymer for fracturing inter-salt shale oil reservoirs', *Petroleum Science*, 16: 816-29.
- Li, Xingang, Ziqi Yang, Hong Sui, Ashish Jain, and Lin He. 2018. 'A hybrid process for oil-solid separation by a novel multifunctional switchable solvent', *Fuel*, 221: 303-10.
- Li, Z. F., K. Geisel, W. Richtering, and T. Ngai. 2013. 'Poly(N-isopropylacrylamide) microgels at the oil-water interface: adsorption kinetics', *Soft Matter*, 9: 9939-46.
- Li, Z. F., W. Richtering, and T. Ngai. 2014. 'Poly(N-isopropylacrylamide) microgels at the oil-water interface: Temperature effect', *Soft Matter*, 10: 6182-91.
- Liang, Chen, Qingxia Liu, and Zhenghe Xu. 2014. 'Surfactant-free switchable emulsions using CO₂-responsive particles', *ACS Applied Materials & Interfaces*, 6: 6898-904.
- Liu, Dongfang, Hongsheng Lu, Ying Zhang, Peiyao Zhu, and Zhiyu Huang. 2019. 'Conversion of a surfactant-based microemulsion to a surfactant-free microemulsion by CO₂', *Soft Matter*.

- Liu, Xingli, Yu Wang, Zhiyong Lu, Quansheng Chen, and Yujun Feng. 2012. 'Effect of inorganic salts on viscosifying behavior of a thermoassociative water-soluble terpolymer based on 2-acrylamido-methylpropane sulfonic acid', *Journal of Applied Polymer Science*, 125: 4041-48.
- Long, Jun, Hongjun Li, Zhenghe Xu, and Jacob H. Masliyah. 2011b. 'Improving oil sands processability using a temperature-sensitive polymer', *Energy & Fuels*, 25: 701-07.
- Lu, H. S., X. Q. Guan, S. S. Dai, and Z. Y. Huang. 2014. 'Application of CO₂-triggered switchable surfactants to form emulsion with Xinjiang heavy oil', *Journal of Dispersion Science and Technology*, 35: 655-62.
- Lu, H. S., X. Q. Guan, B. G. Wang, and Z. Y. Huang. 2015. 'CO₂-switchable oil/water emulsion for pipeline transport of heavy oil', *Journal of Surfactants and Detergents*, 18: 773-82.
- Lu, Yi, Dejun Sun, John Ralston, Qingxia Liu, and Zhenghe Xu. 2019. 'CO₂-responsive surfactants with tunable switching pH', *Journal of Colloid and Interface Science*, 557: 185-95.
- Lu, Yi, Yeling Zhu, Dejun Sun, Qingxia Liu, and Zhenghe Xu. 2019. "Controlling interfacial property through cost-efficient, CO₂-responsive assemblies for the enhancement of bitumen recovery." in *Abstracts of papers of the American Chemical Society*. Orlando: American Chemical Society, 1155 16th st, NW, Washington, DC 20036 USA.
- Lu, Yi, Yeling Zhu, Zhenghe Xu, and Qingxia Liu. 2019. 'Pseudo-Gemini biosurfactants with CO₂ switchability for enhanced oil recovery (EOR)', *Tenside Surfactants Detergents*, 56: 407-16.
- Martínez-Balbuena, L., Araceli Arteaga-Jiménez, Ernesto Hernández-Zapata, and César Márquez-Beltrán. 2017. 'Applicability of the Gibbs Adsorption Isotherm to the analysis of experimental surface-tension data for ionic and nonionic surfactants', *Advances in Colloid and Interface Science*, 247: 178-84.
- Masliyah, J, J Czarnecki, and Z Xu. 2010. *Handbook on theory and practice of bitumen recovery from Athabasca oil sands* (Kingsley Knowledge Publishing).
- Masliyah, Jacob, Zhiang Joe Zhou, Zhenghe Xu, Jan Czarnecki, and Hassan Hamza. 2004. 'Understanding water- based bitumen extraction from Athabasca oil sands', *The Canadian Journal of Chemical Engineering*, 82: 628-54.

- McElfresh, Paul M., David Lee Holcomb, and Daniel Ector. 2012. "Application of nanofluid technology to improve recovery in oil and gas wells." In *SPE International Oilfield Nanotechnology Conference and Exhibition*, 6. Noordwijk, The Netherlands: Society of Petroleum Engineers.
- McLean, Douglas S, David Vercoe, Karen R Stack, and DE Richardson. 2005. 'The colloidal pK_a of lipophilic extractives commonly found in *Pinus radiata*', *Appita Journal*, 58: 362-66.
- Merchan-Arenas, Diego R, and Cindy Carolina Villabona-Delgado. 2019. 'Chemical-enhanced oil recovery using N,N-dimethylcyclohexylamine on a Colombian crude oil', *International Journal of Chemical Engineering*, 2019.
- Mihut, A. M., A. P. Dabkowska, J. J. Crassous, P. Schurtenberger, and T. Nylander. 2013. 'Tunable adsorption of soft colloids on model biomembranes', *ACS Nano*, 7: 10752-63.
- Milani, Silvia, Göran Karlsson, Katarina Edwards, Piero Baglioni, and Debora Berti. 2011. 'Association of polynucleotides with nucleolipid bilayers driven by molecular recognition', *Journal of Colloid and Interface Science*, 363: 232-40.
- Mohajeri, Ali, Alimorad Rashidi, Kheirollah Jafari Jozani, Payman Khorami, Bahman Amini, Dorsa Parviz, and Mansour Kalbasi. 2010. "Hydrodesulphurization nanocatalyst, its use and a process for its production." In *U.S. Patent*, No. 12/629,835..
- Mossop, Grant D. 1980. 'Geology of the Athabasca oil sands', *Science*, 207: 145-52.
- Mozhdehei, Armin, Negahdar Hosseinpour, and Alireza Bahramian. 2019. 'Dimethylcyclohexylamine switchable solvent interactions with asphaltenes toward viscosity reduction and *in situ* upgrading of heavy oils', *Energy & Fuels*, 33: 8403-12.
- Nazar, M. F., S. S. Shah, and M. A. Khosa. 2011. 'Microemulsions in enhanced oil recovery: A review', *Petroleum Science and Technology*, 29: 1353-65.
- Negin, Chegenizadeh, Saeedi Ali, and Quan Xie. 2017. 'Most common surfactants employed in chemical enhanced oil recovery', *Petroleum*, 3: 197-211.
- Nicolaidis, Charalambos, and Ioannis Vyrides. 2014. 'Closing the water cycle for industrial laundries: An operational performance and techno-economic evaluation of a full-scale membrane bioreactor system', *Resources Conservation and Recycling*, 92: 128-35.

- Novales, Bruno, Laurence Navailles, Monique Axelos, Frédéric Nallet, and Jean-Paul Douliez. 2008. 'Self-assembly of fatty acids and hydroxyl derivative salts', *Langmuir*, 24: 62-68.
- Onda, Mitsuhiko, Kanami Yoshihara, Hiroshi Koyano, Katsuhiko Ariga, and Toyoki Kunitake. 1996. 'Molecular recognition of nucleotides by the guanidinium unit at the surface of aqueous micelles and bilayers: A comparison of microscopic and macroscopic interfaces', *Journal of the American Chemical Society*, 118: 8524-30.
- Pan, Fang, Zhiming Lu, Ian Tucker, Sarah Hosking, Jordan Petkov, and Jian R. Lu. 2016. 'Surface active complexes formed between keratin polypeptides and ionic surfactants', *Journal of Colloid and Interface Science*, 484: 125-34.
- Paul, Brown, Bushmelev Alexey, Butts Craig P., Cheng Jing, Eastoe Julian, Grillo Isabelle, Heenan Richard K., and Schmidt Annette M. 2012. 'Magnetic control over liquid surface properties with responsive surfactants', *Angewandte Chemie International Edition*, 51: 2414-16.
- Perazzo, Antonio, Giovanna Tomaiuolo, Valentina Preziosi, and Stefano Guido. 2018. 'Emulsions in porous media: From single droplet behavior to applications for oil recovery', *Advances in Colloid and Interface Science*, 256: 305-25.
- Philippova, O. E., and A. R. Khokhlov. 2010. 'Smart polymers for oil production', *Petroleum Chemistry*, 50: 266-70.
- Qiao, Peiqi, David Harbottle, Zuoli Li, Yuechao Tang, and Zhenghe Xu. 2018. 'Interactions of asphaltene subfractions in organic media of varying aromaticity', *Energy & Fuels*. 32.10: 10478-10485.
- Quinlan, Patrick James, and Kam Chiu Tam. 2015. 'Water treatment technologies for the remediation of naphthenic acids in oil sands process-affected water', *Chemical Engineering Journal*, 279: 696-714.
- Raffa, Patrizio, Antonius A. Broekhuis, and Francesco Picchioni. 2016. 'Polymeric surfactants for enhanced oil recovery: A review', *Journal of Petroleum Science and Engineering*, 145: 723-33.

- Rahmani, Amir Reza, Steven Bryant, Chun Huh, Alex Athey, Mohsen Ahmadian, Jiuping Chen, and Michael Wilt. 2015. 'Crosswell magnetic sensing of superparamagnetic nanoparticles for subsurface applications', *SPE Journal*, 20: 1067-82.
- Sakurai, Minoru, Hirohisa Tamagawa, Yoshio Inoue, Katsuhiko Ariga, and Toyoki Kunitake. 1997. 'Theoretical study of intermolecular interaction at the lipid–water interface. 1. quantum chemical analysis using a reaction field theory', *The Journal of Physical Chemistry B*, 101: 4810-16.
- Sarsenbekuly, Bauyrzhan, Wanli Kang, Hongbin Yang, Bo Zhao, Saule Aidarova, Bin Yu, and Miras Issakhov. 2017. 'Evaluation of rheological properties of a novel thermo-viscosifying functional polymer for enhanced oil recovery', *Colloids and Surfaces A: Physicochemical and Engineering Aspects*, 532: 405-10.
- Scherrer, Robert A., and Susan M. Howard. 1977. 'Use of distribution coefficients in quantitative structure-activity relations', *Journal of Medicinal Chemistry*, 20: 53-58.
- Schramm, Laurier L, and Russell G Smith. 1985. 'The influence of natural surfactants on interfacial charges in the hot-water process for recovering bitumen from the Athabasca oil sands', *Colloids and surfaces*, 14: 67-85.
- Schramm, Laurier Lincoln. 2000. 'Surfactants: Fundamentals and applications in the petroleum industry.' (Cambridge University Press: Cambridge, UK.).
- Shibaev, Andrey V., Mikhail V. Tamm, Vyacheslav S. Molchanov, Andrey V. Rogachev, Alexander I. Kuklin, Elena E. Dormidontova, and Olga E. Philippova. 2014. 'How a viscoelastic solution of wormlike micelles transforms into a microemulsion upon absorption of hydrocarbon: New insight', *Langmuir*, 30: 3705-14.
- Sorbie, KS. 1991. 'Polymer-improved oil recovery, 115 Glasgow', *Scotland: Blackie & Son*: 126-63.
- Sotto, Arcadio, Arman Boromand, Stefan Balta, Jeonghwan Kim, and Bart Van der Bruggen. 2011. 'Doping of polyethersulfone nanofiltration membranes: Antifouling effect observed at ultralow concentrations of TiO₂ nanoparticles', *Journal of Materials Chemistry*, 21: 10311-20.

- Spink, J. A. 1963. 'Ionization of monolayers of fatty acids from C₁₄ to C₁₈', *Journal of Colloid Science*, 18: 512-25.
- Srinivasa, S., C. Flury, A. Afacan, J. Masliyah, and Z. H. Xu. 2012. 'Study of bitumen liberation from oil sands ores by online visualization', *Energy & Fuels*, 26: 2883-90.
- Sui, Hong, Lin Xu, Xingang Li, and Lin He. 2016. 'Understanding the roles of switchable-hydrophilicity tertiary amines in recovering heavy hydrocarbons from oil sands', *Chemical Engineering Journal*, 290: 312-18.
- Suleimanov, B. A., F. S. Ismailov, and E. F. Veliyev. 2011. 'Nanofluid for enhanced oil recovery', *Journal of Petroleum Science and Engineering*, 78: 431-37.
- Sun, Lin, Baojun Bai, Bing Wei, Wanfen Pu, Peng Wei, Daibo Li, and Changyong Zhang. 2019. 'Recent advances of surfactant-stabilized N₂/CO₂ foams in enhanced oil recovery', *Fuel*, 241: 83-93.
- Taber, J. J., F. D. Martin, and R. S. Seright. 1997a. 'EOR screening criteria revisited - Part 1: Introduction to screening criteria and enhanced recovery field projects', *SPE Reservoir Engineering*, 12: 189-98.
- . 1997b. 'EOR screening criteria revisited - Part 2: Applications and impact of oil prices', *SPE Reservoir Engineering*, 12: 199-206.
- Tagavifar, Mohsen. 2015. "Microemulsion viscosity and its implications for chemical EOR : experimental results and a model." In. Research Showcase in Petroleum and Geosystems: The University of Texas at Austin.
- Talari, Jyothsna Varsha. 2014. 'Temperature sensitive supramolecular assemblies for enhanced oil recovery'. *SPE Journal* 19.06 : 1-035.
- Tamagawa, Hirohisa, Minoru Sakurai, Yoshio Inoue, Katsuhiko Ariga, and Toyoki Kunitake. 1997. 'Theoretical study of intermolecular interaction at the lipid–water interface: 2. Analysis based on the Poisson–Boltzmann equation', *The Journal of Physical Chemistry B*, 101: 4817-25.
- Tan, H., K. C. Tam, and R. D. Jenkins. 2001. 'Network structure of a model HASE polymer in semidilute salt solutions', *Journal of Applied Polymer Science*, 79: 1486-96.

- Tang, Juntao, Richard M. Berry, and Kam C. Tam. 2016. 'Stimuli-responsive cellulose nanocrystals for surfactant-free oil harvesting', *Biomacromolecules*, 17: 1748-56.
- Tang, Juntao, Patrick James Quinlan, and Kam Chiu Tam. 2015. 'Stimuli-responsive Pickering emulsions: recent advances and potential applications', *Soft Matter*, 11: 3512-29.
- Tangparitkul, Suparit, Thibaut Charpentier, Diego Pradilla, and David Harbottle. 2018. 'Interfacial and colloidal forces governing oil droplet displacement: Implications for enhanced oil recovery', *Colloids and Interfaces*, 2: 30.
- Tiktopulo, E. I., V. N. Uversky, V. B. Lushchik, S. I. Klenin, V. E. Bychkova, and O. B. Ptitsyn. 1995. 'Domain coil-globule transition in homopolymers', *Macromolecules*, 28: 7519-24.
- Viken, Alette Løbø, Tormod Skauge, Per Erik Svendsen, Peter Aarrestad Time, and Kristine Spildo. 2018. 'Thermothickening and salinity tolerant hydrophobically modified polyacrylamides for polymer flooding', *Energy & Fuels*, 32: 10421-27.
- Wang, C., K. C. Tam, and R. D. Jenkins. 2002. 'Dissolution behavior of HASE polymers in the presence of salt: Potentiometric titration, isothermal titration calorimetry, and light scattering studies', *The Journal of Physical Chemistry B*, 106: 1195-204.
- Wang, Ji, Meiqing Liang, Qirui Tian, Yujun Feng, Hongyao Yin, and Guangliang Lu. 2018. 'CO₂-switchable foams stabilized by a long-chain viscoelastic surfactant', *Journal of Colloid and Interface Science*, 523: 65-74.
- Wang, L., D. Sharp, J. Masliyah, and Z. Xu. 2013. 'Measurement of interactions between solid particles, liquid droplets, and/or gas bubbles in a liquid using an integrated thin film drainage apparatus', *Langmuir*, 29: 3594-603.
- Wang, Louxiang, Zhenghe Xu, and Jacob H Masliyah. 2013. 'Dissipation of film drainage resistance by hydrophobic surfaces in aqueous solutions', *The Journal of Physical Chemistry C*, 117: 8799-805.
- Wang, Xiaofeng, Yi Shi, Robert W. Graff, Doyun Lee, and Haifeng Gao. 2015. 'Developing recyclable pH-responsive magnetic nanoparticles for oil-water separation', *Polymer*, 72: 361-67.

- Wang, Yu, Zhi Yong Lu, Yu Gui Han, Yu Jun Feng, and Chong Li Tang. 2011. 'A novel thermoviscosifying water-soluble polymer for enhancing oil recovery from high-temperature and high-salinity oil reservoirs', *Advanced Materials Research*, 306-307: 654-57.
- Wasan, Darsh T., and Alex D. Nikolov. 2003. 'Spreading of nanofluids on solids', *Nature*, 423: 156-59.
- Wellen, Bethany A., Evan A. Lach, and Heather C. Allen. 2017. 'Surface pK_a of octanoic, nonanoic, and decanoic fatty acids at the air–water interface: applications to atmospheric aerosol chemistry', *Physical Chemistry Chemical Physics*, 19: 26551-58.
- Werner, Jörg G., Saraf Nawar, Alexander A. Solovev, and David A. Weitz. 2018. 'Hydrogel microcapsules with dynamic pH-responsive properties from methacrylic anhydride', *Macromolecules*, 51: 5798-805.
- Wever, D. A. Z., F. Picchioni, and A. A. Broekhuis. 2011. 'Polymers for enhanced oil recovery: A paradigm for structure–property relationship in aqueous solution', *Progress in Polymer Science*, 36: 1558-628.
- Xiang, B. X., Y. C. Zhang, X. D. Huang, T. Kang, S. J. Severtson, W. J. Wang, and P. W. Liu. 2019. 'Tailoring CO₂-responsive polymers and nanohybrids for green chemistry and processes', *Industrial & Engineering Chemistry Research*, 58: 15088-108.
- Xie, Chun-Yan, Shi-Xin Meng, Long-Hui Xue, Rui-Xue Bai, Xin Yang, Yaolei Wang, Zhong-Ping Qiu, Bernard P. Binks, Ting Guo, and Tao Meng. 2017. 'Light and magnetic dual-responsive pickering emulsion micro-reactors', *Langmuir*, 33: 14139-48.
- Xu, Haiyan, Weihong Jia, Sili Ren, and Jinqing Wang. 2018. 'Novel and recyclable demulsifier of expanded perlite grafted by magnetic nanoparticles for oil separation from emulsified oil wastewaters', *Chemical Engineering Journal*, 337: 10-18.
- Xu, P., Z. Wang, Z. Xu, J. Hao, and D. Sun. 2016. 'Highly effective emulsification/demulsification with a CO₂-switchable superamphiphile', *Journal of Colloid and Interface Science*, 480: 198-204.

- Xu, W., H. Gu, X. Zhu, Y. Zhong, L. Jiang, M. Xu, A. Song, and J. Hao. 2015. 'CO₂-controllable foaming and emulsification properties of the stearic acid soap systems', *Langmuir*, 31: 5758-66.
- Yan, Tao, Xiaoqing Chen, Taiheng Zhang, Jingang Yu, Xinyu Jiang, Wenjihao Hu, and Feipeng Jiao. 2018. 'A magnetic pH-induced textile fabric with switchable wettability for intelligent oil/water separation', *Chemical Engineering Journal*, 347: 52-63.
- Yang, Bingqing, and Jean Duhamel. 2015. 'Extraction of oil from oil sands using thermoresponsive polymeric surfactants', *ACS Applied Materials & Interfaces*, 7: 5879-89.
- Yang, Zihao, Xiaochen Li, Danyang Li, Taiheng Yin, Peizhong Zhang, Zhaoxia Dong, Meiqin Lin, and Juan Zhang. 2019. 'New method based on CO₂-switchable wormlike micelles for controlling CO₂ breakthrough in a tight fractured oil reservoir', *Energy & Fuels*, 33: 4806-15.
- Yang, Ziqi, Changqing He, Hong Sui, Lin He, and Xingang Li. 2019. 'Recent advances of CO₂-responsive materials in separations', *Journal of CO₂ Utilization*, 30: 79-99.
- Ye, Y., S. M. Khandrika, and J. D. Miller. 1989. 'Induction-time measurements at a particle bed', *International Journal of Mineral Processing*, 25: 221-40.
- Yegin, Cengiz, B. P. Singh, Ming Zhang, Frontida Biopharm, Karthik Balaji, Anuj Suhag, Rahul Ranjith, Zumra Peksaglam, Zein Wijaya, Dike Putra, Henny Anggraini, and Cenk Temizel. 2017. "Next-generation displacement fluids for enhanced oil recovery." In *SPE Oil and Gas India Conference and Exhibition*, 29. Mumbai, India: Society of Petroleum Engineers.
- Yeung, A, T Dabros, J Czarnecki, and J Masliyah. 1999. 'On the interfacial properties of micrometre-sized water droplets in crude oil', *Proceedings of the Royal Society of London. Series A: Mathematical, Physical and Engineering Sciences*, 455: 3709-23.
- Yin, H., Y. Feng, H. Liu, M. Mu, and C. Fei. 2014. 'Insights into the relationship between CO₂ switchability and basicity: Examples of melamine and its derivatives', *Langmuir*, 30: 9911-9.
- Yoon, Roe-Hoan, and Jorge L Yordan. 1991. 'Induction time measurements for the quartz—amine flotation system', *Journal of Colloid and Interface Science*, 141: 374-83.

- Young, Thomas. 1805. 'III. An essay on the cohesion of fluids', *Philosophical Transactions of the Royal Society of London*: 65-87.
- Zhang, Yan, Yujun Feng, Bo Li, and Peihui Han. 2019. 'Enhancing oil recovery from low-permeability reservoirs with a self-adaptive polymer: A proof-of-concept study', *Fuel*, 251: 136-46.
- Zhang, Yan, Mingwei Gao, Qing You, Hongfu Fan, Wenhui Li, Yifei Liu, Jichao Fang, Guang Zhao, Zhehui Jin, and Caili Dai. 2019. 'Smart mobility control agent for enhanced oil recovery during CO₂ flooding in ultra-low permeability reservoirs', *Fuel*, 241: 442-50.
- Zhang, Yongmin, Yuandi Zhang, Cheng Wang, Xuefeng Liu, Yun Fang, and Yujun Feng. 2016. 'CO₂-responsive microemulsion: Reversible switching from an apparent single phase to near-complete phase separation', *Green Chemistry*, 18: 392-96.
- Zhao, Xiaolin, Suchitra Subrahmanyam, and Kenneth B. Eisenthal. 1990. 'Determination of pK_a at the air/water interface by second harmonic generation', *Chemical Physics Letters*, 171: 558-62.
- Zhong, Chuanrong, Wei Wang, and Mingming Yang. 2012. 'Synthesis and solution properties of an associative polymer with excellent salt-thickening', *Journal of Applied Polymer Science*, 125: 4049-59.
- Zhu, Dingwei, Jichao Zhang, Yugui Han, Hongyan Wang, and Yujun Feng. 2013. 'Laboratory study on the potential EOR use of HPAM/VES hybrid in high-temperature and high-salinity oil reservoirs', *Journal of Chemistry*, 2013.
- Zhu, Yeling, Ci Yan, Qingxia Liu, Jacob Masliyah, and Zhenghe Xu. 2018. 'Biodiesel-assisted ambient aqueous bitumen extraction (BA³BE) from Athabasca oil sands', *Energy & Fuels*. 32: 6565-6576.